2012

Development of a modular dual engine hybrid electric vehicle simulation model

Kenan Baltaci
University of Northern Iowa

DEVELOPMENT OF A MODULAR DUAL ENGINE HYBRID ELECTRIC VEHICLE SIMULATION MODEL

An Abstract of a Dissertation

Submitted

in Partial Fulfillment

of the Requirements for the Degree

Doctor of Technology

Approved:

_____

Dr. Recayi Pecen, Committee Chair

_____

Dr. Michael J. Licari
Dean of the Graduate College

Kenan Baltaci

University of Northern Iowa

July 2012

ABSTRACT

Depleting resources of fossil fuel, climate change impacts, high oil prices, and strict emission requirements are leading to the research on efficient, environmentally friendly, and lowered fossil fuel dependent solutions in the transportation field. While a number of studies used computer modeling and simulation tools to investigate hybrid electric vehicles (HEVs), very few attempted to model and simulate a dual-engine hybrid vehicle. Designing a vehicle engine to meet energy needs in the fully loaded condition is not an optimal solution for manufacturers and customers. The larger the engine, the higher the manufacturing costs for companies, and higher fuel consumption for customers. The integration of dual-engine hybrid technology can help to solve this problem.

The objective of this study was to design and simulate a dual-engine hybrid electric vehicle (DE-HEV) model to investigate whether it can be a fuel efficient and environmentally friendly solution without sacrificing vehicle performance. The simulated DE-HEV uses two small engines instead of one large engine. In the simulated design, a smaller single engine supplies the power if the energy need is not more than a single engine can provide. The second engine turns on when the power demand is greater than the single engine can supply.

Working models for the DE-HEV components, such as an electric motor, generator, battery, and the controller have been developed using the Matlab/Simulink™ simulation package. Each model was validated with test data from the literature. Appropriate power management strategy has been developed to accommodate the dual

engine design. Fuel-efficiency, overall performance, and manufacturing cost for the simulated DE-HEV model have been compared against current commercial models.

Simulation results showed that DE-HEV has between a 2% to 6% higher efficiency than comparable HEVs. Cost analysis results showed that the manufacturing cost of DE-HEV is 11% higher. Performance of the vehicle was tested with standard drive cycles. Test results are satisfactory; although there was significant increase in fuel-efficiency, because of its higher initial manufacturing cost, maintenance, and complexity, DE-HEVs may have challenges in the short term. However, with expected decreases in manufacturing costs of battery storage and power electronics technology, the implementation of DE-HEVs can be feasible transportation options in the near future.

DEVELOPMENT OF A MODULAR DUAL ENGINE HYBRID ELECTRIC VEHICLE SIMULATION MODEL

A Dissertation

Submitted

in Partial Fulfillment

of the Requirements for the Degree

Doctor of Technology

Approved:

_____

Dr. Recayi "Reg" Pecen, Chair

_____

Dr. Hong "Jeffrey" Nie, Co-Chair

_____

Dr. Nilmani Pramanik, Committee Member

_____

Dr. William M. Stigliani, Committee Member

_____

Dr. Otto H. MacLin, Committee Member

_____

Dr. Ayhan Zora, Committee Member

Kenan Baltaci

University of Northern Iowa

July 2012

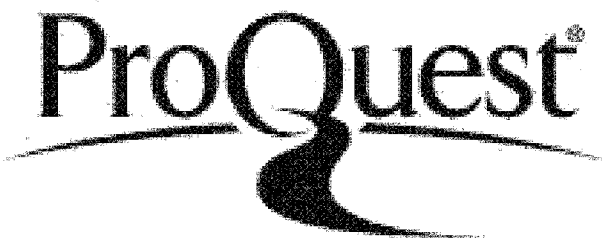

ProQuest LLC
789 East Eisenhower Parkway
P.O. Box 1346
Ann Arbor, MI 48106-1346

ACKNOWLEDGEMENTS

I want to take a moment to thank those who have given of their time, contributions, and effort to make this dissertation a reality. I would like to express my deepest sincere appreciation for all those individuals.

My deepest gratitude is to my advisor, Dr. Recayi Pecen. I have been incredibly fortunate to have an advisor who has supported me throughout my dissertation with his excellent guidance, caring, patience, and knowledge. I attribute the level of my doctorate degree to his encouragement and effort and without him this dissertation, too, would not have been completed or written. One simply could not wish for a better or friendlier advisor.

I would like to express my thanks to Dr. Ayhan Zora, Dr. Hong (Jeffrey) Nie, Dr. Nilmani Pramanik, Dr. Bill Stigliani, and Dr. Otto MacLin for being in my committee and taking their time to review my dissertation.

I am very thankful to Pecen, Zora, Parpucu, and Sengun families for their support and encouragements.

I also would like to thank Dr. Mohammed Fahmy for his support and guidance during my graduate education.

I also would like to thank David Robinson and Allen Larson my supervisors for their flexibility for my work schedule and his understanding of the difficulty of being both doctoral student and part time student employee in Product Engineering Center at John Deere.

I would also like to thank my parents, two sisters, and brother. They were always supporting me and encouraging me with their best wishes.

Finally, I would like to thank my wife, Aysegul Baltaci. She was always there cheering me up and stood by me through the good times and bad.

Finally, I would like to express my sincere appreciation to the faculty, staff, and students in the Industrial technology Department at University of Northern Iowa for their contributions.

TABLE OF CONTENTS

PAGE

LIST OF TABLES

LIST OF FIGURES

FIGURE PAGE

FIGURE PAGE

FIGURE PAGE

CHAPTER I

INTRODUCTION

Due to the depletion of fossil fuel resources, increasing global demand, and environmental concerns such as greenhouse gas emissions and air quality, tremendous advancements are needed in the transportation field. Many scientist and institutions agree that reducing the environmental impact of on-road and off-road vehicles by reducing fossil fuel use is one of the most urgent issues of modern society. Bayindir, Gozukucuk, and Teke (2010) report that "Leading climate alarmists claim that global greenhouse gas emissions need to decrease to 60% below the present levels by 2050 if humans are to avoid catastrophic climate change"(p. 1305). On-road, heavy vehicles such as trucks and buses, and off-road vehicles such tractors, bulldozers, backhoes, etc. are the major consumers of fossil fuel resources today. According to the California Environmental Protection Agency Air Resources Board (CARB) emissions from on-road, heavy-duty vehicles are major contributors to poor air quality: "In particular, diesel vehicles produce emissions in amounts highly disproportionate to the total population of these vehicles" (On-Road Heavy-Duty Vehicle Program, 2011, para. 9). Furthermore, "Continuously increasing legislative and market requirements demand new energy efficient low emission powertrain concepts" (Banjac, Trenc, & Katrasnik, 2009, p. 2865). On the other hand, customers request vehicles with better performance and improved drivability. These contradictory goals required new technologies to come into play. Electric vehicles (EVs), fuel cell vehicles (FCVs), and hybrid electric vehicles (HEVs) are emerging technologies that offer possible solutions:

> Among the alternative power trains being investigated, the HEVs consisting of an internal combustion engine (ICE) and an electric machine (EM) are considered to offer the best short to midterm solution due to the use of smaller battery pack and their similarities with the conventional vehicles. (Katrasnik, 2009, p. 1924).

Power demand from heavy-duty vehicles is high and even higher when a vehicle is fully loaded. However, use of heavy-duty vehicles, or tractors, in fully loaded conditions is rare. Designing such a vehicle engine to meet energy needs in a fully loaded condition is not the optimal solution for producers and the customer because the larger engine size, the higher production cost for producers, and the higher fuel consumption for customer. Use of dual, smaller engine, hybrid technologies can help to solve both problems. Although it is very similar to conventional hybrid vehicle technology, dual-engine hybrid vehicles offer the use of two smaller engines instead of a single large engine, and include use of two generators and two motors. In this design, a single engine supplies all energy needs when low or normal power is needed. The second engine is an auxiliary power source for its tractor, providing extra power when the power demand is more than that of normal operating conditions.

The objective of this study is to design and simulate a dual-engine hybrid vehicle (DE-HEV) model to investigate if the dual-engine hybrid vehicle can be a fuel efficient and environmental friendly solution without sacrificing performance for heavy-duty off-road and on-road vehicles.

Hybrid vehicle technology is relatively complex system compared to the conventional, internal combustion engine vehicle (ICEV) technology; therefore, the powertrain design is more challenging in terms of time spent for research and development cost. Consequently, there is a critical need to develop and validate vehicle

simulations that can predict the performance of the vehicle propulsion system under a variety of driving conditions by accurately modeling all subsystem parameters. Once the validation of the simulation against actual vehicle data was completed, it was used to dependably simulate and test different configurations in variable drive cycles and conditions (Brown, Alexander, Brunner, Advani, & Prasad, 2008).

Statement of the Problem

The problem of this research is to design and analyze a dual engine configuration for hybrid vehicles to determine its viability in terms of emissions, fuel-economy, and performance in comparison to conventional heavy-duty vehicles without compromising performance.

Statement of the Purpose

The purpose of this research study was to develop and validate the dual-engine hybrid vehicle powertrain simulation model for the hybrid vehicles. The objectives of this study that supported this purpose are:

1. Create working models for the dual-engine hybrid vehicle components, such as electric motor, generator, battery, and the controller through simulation using MATLAB®/Simulink® simulation package.
2. Validate each component model with the actual data from previous studies.
3. Develop an appropriate state-of-the-art power management strategy.
4. Compare and contrast the proposed scheme for overall fuel efficiency, cost, emissions, and performance with other commercially available models.

Statement of the Need

The need for this study is based on the importance of increasing the fuel efficiency and reducing the emissions in heavy-duty vehicles. Heavy-duty vehicles can be classified into two groups: on-road heavy-duty vehicles, and off-road heavy-duty vehicles. Studies examining the dual-engine hybrid vehicle are limited. Jackson (2010) wrote, "Emissions reductions have posed many challenges for off-highway applications" (Jackson, 2010, para. 1). The off-highway vehicle industry requires meeting the emission regulations of the U.S. Environmental Protection Agency as well as increasing fuel economy (Moore, 1996). According to the California Environmental Protection Agency Air Resources Board (CARB), emissions from on-road heavy-duty vehicles are major contributors to poor air quality.

There is also need for a reliable simulation model for a dual-engine hybrid vehicle. While a number of studies have used computer modeling and simulation tools to examine HVs, none has attempted to model and simulate dual-engine hybrid vehicles. Hou and Guo (2008) write, "Computer modeling and simulation can be used to reduce the expense and length of the design cycle of hybrid vehicles by testing configurations and energy management strategies before prototype construction begins" (p. 1). HEVs embody more electrical components, featuring many available patterns of combining power flows to meet load requirements, as compared to conventional, internal combustion engine vehicles (ICEVs). Since ICEVs have multiple power sources, several powertrain topologies and different control strategies to control the power can be considered. Banjac et al. (2009) wrote:

Dynamic interactions among various components and the multidisciplinary nature make it difficult to predict interactions among various vehicle components and the systems. Prototyping and testing each design combination is cumbersome, expensive, and time consuming. Modeling and simulation are therefore indispensable for concept evaluation, prototyping, and analysis of HEVs. (p. 1)

Research Hypothesis

The research hypotheses are:

1. Modeling of dual-engine hybrid vehicle components can be developed in MATLAB®/Simulink® simulation software meeting the industry requirements.
2. There will be measurable efficiency increase in the dual-engine hybrid vehicle model compared to the conventional combustion engine.
3. The simulation model developed for the dual-engine hybrid vehicle will perform similarly to actual vehicle operation.
4. The overall cost of the vehicle with dual engines will not be higher than with a conventional combustion engine.

Assumptions

1. It is assumed that test data taken from previous studies, and used in this study, is accurate, and that measurement tools and data acquisition equipment are properly calibrated.

Limitations

1. The model created in this study can run only in Windows XP operating system.
2. This study was limited to a single DE-HEV configuration.

Definition of Terms

Aerodynamic Drag: The force that opposes forward motion through the atmosphere, and is parallel to the direction of the free-stream velocity of the airflow (Anderson, 1997).

Boost (Step-Up) Converter: A power converter with an output DC voltage greater than its input DC voltage. It is a switching-mode power supply that contains at least two semiconductor switches, such as diodes, transistors, and an energy storage element (Reemmer, 2007).

Brushless DC Motor/Generator: A synchronous electric motor powered by direct-current electricity (DC), and has an electronically controlled commutation system instead of a mechanical commutation system based on brushes (How Motors Work, 2008).

CAN: The Controller Area Network (CAN) is a serial bus communications protocol developed by Bosch in the early 1980s. It is designed to allow microcontrollers and devices to communicate with each other within a vehicle without a host computer (Levine & Hristu-Varsakelis, 2005).

Drivetrain: This term, also called a "powertrain," describes all of a vehicle's components that produce power and transmit power to the wheels, engine, transmission, transfer case, drive-shafts, differentials, axle shafts, and wheel hubs (Toyota Gibraltar Stockholdings Ltd., n.d.)

Driving Cycle: A driving cycle is a series of data points representing the speed of a vehicle versus time. Usually speed is in kph (kilometers per hour) or mph, and time in seconds. Driving cycles are formed by different organizations and countries to evaluate vehicles in various ways in terms of performance, fuel consumption, and polluting emissions (Ericsson, 2001).

Duty Cycle: The fraction of a time period that a system is in an active state, and the proportion of time during which a component or a device is operated (Duty Cycle, 2011).

ECU: Electronic control unit (ECU) is an embedded system that controls one or more of the electrical subsystems in a vehicle (Webster's Dictionary, 2011)

Gear Ratio: The relationship between the number of teeth on two gears that are meshed with each other, or on two sprockets connected with a common roller chain (Fl Technical Glossary, 2008).

Gear Set: A group of different sized gears that limit or increase the mechanical speed. The direction and magnitude of change depends on gear ratios (Uses for Gears, 2008).

Global Warming: The term "global warming" describes the observed and projected increase in globally averaged temperatures over time. The Intergovernmental Panel on Climate Change has determined that this increase can be attributed to a combination of natural climate variations and human factors. One of the leading causes under investigation is the greenhouse effect of gasses in the atmosphere (What is Global Warming?, 2011)

Greenhouse Gas: A greenhouse gas (GHG) is a gas that absorbs and releases radiation within our atmosphere. While greenhouse gases allow the sun's energy to enter the atmosphere, instead of letting it re-radiate back into space as infrared radiation, these gasses absorb infrared radiation and trap it in the atmosphere (Ecolife Dictionary, 2011).

ICE: The internal combustion engine is one in which the combustion of a fuel occurs with an oxidizer (usually air) in a combustion chamber. In an internal combustion engine, the expansion of the high-temperature and high-pressure gases produced by combustion applies direct force to some component of the engine, such as pistons, turbine blades, or a nozzle. This force moves the component over a distance, generating useful mechanical energy. The term "internal combustion engine" usually refers to an engine in which combustion is intermittent (Internal Combustion Engine, 2008).

LabVIEW: LabVIEW is a graphical programming environment used by engineers and scientists to develop sophisticated measurements, testing, and control systems using intuitive graphical icons and wires that resemble a flowchart. It offers integration with thousands of hardware devices, and provides hundreds of built-in libraries for advanced analysis and data visualization (What is NI LabVIEW?, 2011).

Lookup Table: Lookup tables are tables that store numeric data in a multidimensional array. Lookup tables provide a means to capture the dynamic behavior of a physical (mechanical, electronic, software) system (TheMathWorks, 2011)

MATLAB®: MATLAB® is a high-level technical computing language and interactive environment for algorithm development, data visualization, data analysis, and numerical computation (The MathWorks, 2011).

Planetary Gear: Planetary gear set of carrier, sun, planet, and ring wheels with adjustable gear ratios and friction losses (The MathWorks, 2011).

Plug-in Hybrid: A plug-in hybrid is a hybrid vehicle that has a high-capacity battery bank that can be re-charged by plugging in to normal, household current, and also uses on-board charging capabilities of normal hybrids (Global Smart Energy, 2011)

PMDC (Permanent Magnet Direct Current) Motor/Generator: The rotor of the permanent magnet motors rotate in synchronicity with the oscillating field or current (Electric Motors and Generators, 2007).

Regenerative Braking: Regenerative braking is a system in which the electric motor that normally drives a hybrid or pure electric vehicle is essentially operated in reverse (electrically) during braking or coasting. Instead of consuming energy to propel a vehicle, the motor acts as a generator that charges the onboard batteries with electrical energy that would normally be lost as heat through traditional, mechanical friction brakes (HybridCARS, 2006).

Rolling Resistance: Resistance from tire deformation, tire penetration, surface compression, tire slippage, and air circulation around the wheel.

RPM: Rotations per minute.

Saber: Saber is a proven platform for modeling and simulating physical systems, enabling full-system virtual prototyping for applications in analog/power electronics, electric power generation/conversion/distribution, and mechatronics (Synopsys, Inc., 2011).

Simulink: Simulink® is an environment for multi-domain simulation and model-based design for dynamic and embedded systems. It provides an interactive, graphical environment and a customizable set of block libraries that let users design, simulate, implement, and test a variety of time-varying systems, including communications, controls, signal processing, video processing, and image processing (TheMathWorks, 2011).

Torque: Torque is a measure of how much force acting on an object causes that object to rotate. A torque is represented by x, and is a vector that measures the tendency of a force to rotate an object about some axis (Serway & Jewett, 2003).

CHAPTER II

REVIEW OF LITERATURE

Although there has been increasing research on hybrid electric vehicles, it is still relatively new technology, and literature on simulating the hybrid electric vehicle is somewhat limited in scope. Work on the fuel efficiency and emission aspects of heavy-duty hybrid vehicles has been even more limited, and as such, even less existing work is available for study. This section is intended to provide a brief review of work being performed on hybrid electric vehicles in general and off-highway hybrid vehicles in particular, both on the whole vehicle concepts and individual component designs. This review of literature has been divided into five categories: (a) the history of hybrid vehicles; (b) hybrid vehicle drivetrain configurations; (c) previous work; and (d) the benefits of hybrid electric vehicles to humanity.

The History of Hybrid Vehicles

In the early days, electrical motor engineering was more advanced than internal combustion engine (ICE) engineering. Electric cars were more expensive than gasoline cars. Electric vehicles were considered more reliable, safer, and more convenient. Despite its many advantages, the limited range of the electric car was a big disappointment. As Fuhs (2009) wrote, "Moreover, the inconvenience of recharging and the long recharge times reduced its appeal" (p. 4). Engineers recognized that the good features of gasoline engines could be combined with the good features of electric motors to produce a superior car: "The purpose of hybrids was basically to improve the handicaps of the single propulsion systems" (Tóth-Nagy, 2000, p. 6). The gasoline engine has the

favorable range capability, while the electric car offers quiet comfort and ease of control. A combination of the two yields the hybrid vehicle, with better performance and reliability. Starting ICE vehicles was a big problem, whereas, hybrid vehicles could be started with the simple motion of pushing a button; this was a major advantage (Fuhs, 2009).

Hybrid vehicle technology may seem like new technology, but in fact, it has been around for more than a century. Some researchers agree: "Surprisingly, the concept of a hybrid electric vehicle is almost as old as the automobile itself" (Ehsani, Gao, Gay, & Emadi 2010, p. 14).

The first hybrid vehicles were introduced at the Paris Salon of 1899 (Wakefield, 2008). Ehsani et al. (2010) wrote,

> These vehicles were built by the Pieper establishments of Liège, Belgium and by the Vendovelli and Priestly Electric Carriage Company, France. The Pieper vehicle was a parallel hybrid with a small air-cooled gasoline engine assisted by an electric motor and lead–acid batteries. It is reported that the batteries were charged by the engine when the vehicle coasted or was at a standstill. When the driving power required was greater than the engine rating, the electric motor provided additional power. (p. 14)

The other hybrid vehicle reported at the Paris Salon of 1899 was the first series hybrid electric vehicle. It was derived from a pure electric vehicle and was commercially built by the French firm, Vendovelli and Priestly (Husain, 2005). Ehsani et al. (2010) continue:

> This vehicle was a tricycle, with the two rear wheels powered by independent electric motors. An additional 3/4 hp gasoline engine coupled to a 1.1 kW generator was mounted on a trailer and could be towed behind the vehicle to extend its range by recharging the batteries. (p. 15)

Table 1

Early Hybrids in Europe and United States Early Hybrid Vehicles

Manufacturer or Engineer	Country	Year
Pieper	France	1898[a]
Vendovelli & Priestly	France	1899[a]
Jenatzy	Belgian	1901[a]
Krieger	France	1902
Lohner-Porsche	Germany	1903
Auto-Mixie	Germany	1906
Mercedes-Mixie	Germany	1907
Pope	United States	1902[b]
Baker	United States	1917
Woods	United States	1917

[a] Concept vehicle for Paris Automobile Salon; [b] Prototype caught fire and burned on the first test run.

As shown on Table 1, many other parallel and series hybrid vehicles were built during a period ranging from 1899 to 1917. With the development of the starter motor for the gasoline engine, and their improved range, the public's interest turned from electric vehicles to gasoline engine vehicles after 1913. In the same year, Henry Ford set up an assembly line, taking only ninety-three minutes to assemble the famous T Model (The Library of Congress, 2007). Hybrid vehicles could no longer compete with the greatly improved gasoline engines developed after World War I. Ehsani et al. (2010) state, "The gasoline engine made tremendous improvements in terms of power density, the engines became smaller and more efficient, and there was no longer a need to assist them with electric motors" (p. 15). Moreover, early hybrid designs had to cope with the difficulty of controlling the electric machine. The technology of power electronics did not become

available until the mid-1960s, and early electric motors were controlled by mechanical switches and resistors. They had a short operating range, which meant inefficient operation. It was very hard to make them compatible with the operation of a hybrid vehicle because of the technology available at that time. Although engineers never stopped designing electric and hybrid vehicles, the lack of advanced batteries, efficient control, and cheap gasoline prices pushed electric and hybrid electric vehicle development into the background until late 60s (Tóth-Nagy, 2000).

Interest in hybrid vehicle started again with the Arab oil embargoes and gasoline shortages during the 1973. The U.S. Department of Energy ran tests on many electric and hybrid vehicles produced by various manufacturers, including a hybrid known as the "VW Taxi," produced by Volkswagen in Wolfsburg, West Germany. This parallel hybrid vehicle, despite logging over 13,000 km in test drives, and being shown in many automotive industry shows, never reached production. In 1976, U.S. Congress enacted Public Law 94-413, the Electric and Hybrid Vehicle Research, Development, and Demonstration Act of 1976, which objectives were to work with industry to improve batteries, motors, controllers, and other hybrid-electric components (History of Hybrid Vehicles, 2006).

Despite the two oil crises of 1973 and 1977, growing environmental concerns, and efforts done by the U.S. government, no hybrid electric vehicle made it to the market for years. The lack of interest in hybrid electric vehicles during this period may be attributed to advances in ICE technology and the lack of practical power electronics, modern electric motors, and battery technologies. The 1980s witnessed a reduction in

conventional ICE-powered vehicle sizes, the introduction of catalytic converters, and the generalization of fuel injection (Ehsani et al., 2010).

Decreasing fossil fuel resources and increasing environmental concerns breathed life into hybrid electric vehicles in the 1990s. The most significant effort in the development and commercialization of hybrid electric vehicles was made by Toyota and Honda. In 1997, Toyota released the Prius sedan in Japan. Honda also released its Insight and Civic Hybrid. They both have achieved significant improvement in fuel consumption: "Toyota Prius and Honda Insight vehicles have a historical value in that they are the first hybrid vehicles commercialized in the modern era to respond to the problem of personal vehicle fuel consumption" (Ehsani et al., 2010, p. 17).

Hybrid Vehicle Drivetrain Configurations

Definition of Hybrid Vehicle

As the technology is still in the development stage, the terminology used by the industry is sometimes unclear and confusing. The International Electrotechnical Commission (IEC) proposed the following definition for HVs: "A hybrid road vehicle is one in which propulsion energy, during specified operational missions, is available from two or more kinds or types of energy stores, sources, or converters. At least one store or converter must be on-board" (Husain, 2005, p. 4). More specifically, a sub-category of hybrid electric vehicle (HEV) is defined as: "A hybrid electric vehicle is a hybrid vehicle in which at least one of the energy stores, sources, or converter can deliver electric energy" (Chau & Chan, 2001, p. 49). The latter HEV term is commonly used to describe any hybrid vehicle. The first definition for HV may be used instead of term "HEV," since

the term "electric" is largely redundant. Unless the hybrid consists of two fuels combusted separately in the same vehicle, there will inevitably be one or more electrical motor (EMs) in the powertrain (Wishart, 2009).

HEV Configurations

Fuel consumption can be reduced without sacrificing performance through proper design of the powertrain components and well-designed power management strategies. Based on their area of use, different vehicles have different speed and torque requirements; for example, transportation buses, military vehicles, and automobiles may require different speed-torque drive characteristics (Fang & Qin, 2006). Hence, different configurations of HEVs are developed for various vehicular applications (Hou & Guo, 2008). One of the most common ways to classify a HEV is based on drivetrain configuration. Conventionally, HEVs are classified into two basic types: series and parallel (Ehsani et al., 2010); however, with improvements in vehicle technologies, some new HEVs are designed using combinations of these two basic concepts, extending the classification. HEVs, then, are presently classified into four kinds: series hybrid, parallel hybrid, series–parallel hybrid, and complex Hybrid (Husain, 2005).

Series HVs

IEC defines the series hybrid electric vehicle as "an HEV in which only one energy converter can provide propulsion power" (Wouk , 1995, p. 17). Although it is very similar to IEC's definition, the definition from Ehsani at al. (2010) is comprehensible: "A series hybrid drive train is a drive train in which two electrical power sources feed a single electrical power plant (electric motor) that propels the vehicle" (p.

128). Since there is no direct mechanical connection between the ICE and the wheels, it has the simplest control structure. All the propulsion power comes from the EM, while the ICE is used to charge the battery to power the EM or its battery.

In this configuration, as shown in Figure 1, the ICE is used to generate electricity in a generator. Generated electricity needs to be processed by the power electronics components to feed the battery and the electric motor with appropriate electric energy mode, in terms of waveform, voltage, current, and phasing. Energy regulated by the power electronics components goes to either the motor or the battery bank. The hybrid power is then combined at the motor.

Figure 1 shows that the series HEV has only two draft shafts. These are not connected, so the engine can run at optimum speed, torque, and throttle setting to give minimum fuel consumption. Moreover, being able to control the operating point of the engine enables the vehicle to minimize emissions. Since the engine and the generator are not connected together electromechanically, they are considered individually in the design process when it comes to locating them in the drivetrain.

As well as its advantages, as shown in the series configuration in Figure 1, the series has some disadvantages. The generator, an essential component of the series configuration, is very heavy (Fuhs, 2009). A double energy conversion principle takes place in the series hybrid vehicle drivetrain as follows:

Gas engine → Electrical generator →Electrical motor →Differential gear

As seen in Figure 1; first, mechanical energy is converted to electrical energy via the generator. Then electrical energy is converted to mechanical energy via the electrical motor. Each conversion results in some energy loss.

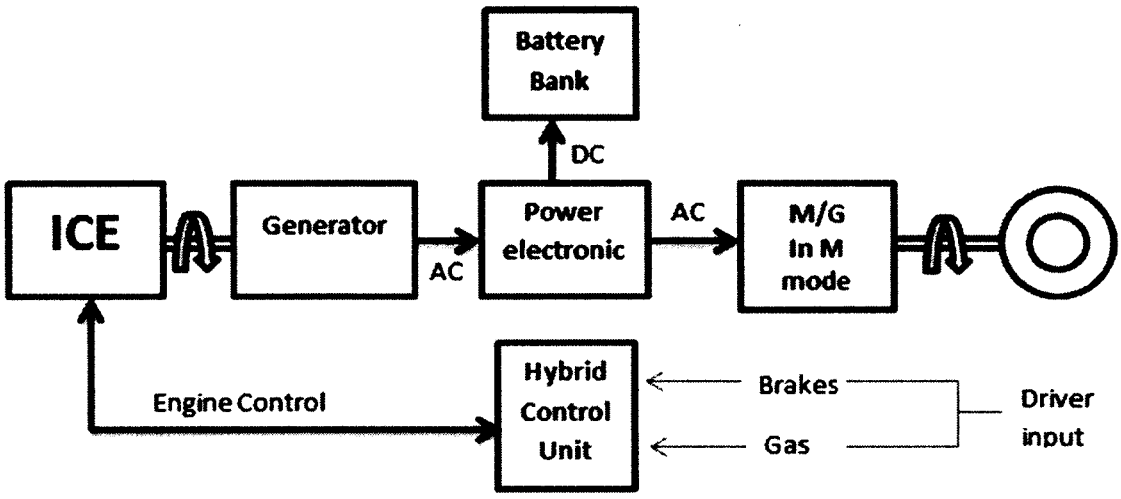

Figure 1. Configuration of a series HEV drivetrain in normal cruise operation.

As shown in Figures 1 through 4, the series hybrid has four different running modes:

1. Normal cruise mode: Vehicle uses power from the engine. The generator can deliver the required power at different rpm so the engine can run on its optimum operating point for minimum fuel consumption; as seen in Figure 1.
2. Acceleration mode: Both the generator and the battery work to supply high power demand (acceleration, going uphill, etc.); as seen in Figure 2.

3. Regenerative braking mode: Hybrid vehicles have the ability to recapture some of the energy used to accelerate the vehicle during braking. In this mode, the electrical motor, coupled with the wheels, work as a generator; as seen in Figure 3.
4. Battery charging mode: In this mode, the generator feeds the electrical motor as well as the battery; as seen in Figure 4.

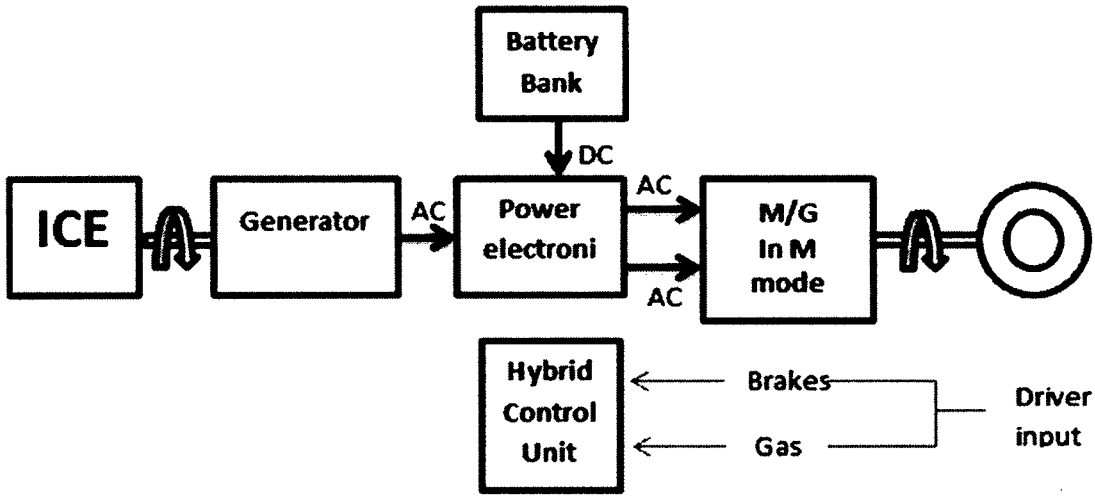

Figure 2. Configuration of a series HEV drivetrain in acceleration mode.

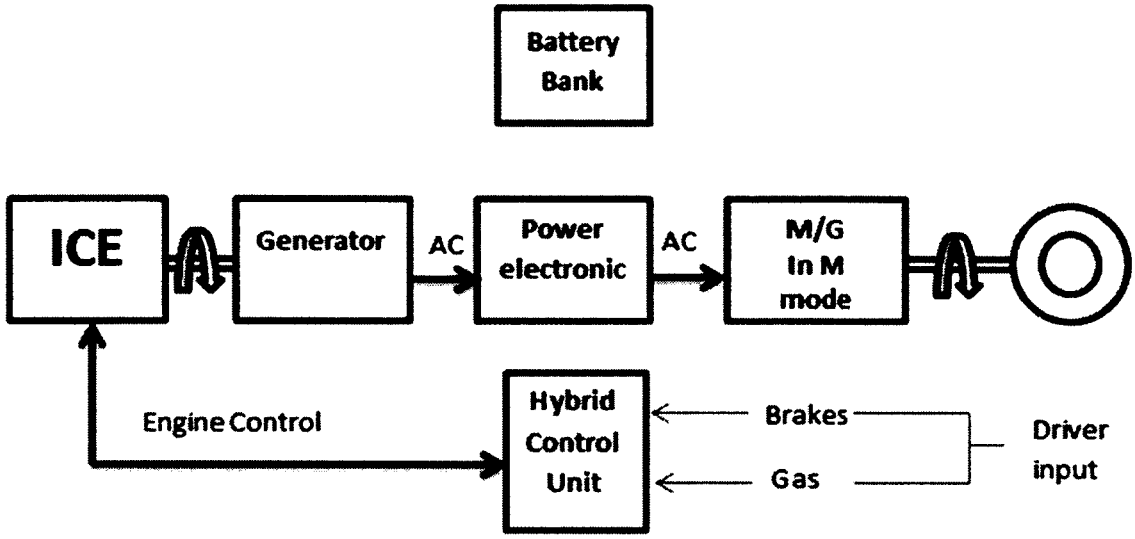

Figure 3. Configuration of a series HEV drivetrain in regenerative braking mode.

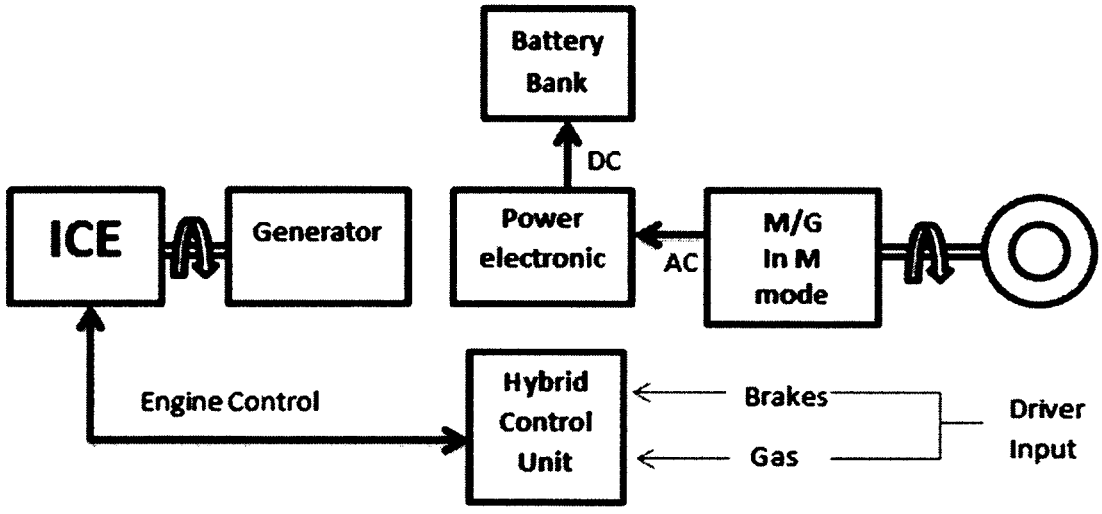

Figure 4. Configuration of a series HEV drivetrain in battery charging mode.

Parallel HEVs

A parallel hybrid is an HEV in which more than one energy converter can provide propulsion power (Wouk, 1995). In parallel configurations, both the engine and the motor, coupled with drive shaft, provide traction power to the wheels via a three-way gear box. Thus, both the engine and the motors can be downsized, making the parallel configuration more viable with lower costs and higher efficiency (Chau & Chan, 2001).

Figures 5 through 8 show a parallel hybrid has four different running modes:

1. Normal cruise mode: The engine is the only torque provider in normal cruise mode. A hybrid controlled unit determines the best gear ratio for optimum performance and fuel efficiency; as seen in Figure 5.
2. Acceleration mode: Both the engine and the motor clutch are engaged with a three-way gear box to supply high torque demand (Acceleration, going uphill, etc.); as seen in Figure 6.
3. Regenerative braking mode: This is the reverse version of the electric-only mode. The electric motor, coupled with a three-way gear box, works as a generator and feeds the battery with electric power; as seen in Figure 7.
4. Electric only mode: It is the best operation mode for achieving good fuel efficiency and mpg. In this mode, the engine is not running and all power is supplied by a battery pack; as seen in Figure 8.

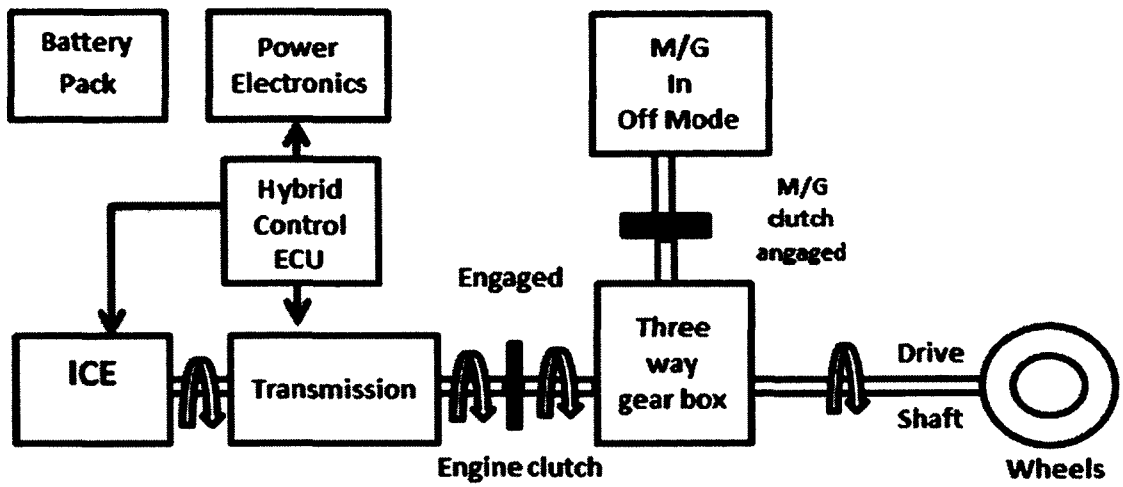

Figure 5. Configuration of a parallel HEV drivetrain in normal cruise operation.

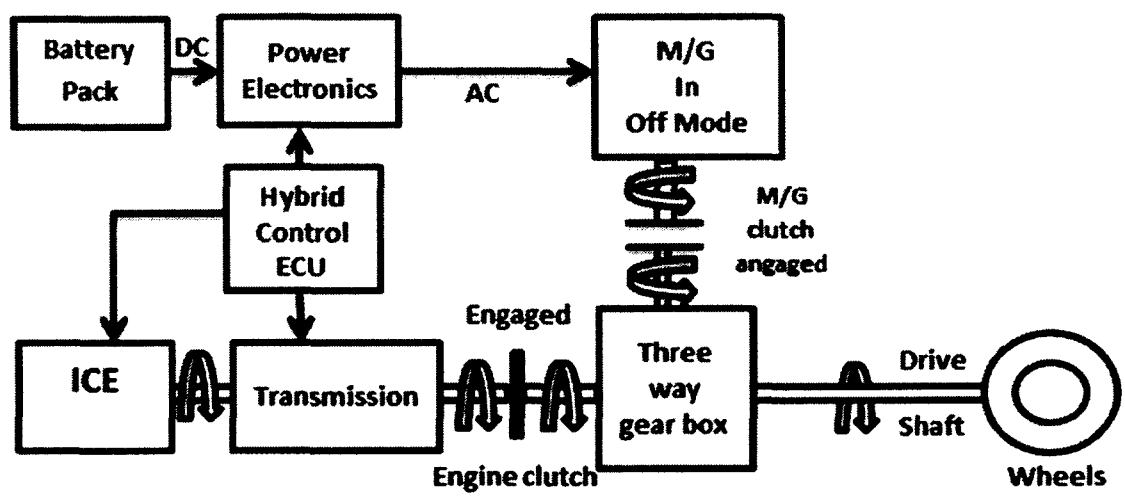

Figure 6. Configuration of a parallel HEV drivetrain in acceleration mode.

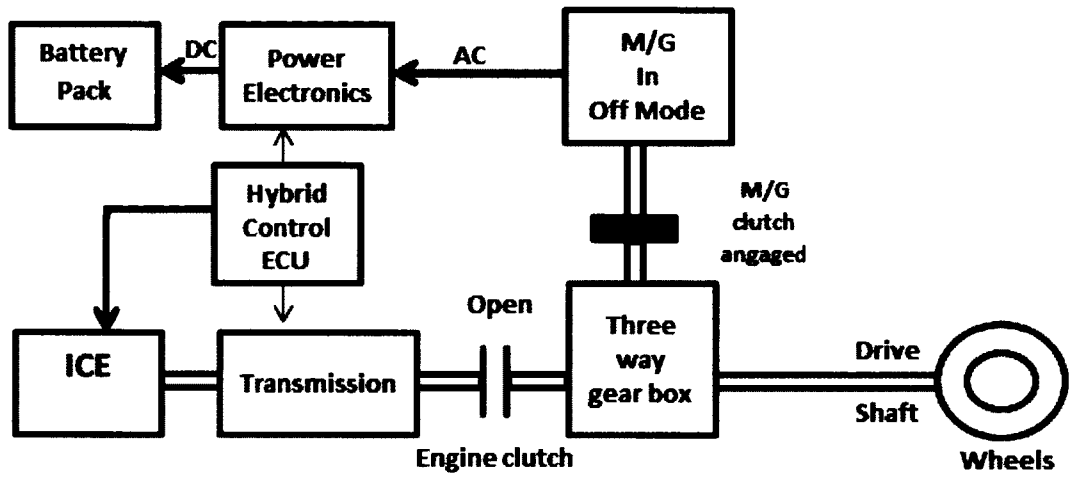

Figure 7. Configuration of a series HEV drivetrain in regenerative braking mode.

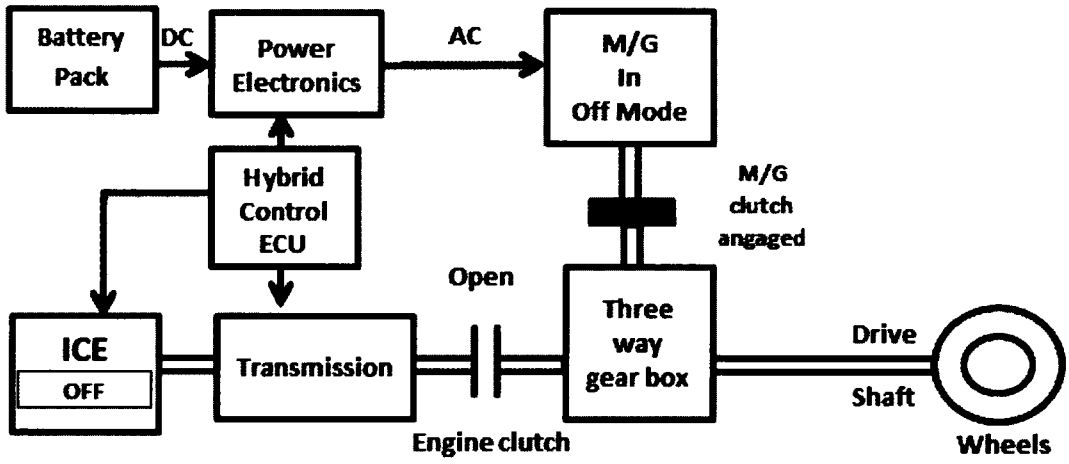

Figure 8. Configuration of a series HEV drivetrain electric only mode.

Series-Parallel HVs

Despite their many advantages, parallel and series hybrid configurations have some disadvantages. Fuhs (2009) writes, "Series only or parallel only designs often do not meet performance requirements" (p. 81). Husain (2005) adds, "Although HEVs initially evolved as series or parallel, manufacturers later realized the advantages of a combination of the series and parallel configurations for practical road vehicles" (p. 634), and finally, "Mixed designs, rather than series or parallel designs, offer more flexibility" (Fuhs, 2009, p. 81).

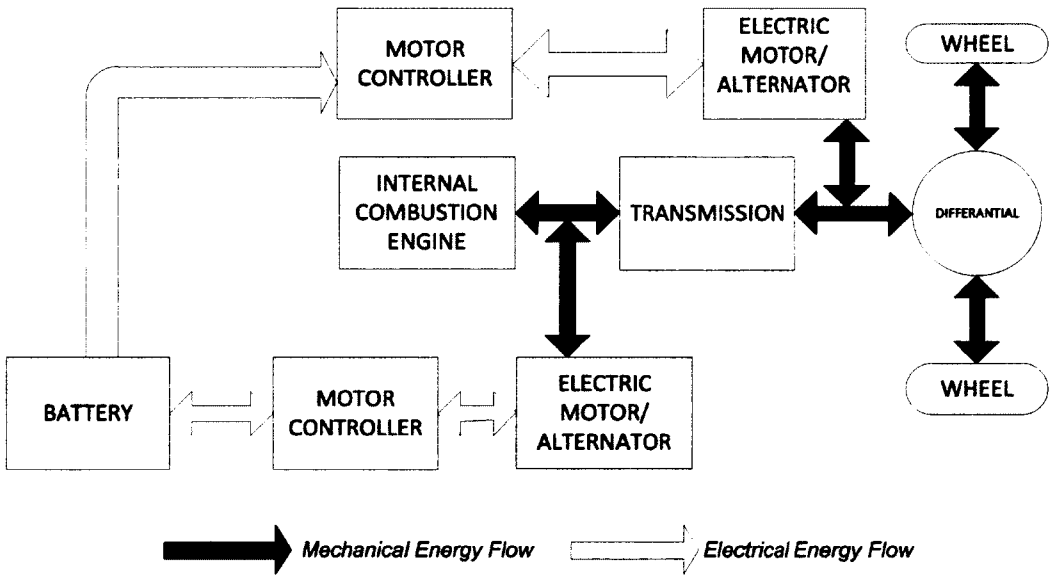

Figure 9. Power Flow Diagram for the Series-Parallel HEV.

With mixed configuration hybrid vehicles, depending on driving conditions, the various modes can be selected to use the most advantageous individual mode (Tóth-Nagy, 2000). That means that an ICE either can directly supply torque to the wheels via a transmission, as is conventional.

Selecting a hybrid design configuration—series, parallel, or mixed—depends on driving cycle (freeway, highway, urban) and the vehicle`s function (car, bus, truck, off-highway). As seen in Figure 9, the series-parallel hybrid offers all operation modes that the parallel and the series hybrid designs offer. The series-parallel hybrid module provides high performance by utilizing both electric motor and combustible engines together, similar to a parallel hybrid design. It also offers high fuel efficiency during normal cruise mode.

Benefits of Hybrid Electric Vehicles

Optimize Fuel Economy

Hybrid vehicles increase fuel efficiency by optimizing the operating point of ICE, reducing the ICE`s size, stopping the ICE if it is not needed, and recovering kinetic energy at braking. Improving engine operation efficiency contributes to improving the vehicle`s fuel economy (Ehsani et al., 2010). Hybrid vehicles increase fuel efficiency by operating the internal combustion engine at a much higher efficiency. Conventional vehicle engines are sized to meet the vehicle`s peak power demand, which means that the rest of the time they run at a fraction of their potential power output:

> Hybridization allows the engine to be downsized, because the electric motor can augment the peak power requirements under various driving conditions while the

> engine works to meet the average power requirements. This allows the engine to run much closer to its peak power output potential. (Kellermeyer III, 1998, p. 2)

All types of HEVs can make more efficient use of fuel because hybridization permits not only the use of smaller engines operating more efficiently, but also partial recovery of vehicle's kinetic energy when the vehicle decelerates or goes downhill. In addition, plug-in HEVs permit substituting electricity as propulsion "fuel" for part of the fuel (Sanna, 2005).

Reduce Emissions

Hybrid vehicles are mostly developed to reduce fuel consumption, but they can also provide other advantages, including reducing pollutant emissions due to the higher flexibility in controlling engine operations in comparison to conventional vehicles (Lorenzo, 2009).

According to a report titled, *Comparing the Benefits and Impacts of Hybrid Electric Vehicle Options*, published by EPRI (2006) "HEV designs offer major efficiency improvements and reductions in the consumption of petroleum-based fuels, as well as substantial reductions in the emissions of air pollution precursors (nitrogen oxides and reactive organic gases) and of carbon dioxide" (p. X). Emission reduction depends on the design of the hybrid vehicle; the same study shows that "emissions decrease with increasing degree of hybridization" (Electric Power Research Institute [EPRI], 2001, p. 2.7).

For example, while the HEV 0 (HEV with 0-mile, all-electric range) can reduce smog precursor emissions by up to 15%, and petroleum consumption and CO_2 emissions by 25% in representative driving, when compared to conventional vehicles (CV), the

HEV 60 (HEV with 60-mile, all-electric range), fully charged every night, can reduce emissions, energy use, and CO_2 emissions by 50%, and petroleum consumption by over 75%; as seen in Figure 10.

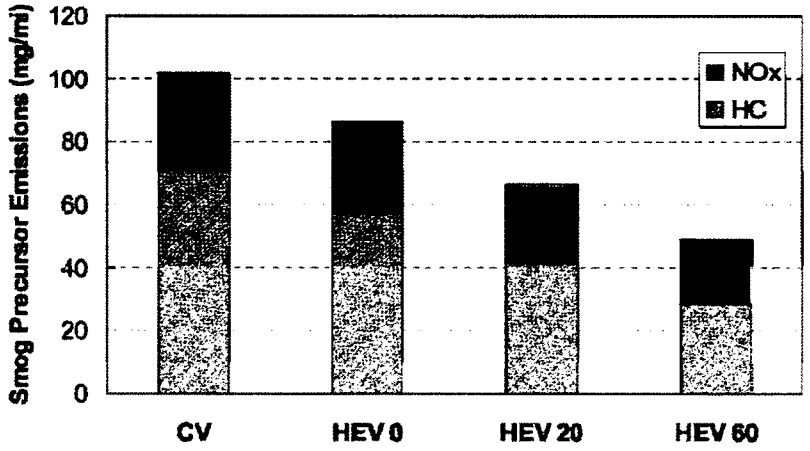

Figure 10. Emissions for different all-electric range Mid-Size Cars (EPRI, 2001)

Quiet Operation

Hybrid vehicles are quieter than conventional vehicles (CV). First, hybrid vehicles use a smaller engine, which means less noise. Second, hybrid vehicles use an advanced control system, which eliminates unnecessary use of engine and motor operations, thereby reducing noise. According to Mi (2004), "There is no noise at low speed because the ICE is stopped" (p. 6). The motor module is stopped when the vehicle comes to a stop.

CHAPTER III

METHODOLOGY

Overview of Approach

In order to simulate a dual-engine hybrid vehicle powertrain that meets the performance, efficiency, and cost constraints, the following methodology was used:

- Component models for engine, generator, motor, and AC/DC converters were developed;
- Models were validated by means of published lab tests that have been completed in the literature and manufacturer's datasheet for actual components;
- Powertrain energy management strategy was established;
- Total powertrain system was simulated using developed component models and the proposed energy management system;
- Necessary changes in component models and the energy management strategy was based on the simulation results to find optimum configuration and energy management strategy in terms of performance, fuel economy, and cost; and
- Simulation results were compared with actual vehicles on the market to see if the dual-engine powertrain model is a viable option for heavy-duty vehicles.

In this study, and as shown in Figure 11, developing and verifying of the dual-engine HEV simulation process is divided into four major phases. Phase 1 includes the research conducted on HEV components and control systems. Phase 2 briefly describes the overall design process of a HEV, including a description of component selection and

sizing. HEV component models were designed using the MATLAB®/Simulink® software package. Phase 3, the main the part of the dissertation, presents the vehicle control system development for the methodology. The HEV energy management system was designed using National Instruments` LabView™ software package. Phase 4 presents the validation of the software model by comparing experimental testing in the literature for the HEV model developed in this study with the manufacturer's datasheet.

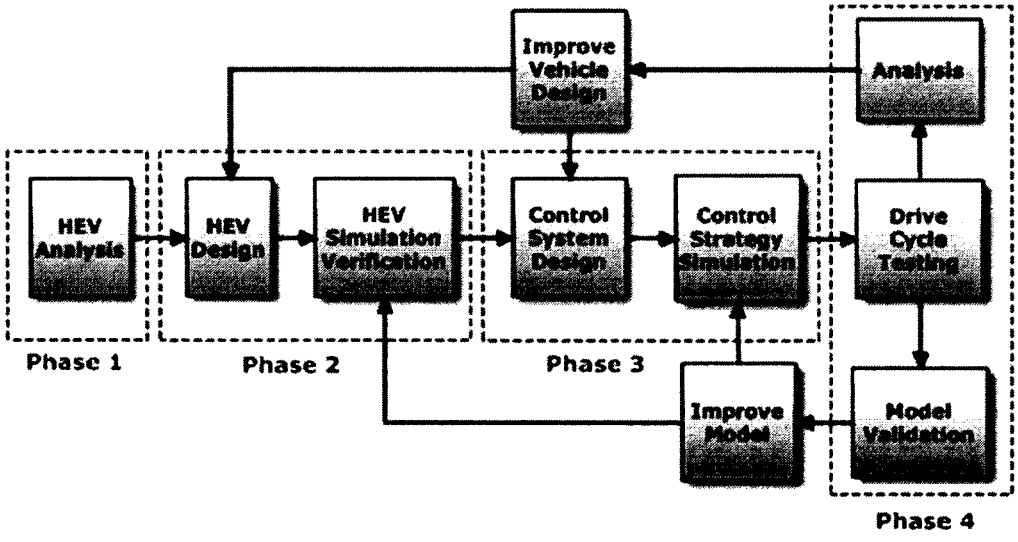

Figure 11. Flowchart of the Phases of the study.

Approach to Modeling HEVs

Hybrid vehicle models can be classified as forward-looking models or backward-facing models (Emadi, Mi, & Gao, 2007).

Backward-Looking Approach

A backward-looking approach answers the question: "Assuming the vehicle met the required trace, how much does each component perform?" There is no need to model driver behavior in such models. Instead, the force required to accelerate the vehicle with respect to time step can be calculated directly from the proposed speed trace, based on driving cycle. Then, calculated force is translated into a torque, taking efficiency into account. In the same way, the vehicle's linear speed is needed to be translated into a required rotational speed. As shown in Figure 12, this process needs to be carried out backwards through the drivetrain; in other words, against the tractive power-flow direction, and measured component by component to calculate fuel or electrical energy use necessary to meet the trace in the driving cycle.

If components used in the model are tested beforehand, and efficiency maps for components are already known, using the backward-looking approach is more convenient: "This means that a straightforward calculation can determine a component's efficiency and allow the calculation to progress. The explicit nature of the efficiency/loss calculation also allows very simple integration routines to be used with relatively large time" (Wipke, Cuddy, & Burch, 1999, p. 1752). Therefore, simulations that use the backward-looking approach tend to run faster than in the forward-looking approach.

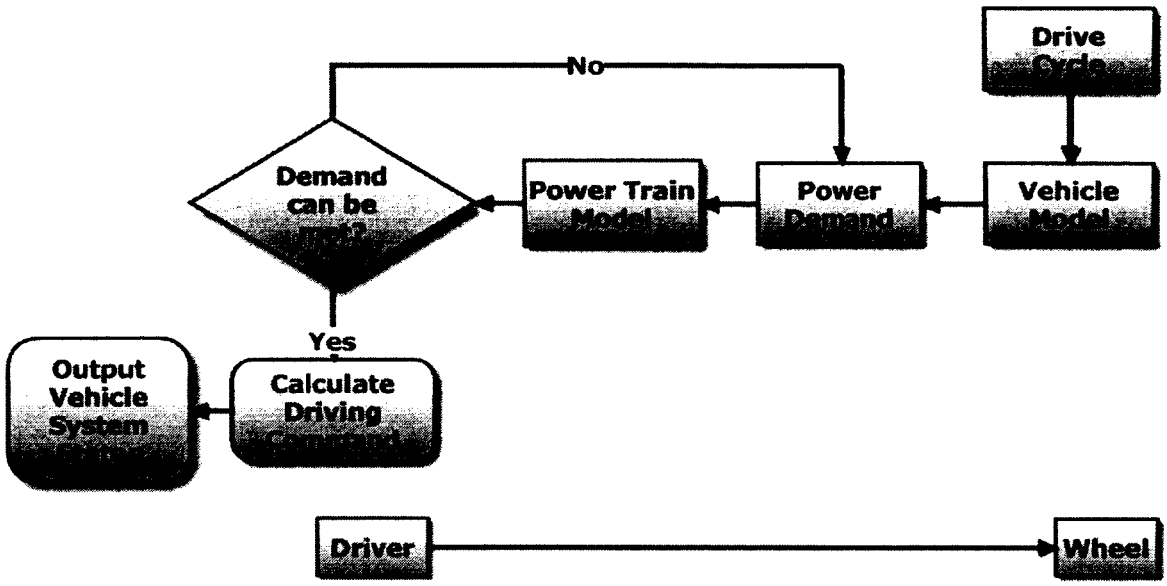

Figure 12. Schematic representation of backward-looking structure model (Wishart, 2008).

Maps of use of efficiency or loss assume that the trace for drive cycle is met, bringing a disadvantage aside from the aforementioned advantage. Wipke et al. (1999) wrote that, "Because the backward-facing approach assumes that the trace is met, this approach is not well suited for computing best-effort performance, such as occurs when the accelerations of the speed trace exceed the capabilities of the drivetrain" (p. 1752). Since efficiency maps are typically created by steady-state testing, dynamic effects are not included in the maps or in the backward-looking model's estimation of energy use.

Forward-Looking Approach

As shown in Figure 13, models that use a forward-looking approach contain a driver model, which considers the required and the existing speed to create correct

throttle and brake commands (Wipke et al., 1999). After that, the throttle command is rendered into a torque supplied by the engine (and/or motor) and an energy usage rate. The transmission model receives torque provided by the engine as an input, and transforms it according to the transmission's efficiency and gear ratio. Wipke et al. described, "In turn, the computed torque is passed forward through the drivetrain, in the direction of the physical power flow in the vehicle, until it results in a tractive force at the tire/road interface" (p. 1752).

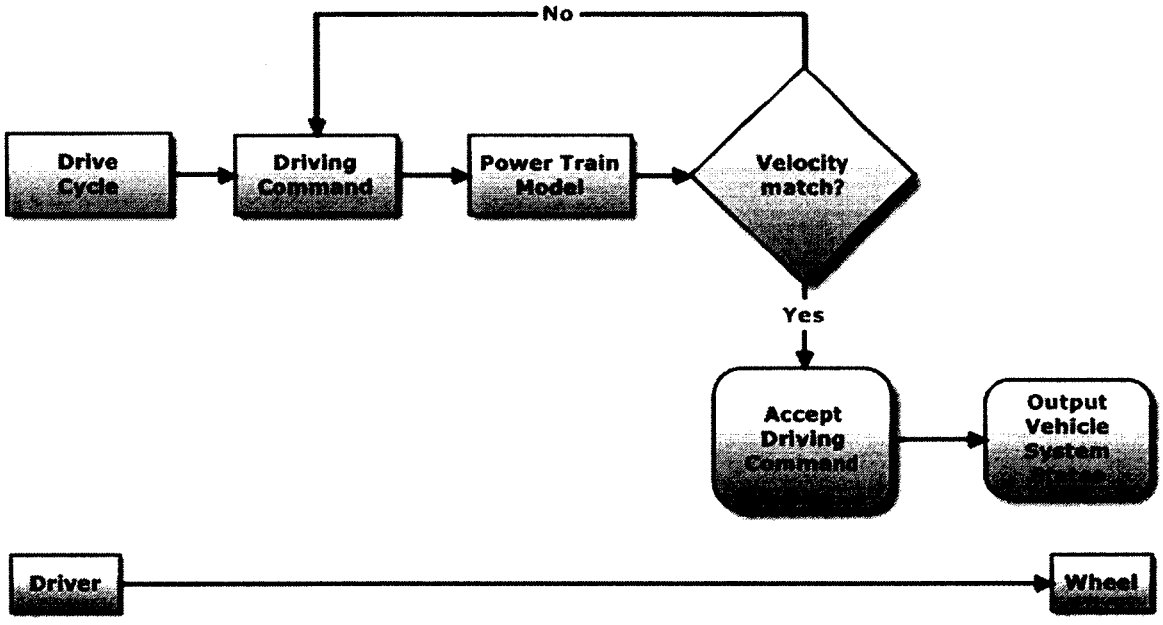

Figure 13. Schematic representation of forward-looking structure model (Wishart, 2008).

The forward-looking approach has some advantages over the backward-looking approach. McBroom (1997) stated, "The forward-looking technique allows development of realistic control algorithms" (p.13). The forward-looking approach is particularly appropriate for hardware development and detailed hybrid vehicle simulations. Because forward-facing models deal in measurable quantities in a physical drivetrain, vehicle controllers can be developed and effectively tested in simulations. Another advantage is that dynamic models can be used in vehicle models that also use a forward-looking approach.

The forward-looking approach is slower than the backward-looking approach. According to some researchers, "Drivetrain power calculations rely on the vehicle states, including drivetrain component speeds that are computed by integration. Therefore, higher order integration schemes using relatively small time steps are necessary to provide stable and accurate simulation results" (Wipke et al., 1999, p. 1752).

Dual-Engine Hybrid Vehicle Design

The proposed dual-engine hybrid vehicle model architecture is shown in Figure 14. It is characterized by the use of two engines, two generators coupled with the engines, a battery bank as an energy storage device, and the presence of two electric motors. In this design, the engines do not have direct mechanical connections with wheels. Rather, the engines drive generators mechanically. Generators feed the electric bus. After necessary AC/DC conversions, traction motors are powered by the electric bus. Required torque is transferred to the wheels from the traction motor via the gearing mechanism.

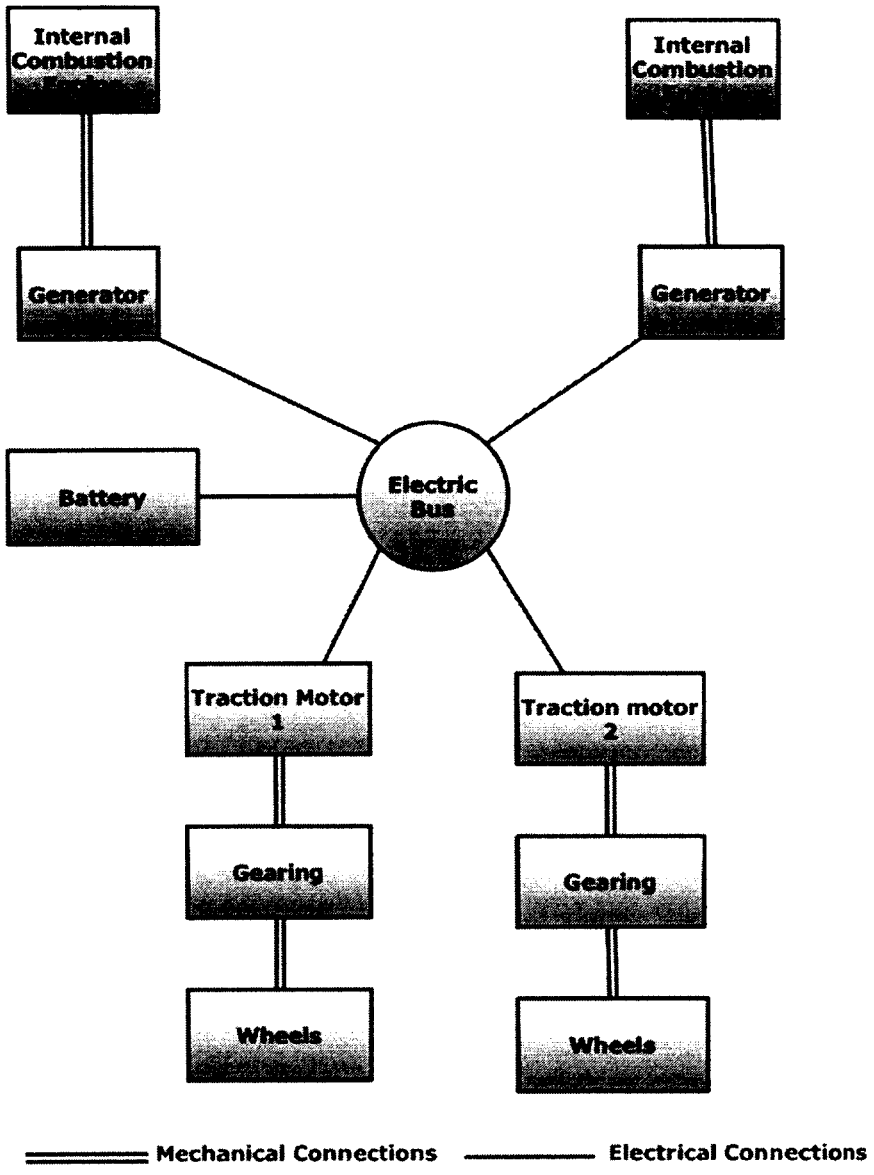

Figure 14. Dual-engine hybrid vehicle model architecture.

Input-output relation between components for the proposed dual-engine hybrid vehicle architecture is shown in Figure 15.

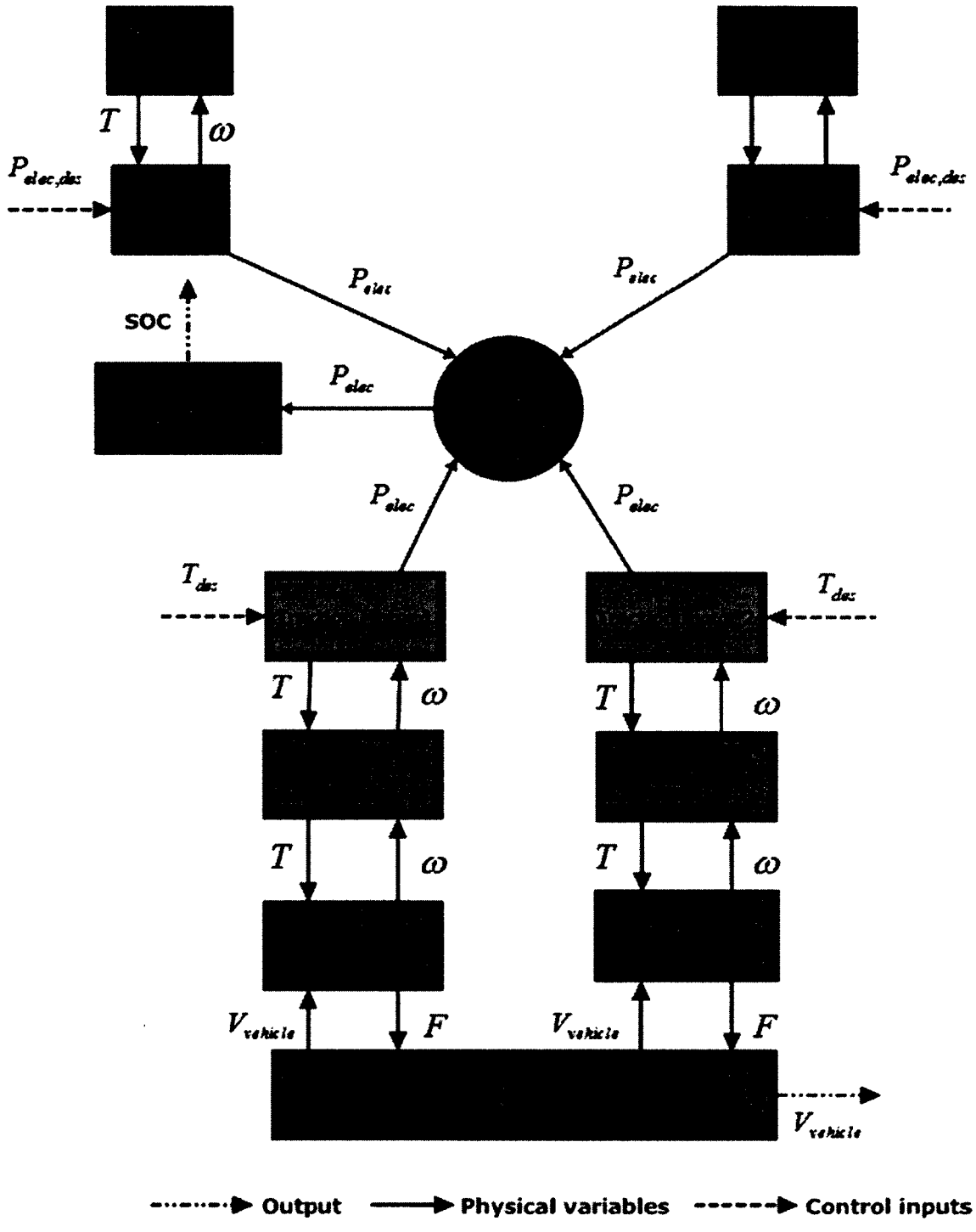

Figure 15. Component input and output modules.

Vehicle Simulation Tools

Modeling and simulation play an important role in the analysis of HEV designs (Gao & Musunuri, 2006). There are many available modeling and hybrid vehicle analysis tools, such as PSAT, ADVISOR, and Saber®. Also, major automotive companies typically have their own hybrid vehicle modeling, simulation, and analysis tools. Most of these existing tools are developed in the MATLAB®/Simulink® environment. They can be used to analyze fuel economy, performance, or emissions of an HEV design.

PSAT

According to the Vehicle Technologies Program (2004), "The Powertrain System Analysis Toolkit (PSAT) is a state-of-the-art flexible and reusable simulation package developed by Argonne National Laboratory (ANL) and sponsored by the U.S. Department of Energy (DOE)" (p. 1). The Argonne National Laboratory (2010) reported that the "PSAT was designed to be a single tool that can be used to meet the requirements of automotive engineering throughout the development process, from modeling to control" (para. 11).

PSAT was created with MATLAB®/Simulink, and is assembled with a graphical user interface (GUI) written in C#, so it is user-friendly (See Figure 16). The large library of component data allows users to simulate light, medium, and heavy-duty vehicles. It uses quasi-steady models and control strategies for propelling, shifting, and braking, which is one of the important features other steady state simulation tools like ADVISOR does not have. According to Emadi et al. (2007) this feature allows PSAT to predict the

fuel economy and performance of a vehicle more accurately, and "Its modeling accuracy has been validated against the Ford P2000 and Toyota Prius" (Emadi et al., 2007, p. 369).

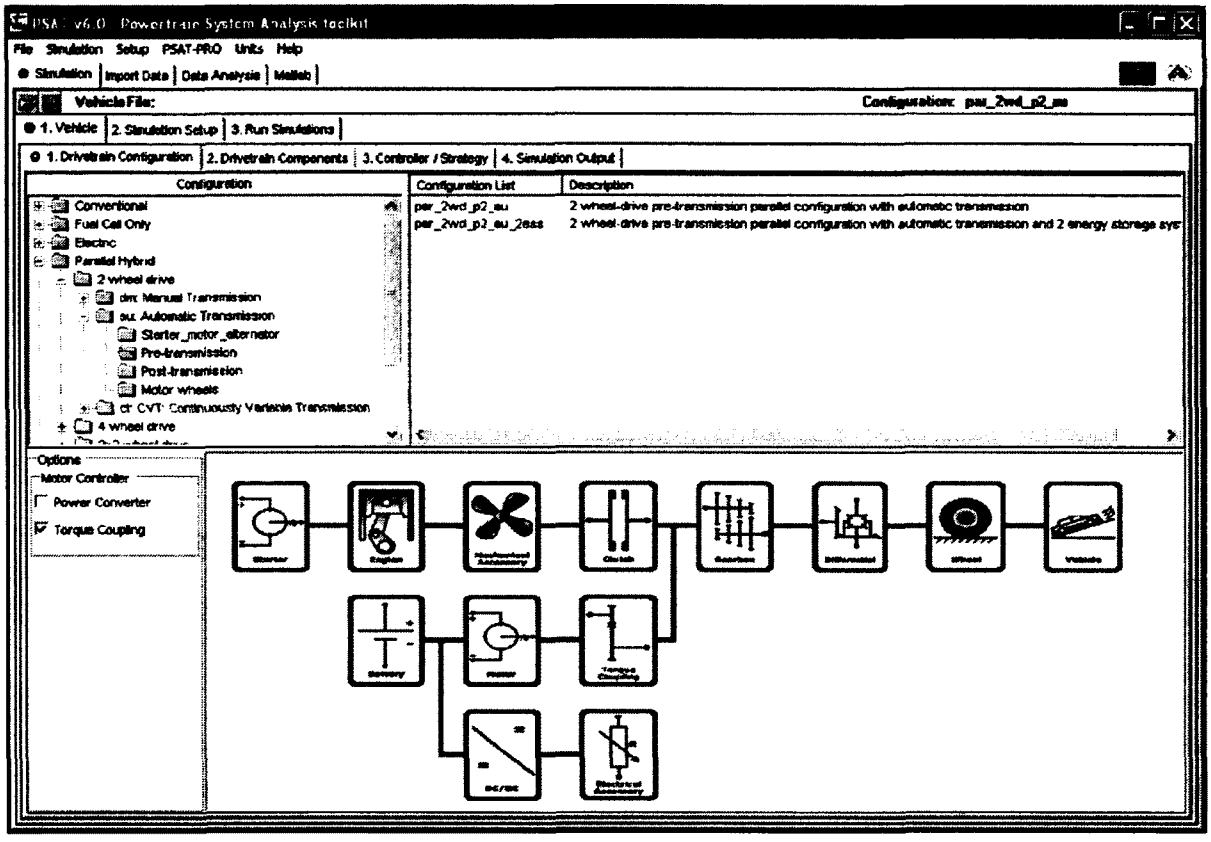

Figure 16. PSAT user interface (Emadi et al., 2007).

MATLAB®/ Simulink®

MATLAB®, developed by MathWorks Inc., is a software package for high-performance numerical computation and visualization (Petinrin, 2010). It is a high-level computing language, providing a user interactive environment for algorithm

development, data visualization, data analysis, and numeric computation. MathWorks described Simulink® as "an interactive environment for modeling, simulating, and analyzing dynamic, multi domain systems. It lets you build a block diagram, simulate the system's behavior, evaluate its performance, and refine the design" (The MathWorks, 2005, p. 3-4).

ADVISOR

ADVISOR (ADvanced VehIcle SimulatOR) was developed in 1994 by the U.S. Department of Energy's National Renewable Energy Laboratory's (NREL) Center for Transportation Technologies and Systems to support the U.S. Department of Energy hybrid propulsion system program (NREL, 2002).

It supports both linear and non-linear systems, and offers a very user-friendly interface, as shown in Figure 17. ADVISOR employs both backward and forward modeling approaches and contains an extensive model library. It uses models for engines, transmissions, electric motors, and fuel cells modules from its own library, and users can customize those models. Speed and torque values are requested for each model as an input, and achieved speed and torque values are passed to the next model as an output. These models also include information on the efficiency of components, which is a value that is constant for simple components. It uses lookup tables for more complex components, such as the electric motor and the engine.

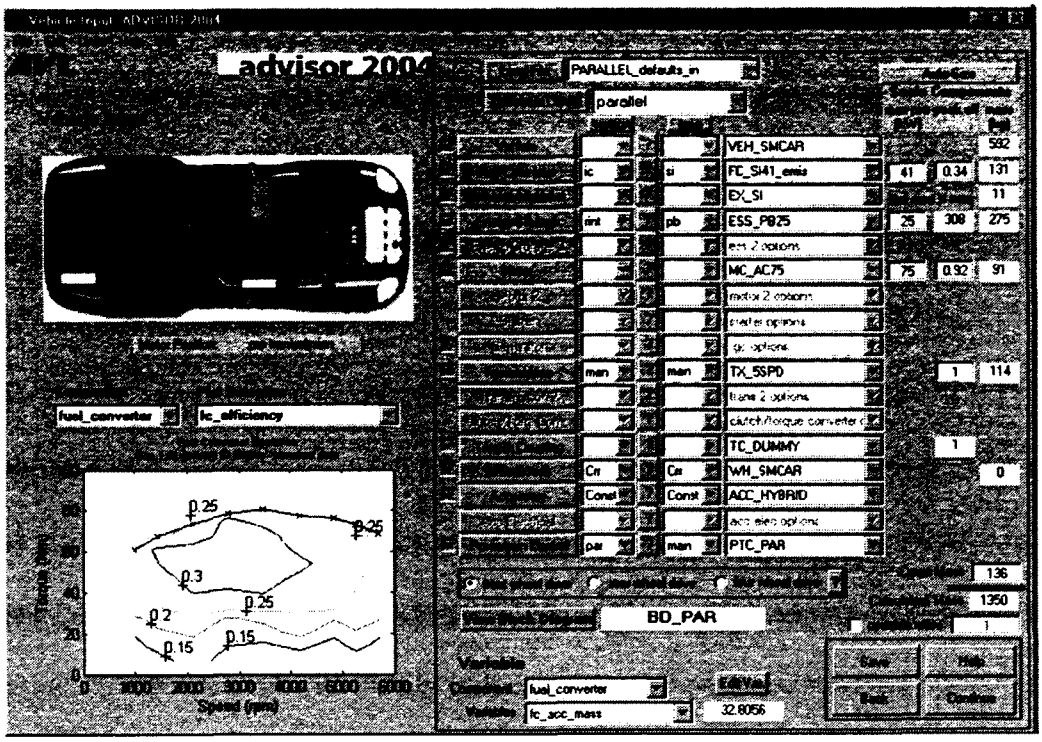

Figure 17. ADVISOR user interface (Markel et al., 2002)

Saber®

Vlach (1990) reported that "The Saber® simulator is a comprehensive simulator spanning analog and digital domains and capable of simulating systems described by a mixture of models at the primitive, functional, and behavioral levels" (p. 1). Saber® has the capability to simulate, analyze, and verify interactions between multiple physical domains such as mechanical, electrical, hydraulic, magnetic, thermal, etc. (Synopsys, Inc., 2006). Saber® software offers the capability to model at different levels of abstraction, from high-level behavioral models down to detailed component levels, using available models developed for automotive use. Saber® uses the analog hardware

description language, MAST. It allows Saber® to separate the modeling and simulation aspects of creating a practical simulation environment. Saber does not restrict users to any single technology. Users can model and simulate anything, as long as it is transformed to an electrical equivalent (Vlach, 1990).

Saber® uses a Robust Design called the Taguchi Method, pioneered by Dr. Genichi Taguchi, to manage complex energy generation and distribution problems (Synopsys, Inc., 2011). According to Jensen (2006):

> Robust design is a general but proven development philosophy focused on improving the reliability of a process or product. Improving reliability requires that Robust Design principles be an early and integral part of the development cycle. The objective is to make the end-product immune to factors that could adversely affect reliability. (p. 1)

LabVIEW™

LabVIEW™, short for Laboratory Virtual Instrument Engineering Workbench, is a programming environment. National Instruments LabVIEW™ is a graphical programming language that has been widely adopted throughout industry, academia, and research labs as the standard for data acquisition and instrument control software (Travis & Kring, 2007). LabVIEW™ is a general purpose programming language used for developing projects graphically. It can also be called an application-specific development environment (ADE). As shown in Figure 18, it is a revolutionary programming language that depicts program code graphically rather than textually (Pogula, 2005). LabVIEW™ departs from the sequential nature of traditional programming languages and features an easy-to-use graphical programming environment, including the tools necessary for data acquisition (DAQ), data analysis, and presenting results (Travis & Kring, 2007).

Engineers and scientists in research, development, production, testing, and service industries as diverse as automotive, semiconductor, aerospace, electronics, chemical, telecommunications, and pharmaceuticals have used, and continue to use, LabVIEW™ to support their work.

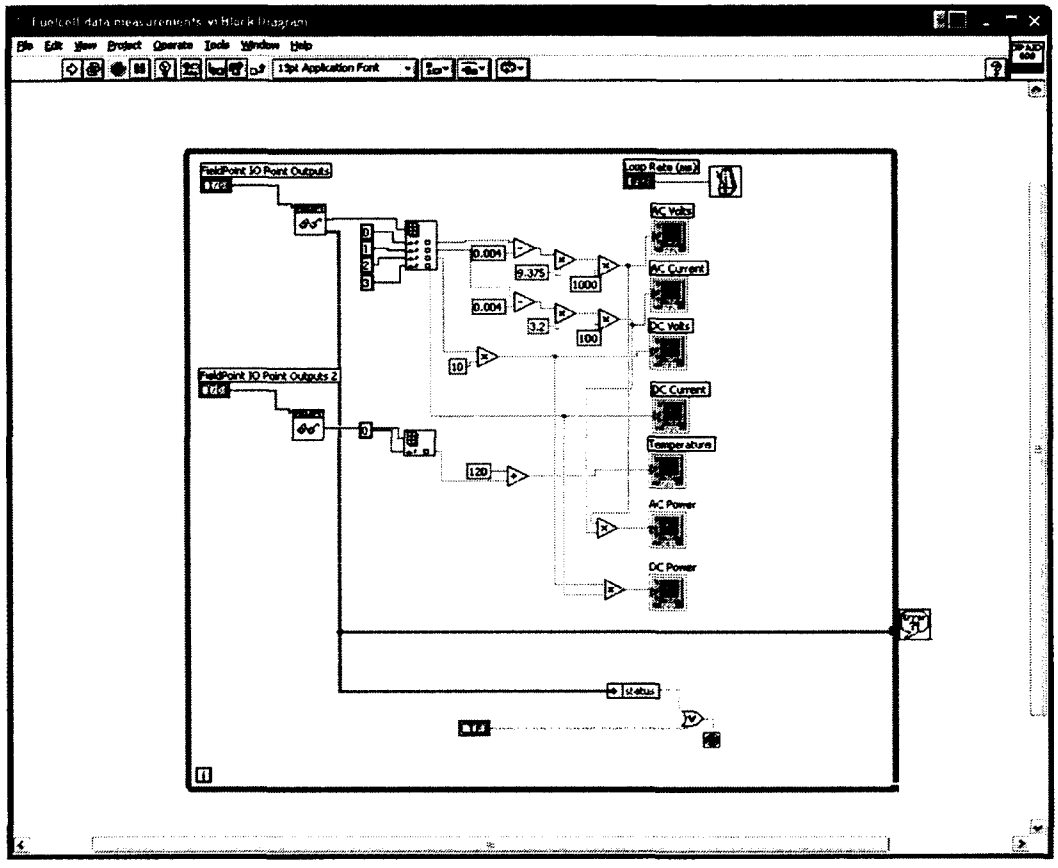

Figure 18. LabVIEW™ graphical programming interface.

LabVIEW™ is a major player in the area of testing and measurement, industrial automation, and data analysis. For example, scientists at NASA's Jet Propulsion

Laboratory used LabVIEW™ to analyze and display engineering data on the Mars Pathfinder Sojourner rover, including the position and temperature of the rover, how much power remained in the rover`s battery, and to generally monitor the Sojourner`s overall health (Yue, 2011). The programs of LabVIEW™ are called virtual instruments (Vis) because their appearance and operation imitate physical instruments, such as oscilloscopes and millimeters. LabVIEW™ contains a comprehensive set of VIs and functions for acquiring, analyzing, displaying, and storing data, as well as tools for troubleshooting code (Travis & Kring, 2007). LabVIEW™ VIs contains three main components: the front panel window, the block diagram, and the icon/connector pane.

VIs include an interactive interface between the user and the software, which is called the front panel, since it stimulates the panel of physical instruments. The front panel can include knobs, push buttons, graphs, and other controls and indicators, as shown in Figure 19. Data is obtained by the front panel using a keyboard and mouse; results can be viewed on the computer screen.

VIs get instructions from a block diagram, which is created in LabVIEW™'s programming language, "G." The block diagram provides an illustrative solution to a programming problem, and graphically represents written code familiar to most programmers (e.g., "while loops"; "for loops"; "if/then cases"; "formula nodes"; etc.). The means whereby front panel items are wired to the rest of the program are also displayed. In other words, the block diagram contains the source code for any given VI (Huff, 1999).

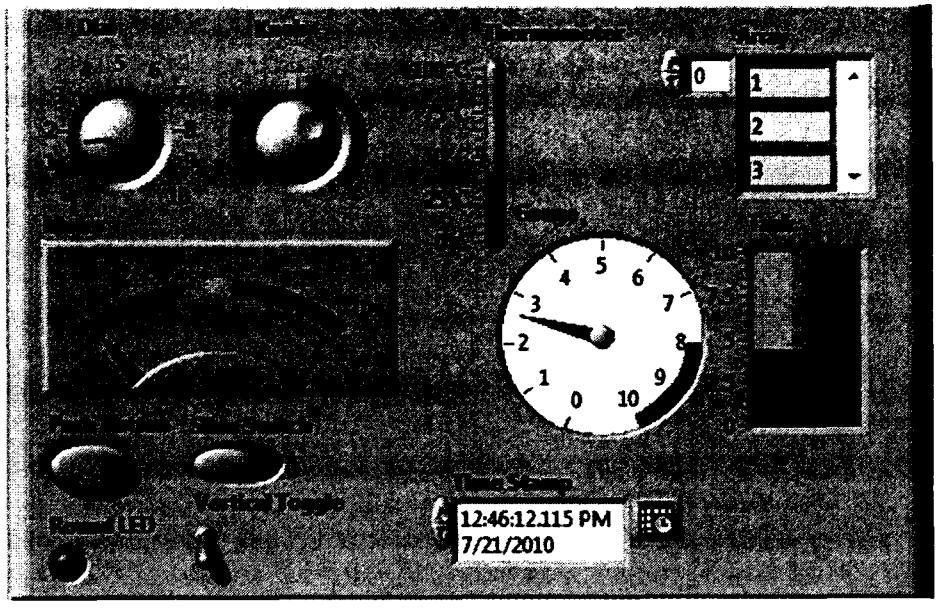

Figure 19. Engineering Controls and Indicators (National Instruments, 2011).

The power of LabVIEW™ lies in the hierarchical and modular nature of the VIs. They can be developed as top-level programs, or as subprograms within other programs or subprograms. When a VI is encapsulated within another VI, it is called a subVI. The icon and connector panel of a VI works like a graphical parameter list, so that other VIs can pass data to it as a subVI. The above descriptions collectively comprise what is known as modular programming (Huff, 1999). Modular programming can be used to break up a large program into manageable units, or to create code that can be easily re-used.

Selection of Vehicle to be Simulated

Verification of developed simulation depends on the validity of component models used in the simulation. The validation process requires valid data about the

characteristics of powertrain components to be modeled. There are two ways of collecting data for vehicle simulation. The first is to test the actual vehicle and powertrain components. This is quite expensive and beyond the scope of this study. A second method is to search the literature. Even though there is a tremendous amount of literature on HEV simulation, it is still difficult to obtain sufficient enough information to model each powertrain component of the vehicle in a single study. Since each study has its unique conditions, gathering test data for a single component from different studies is not a viable approach. The literature review showed that there is a significant amount of extensive research, including testing and simulation about two well-known brands: Toyota Prius and Toyota Camry. These two vehicles were chosen as base vehicles in this study. Studies such as "Evaluation of the 2007 Toyota Camry Hybrid Synergy Drive System," written by Burress, Coomer, Campbell, Seiber, and Marlino and "Evaluation of 2004 Toyota Prius Hybrid Electric Drive System," written by Staunton, Ayers, Marlino, Chiasson, and Burress in 2008 and 2006, respectively were used for baseline data. Both studies performed in U.S. Department of Energy`s Oak Ridge National Laboratory and have highly detailed, hands-on test data about each powertrain component of these vehicles. Toyota Hybrid Camry is retrofitted with dual engine. As shown in Table 2, its engine electric motor has approximately twice the peak power rating than the 2004 Toyota Prius, which means that the Prius's engine can be used as a retrofitted Camry engine. The 2007 Toyota Camry, the 2007 Toyota hybrid Camry, and the 2004 Toyota Prius were used as reference vehicles in this study. The 2007 Toyota Hybrid Camry was retrofitted as a dual-engine hybrid vehicle (DE-HEV).

Table 2

Comparison of Hybrid Camry and the Prius Specifications

Design Future	**2007 Hybrid Camry**	**2004 Prius**
Motor peak power rating	105 kW @ 4500 rpm	50 kW @ 1200–1540 rpm
Top rotational speed	14,000 rpm	6,000 rpm

HEV Powertrain Components

Internal Combustion Engine (ICE)

A conceptual drawing of a static engine model is shown in Figure 20. Since it is a static model, dynamic variables such as crank-angle dynamics, torque oscillations, and combustion cycles, are neglected. The torque derived from the engine is dependent on the throttle opening, and is passed through the crankshaft and flywheel, and then combined. The load torque demand from the rest of the powertrain is met by this combined torque. The torque generated by the engine can be calculated using a torque map. A torque map is "a table interpolation based on the maximum available torque at the current speed and the percentage of load desired α. The fuel consumption is estimated using another table of interpolation, as a function of torque and speed" (Lorenzo, 2009, p. 39).

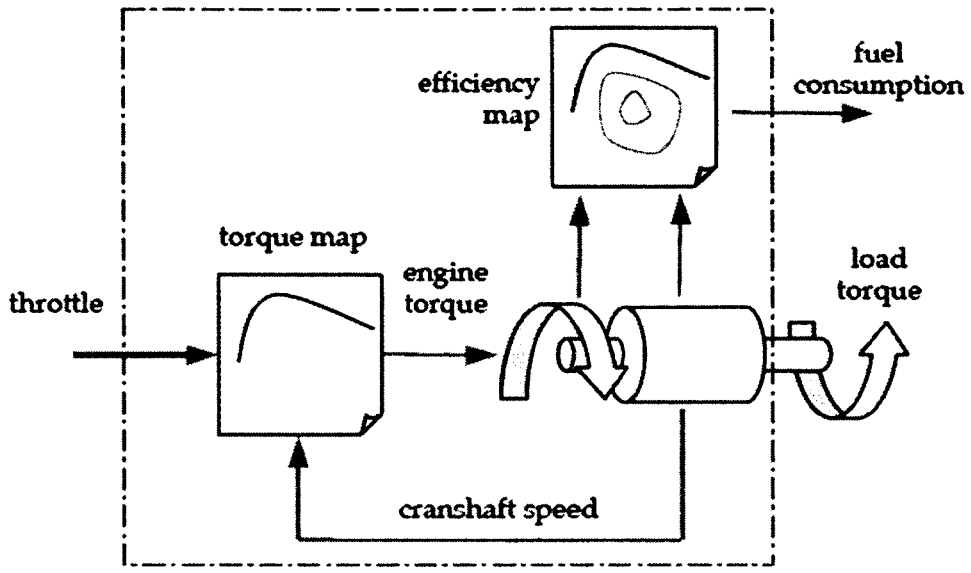

Figure 20. Engine model.

Engine torque is given by equation 1:

$$T_{ice} = \propto \left(T_{ice,max} - T_{ice,min}\right) + T_{min} \quad (1)$$

where,

$T_{ice,max}(\omega)$ is the maximum torque; and

$T_{ice,min}(\omega)$ is the friction torque.

Electrical Machines

An electric machine can be used as motor or as a generator. In motor mode, the electrical machine converts electrical energy from the generator or the battery pack to mechanical power into the transmission. In generator mode, an electric machine converts mechanical energy from the engine and from braking into electrical energy to be used to supply energy to the motor and charge the battery pack. Golbuff (2007) reported that

"There are two main types of electric motors used in HEVs. The first one is permanent magnet motors which uses a permanent magnet to create the magnetic field needed to produce power" (p. 10). The second is an induction motor, which uses current to create a magnetic field. Since they eliminate the power consumption of the field winding, and minimize overall weight and size, permanent magnet motors are more common in HEV applications.

Figure 21 shows the relationship between input-output variables and losses in an electrical machine. In motor mode, the electrical machine takes voltage and current as input, and provides torque and angular velocity as output, after consuming between 5% and 15% of the energy as loss. These losses are copper losses, iron losses, and mechanical (friction) losses, all which cause an increase of the machine's temperature and a reduction in its efficiency.

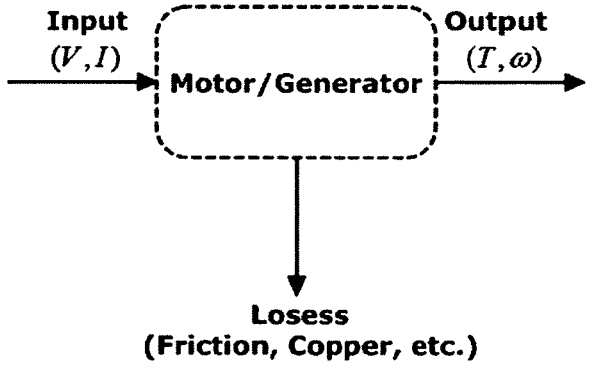

Figure 21. Relationship between input-output variables and losses in electrical machine.

In generator mode, the machine performs same process, but in an opposite direction. Losses occurring in motor mode are the same as in generator mode. A system-level approach, similar to the one used for the engine, can be used for electric machines using maps of torque and efficiency, as shown in Figures 22 and 23. Desired values of electrical power or torque can be used as a control input.

Motor Mode: Electric power is the input, and the torque needed at the shaft of the machine is calculated as shown in equation 2, using the efficiency map:

$$P_{mech} = T\omega = \frac{P_{elec}}{\eta(\omega, P_{elec})} \Rightarrow T = \frac{1}{\omega} \frac{P_{elec}}{\eta(\omega, P_{elec})} \quad (2)$$

where T is the torque; ω is the angular velocity (rad/s); P_{elec} is electric power; and $\eta(\omega,\ P_{elec})$ is efficiency, as a function of speed and electric power.

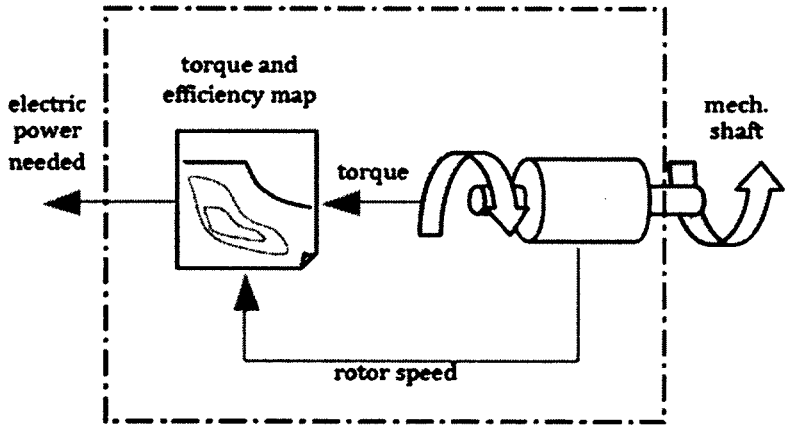

Figure 22. Electrical machine in motor mode.

Generator Mode: Torque demand is the input, and electric power must be calculated given the torque request, as shown in equation 3:

$$P_{elec} = \frac{P_{mech}}{\eta(\omega,T)} = \frac{\omega T}{\eta(\omega,T)} \tag{3}$$

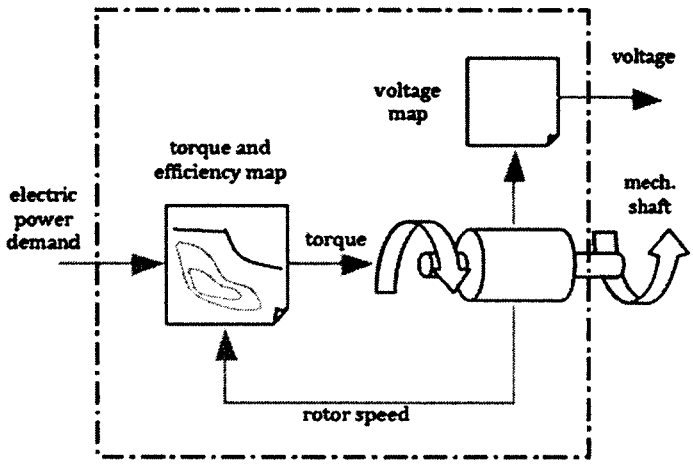

Figure 23. Electrical machine in generating mode.

Power losses can be calculated for both the motoring mode and the generating mode, as shown in equation 4:

$$P_{loss} = \begin{cases} P_{elec} - P_{mech} = \frac{\omega T}{\eta(\omega,T)} - \omega T = \omega T\left(\frac{1}{\eta} - 1\right) = \omega T\left(\frac{1-\eta}{\eta}\right) \\ \qquad\qquad\qquad\qquad motoring, \omega T \geq 0 \\ |P_{mech}| - |P_{elec}| = P_{elec} - P_{mech} = \eta\omega T - \omega T = -\omega T(1-\eta) \\ \qquad\qquad\qquad\qquad generating, \omega T < 0 \end{cases} \tag{4}$$

Energy Storage Systems

Energy storage systems are devices that store energy, deliver energy outside (discharge), and accept energy from outside (charge). There are several types of energy storage devices that can be used for hybrid electric vehicle (HEV) applications. These are chemical batteries, ultra capacitors, and ultrahigh-speed flywheels.

Energy storage systems need to meet a number of requirements, such as specific energy, specific power, efficiency, maintenance requirements, management, cost, environmental adaptation and friendliness, and safety for HEV applications. A battery model is used as an energy storage system in this study, such that: "Batteries are electrochemical devices that convert electrical energy into potential chemical energy during charging and convert chemical energy into electric energy during discharging" (Ehsani & Gao, 2006, p. 375). The objective of the battery model in a vehicle simulation is to predict the change in the state of charge (SOC) given the electrical load. "The SOC is defined as the ratio of the remaining capacity to the fully charged capacity as shown in equation 5. With this definition, a fully charged battery has an SOC of 100% and a fully discharged battery has an SOC of 0%" (Adeli & Sarvi, 2010).

$$SOC(t) = \frac{\int_0^t I(\tau)d\tau}{Q_{batt}} \tag{5}$$

where,

Q_{batt} is the charge capacity (the amount of charge the battery can accept); and

$\int_0^t I(\tau)d\tau$ is the amount of charge actually stored in the battery.

The battery model for vehicle simulation is shown in Figure 24. It has a control input corresponding to power demand, and a control output corresponding to the state of charge (SOC). The decision of charging or discharging the battery is taken based on these control parameters. Figure 25 shows the equivalent circuit for a battery model.

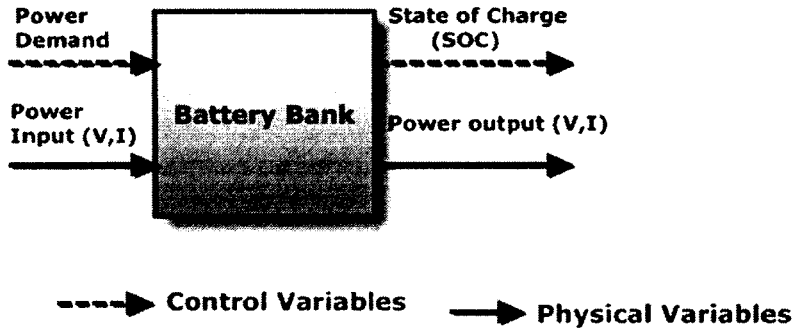

Figure 24. General model of energy storage system.

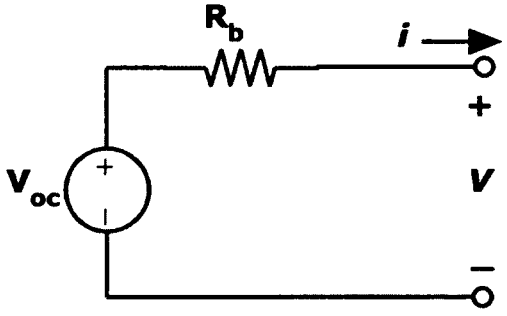

Figure 25. Equivalent circuit diagram for battery.

Battery voltage can be written as follows:

$$V = \frac{P_b}{I} = V_{OC} - R_b * I \quad (6)$$

$$\Rightarrow R_b * I^2 - V_{OC} * I + P_b \quad (7)$$

Solving this equation, we get:

$$I = \frac{V_{OC} - \sqrt{V_{OC}^2 - 4 * R_b * P_b}}{2 * R_b} \quad (8)$$

where,

V_{OC} is the lookup table (SOC, temperature); and R_b is the lookup table (SOC, temperature).

Using equations 6 and 8, the voltage (V) and current (I) of the battery can be estimated in the battery model.

Permanent Magnet DC (PMDC) Machine Simulation

A schematic diagram of a permanent magnet DC machine (motor and generator operation) is illustrated in Figure 26. A mathematical model of a PMDC motor is developed based on this figure.

The flux, established by the permanent magnets, is constant. Applying Kirchhoff's Voltage, and Newton's second laws, the differential equations for permanent magnet DC motors are derived using the motor representation shown in Figure 26. Denoting the back emf and torque constants as k_a, we have the equations (7), (8), and (9) that describe the armature winding and torsional-mechanical dynamics.

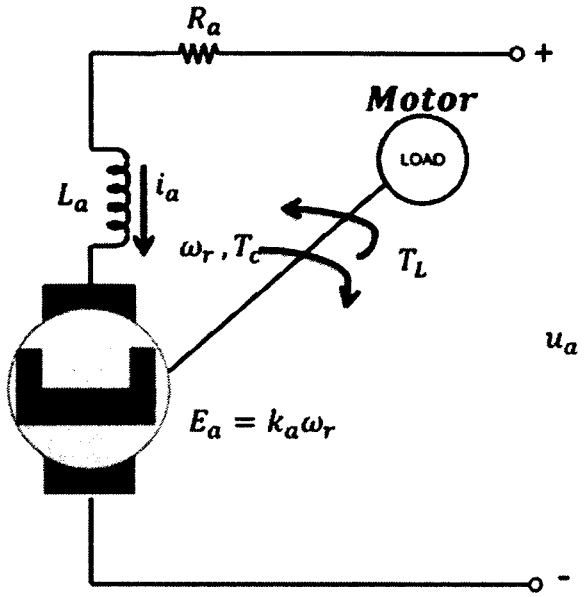

Figure 26. Schematic diagram of a permanent-magnet DC motor.

The field winding is a permanent magnet in PMDC. Permanent magnets offer a number of useful benefits; they do not require external excitation, there is less space required, and they are cheaper. The equivalent circuit of permanent magnet DC machine is shown in Figure 27, and the equations are given by (9), (10), and (11), as follows:

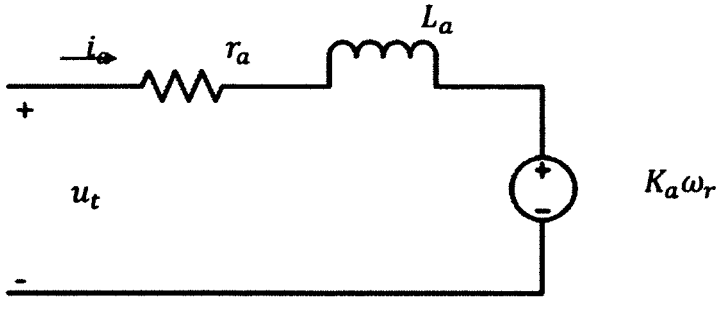

Figure 27. The equivalent circuit of permanent magnet DC motor.

$$u_t = i_a r_a + L_a \frac{di_a}{dt} + K_a \omega_r \tag{9}$$

$$T_e = K_a i_a \tag{10}$$

$$J \frac{d\omega_r}{dt} = T_e - T_L - B_m \omega_r \tag{11}$$

where u_t is the DC source voltage (V); i_a is the armature current (A); r_a is the armature resistance (ohms); L_a is the armature inductance (mH); K_a is the torque constant (V.s/rad); ω_r is the motor speed (rpm); T_e is the electromagnetic torque (Nm); T_L is the load torque (Nm); B_m is the constant (N.m.s); and J is the inertia constant (Kg. m^2).

Equations (1), (2), and (3) can be re-arranged, as in (4) and (5), to construct the block diagram.

$$\frac{di_a}{dt} = \frac{1}{L_a}(u_t - i_a r_a - K_a \omega_r) \tag{8}$$

$$\frac{d\omega_r}{dt} = \frac{1}{J}(T_e - T_L - B_m \omega_r) \tag{9}$$

$$\frac{di_a}{dt} = -\frac{r_a}{L_a} i_a - \frac{k_a}{L_a} \omega_r + \frac{1}{L_a} u_a \text{ (Motor circuitry dynamics)} \tag{11}$$

$$\frac{d\omega_r}{dt} = \frac{k_a}{J} i_a - \frac{B_m}{J} \omega_r - \frac{1}{J} T_L \text{ (Torsional-mechanical dynamics)} \tag{12}$$

Equations (8) and (9) can be written in matrix format, as shown in equation (8):

$$\begin{bmatrix} \frac{di_a}{dt} \\ \frac{d\omega_r}{dt} \end{bmatrix} = \begin{bmatrix} -\frac{r_a}{L_a} & -\frac{k_a}{L_a} \\ \frac{k_a}{J} & -\frac{B_m}{J} \end{bmatrix} \begin{bmatrix} i_a \\ \omega_r \end{bmatrix} + \begin{bmatrix} \frac{1}{L_a} \\ 0 \end{bmatrix} u_a - \begin{bmatrix} 0 \\ \frac{1}{J} \end{bmatrix} T_L \tag{13}$$

A block diagram for the system can be developed from the differential equations given in equations (6) and (7). Taking the Laplace transformation of each equation yields:

$$sI_a(s) - i_a(0) = -\frac{r_a}{L_a} I_a(s) - \frac{k_a}{L_a} \Omega_r(s) + \frac{1}{L_a} u_a(s) \tag{14}$$

$$s\Omega_a(s) - \omega_a(0) = \frac{k_a}{J} I_a(s) - \frac{B_m}{J}\Omega_a(s) - \frac{1}{J}T_L(s) \quad (15)$$

If perturbations around some steady state value are considered, the initial conditions go to zero, and all the variables become some change around a reference state. The equations can be expressed as follows:

$$I(s) = \frac{-k_a\Omega_a(s)+u_a}{L_a s+r_a} \quad (16)$$

$$\Omega(s) = \frac{-k_a I_a(s)+T_L}{L_a s+B_m} \quad (17)$$

An s-domain block diagram of permanent-magnet DC motors is developed and shown in Figure 28.

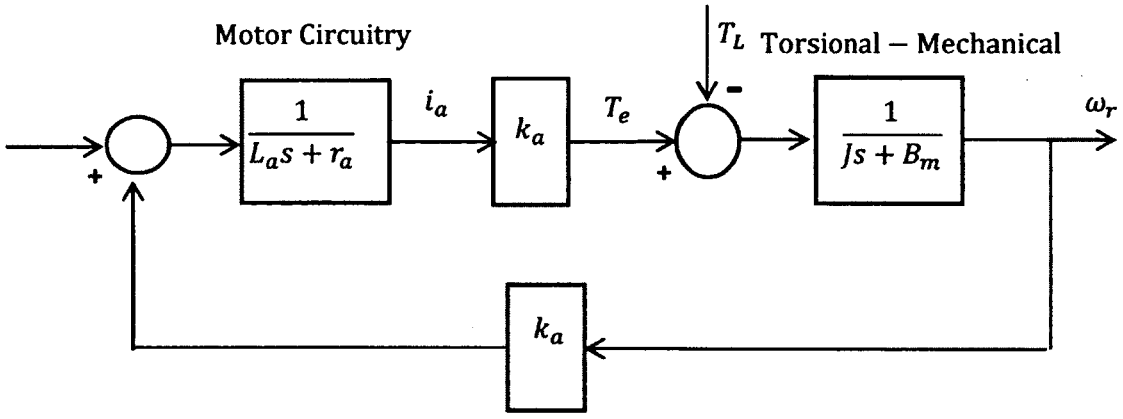

Figure 28. Functional block diagram of permanent-magnet DC motor.

Electrical Motor and Generator Subsystem

One of the main components of an HEV is an electrical machine. There are many types of electrical machines to choose from, such as synchronous machines,

asynchronous machines (induction machines), and DC machines. One of the main demands on electrical machines in HEV is high torque. There are variations within the different types of machines. All of them have quite different characteristics, such as starting torque, maximum torque, speed, etc. The type of machine can be determined based on what is expected from the machine. For example, high power and torque density, simple torque control, high efficiency, fast response, and wide speed range are some of the important characteristics machines should have in HEVs.

Even though a PMDC has a high cost, low thermal robustness, and has high sensitivity to heavy vibration, it is the best match for the aforementioned characteristic. Hence, a PMDC machines model is used in the dual-engine HEV (DE-HEV) simulation in this study.

The motor's maximum speed, maximum torque, and other parameters shown in Table 3, are defined by the manufacturer torque-speed envelope and the specification plate.

Table 3

Electric Motor Parameters

Parameter	**Values**	**Units**
Vector of rotational speeds	1200 2000 3000 4000 6000 6500 1000	rpm
Vector of maximum torque values	[400 400 250 150 110 90 0 0]	N*m
Torque control time constant, Tc	0.02	s
Motor and driver overall efficiency	90	%
Speed at which efficiency is measured	2000	rpm
Torque at which efficiency is measured	200	N*m
Torque-independent electrical losses	0	W
Supply series resistance	0	Ohm

The electric motor subsystem consists of an electric motor model, an inertia block parameter, a torque sensor, and a rotational motion sensor.

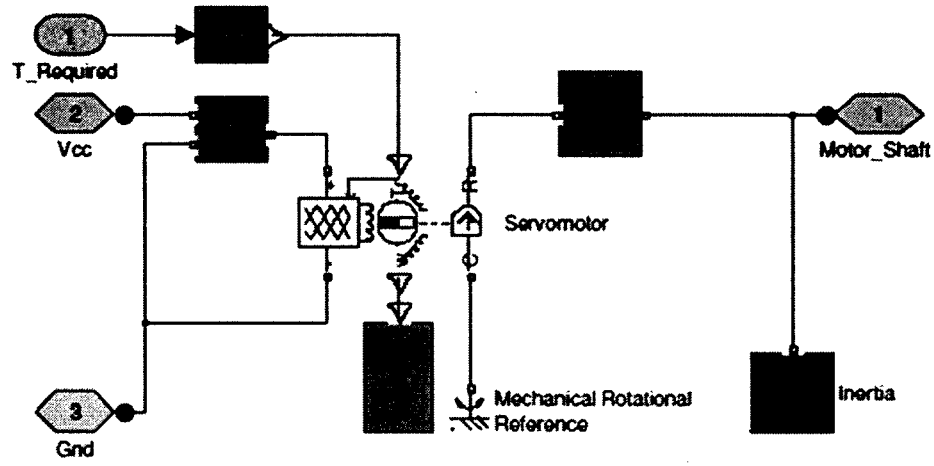

Figure 29. Electrical Motor Subsystem in Simulink.

As shown in Figure 29, an electrical motor has two inputs and one output. The first input is the electrical input, which is connected to the battery. The second input is the control input, which is connected to the control subsystem. The electric motor subsystem has two measurement blocks.

Figure 30 shows the electrical power calculation block in detail. The block between the voltage and electrical input pins calculates electrical power consumed by the electric motor. It first measures the applied voltage and the current. Then, it multiples the

measured voltage and current to calculate electrical power. Finally, it converts the unit from watts (W) to kilowatts (kW), as shown in Figure 30.

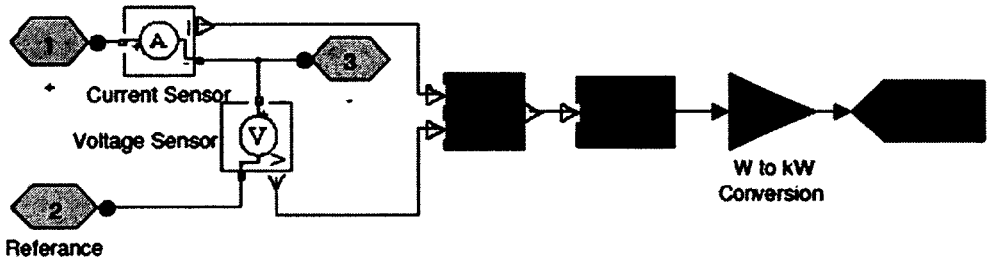

Figure 30. Electrical power calculation.

The only mechanical output in the electrical motor subsystem model is the motor shaft. Figure 31 illustrates the mechanical power calculation block. The block between the mechanical rotational conserving port (R) and the ideal mechanical rotational inertia block calculates the mechanical power produced by the electric motor. First, it measures generated torque and rotational speed. Then, it multiples measured torque and rotational speed to calculate mechanical power. Finally, it converts unit from W to kW. The "goto" source block (Pm_motor1) passes calculated mechanical power to its corresponding source blocks, called "from."

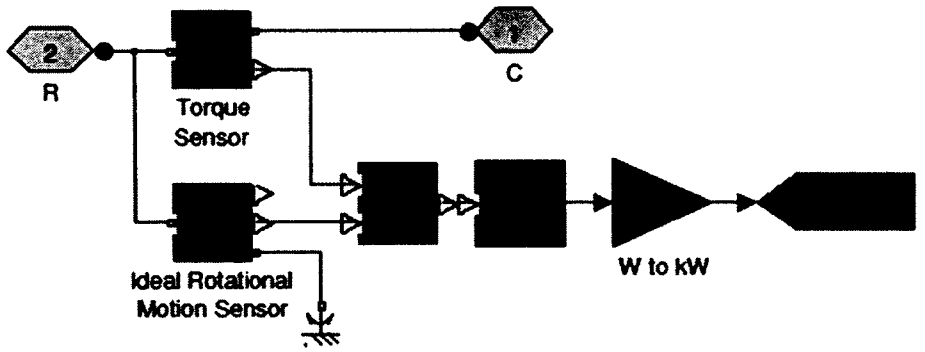

Figure 31. Mechanical power calculation.

As seen in Figure 32, the block between the required torque input and the reference torque demand (Tr) port of the electric motor model converts the unit-less Simulink input signal to a physical signal by using a Simulink-PS converter block. It also delivers the required torque input to the corresponding blocks, as shown in Figure 34.

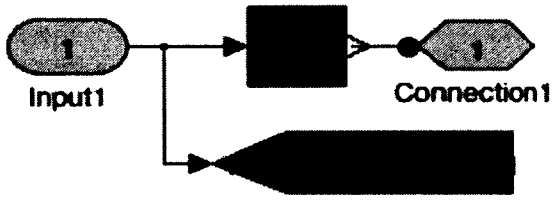

Figure 32. Input conversion and transfer block.

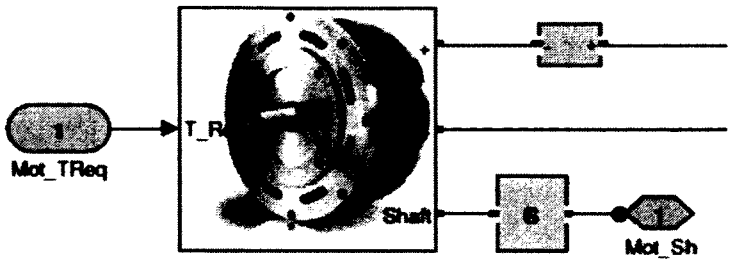

Figure 33. Electrical motor subsystem inputs/outputs.

As shown in Figure 33, the electrical motor subsystem has four inputs/outputs. These are: a required torque control input; two electrical inputs/outputs; and a mechanical input/output. Electrical pins are connected to the DC-DC converter subsystem. The motor shaft pin is connected to the vehicle's dynamic power-split device subsystem. There is also a speed sensor between these subsytems to measure motor shaft speed in rpm, as illustrated in Figure 34.

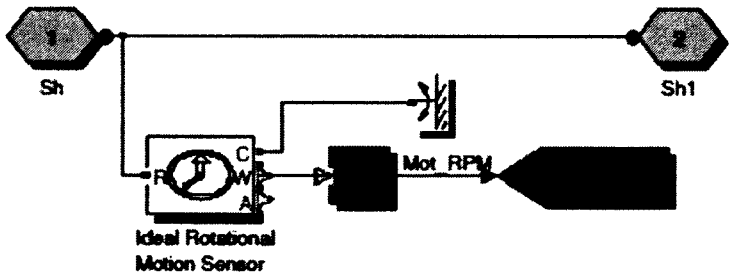

Figure 34. Electric motor subsystem shaft speed sensor.

The electric generator subsystem model is exactly similar to the electric motor subsystem model, except for the measurement block between the mechanical rotational conserving port (R) and the mechanical rotational inertia block. As shown in Figure 35, this block contains the torque sensor as well as the mechanical power, torque measurement, and a calculation block to calculate output torque.

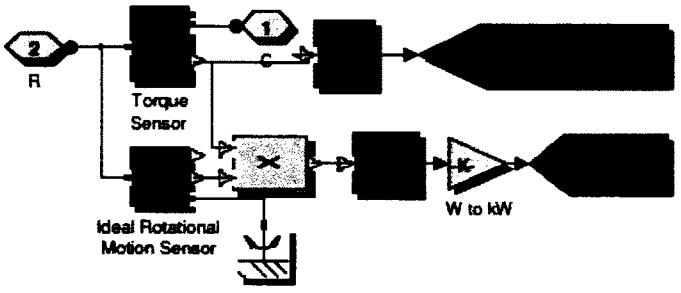

Figure 35. Electric generator subsystem power and torque measurement block.

Electric Motor/Generator Model Validation

A technical report titled, "Evaluation of 2004 Toyota Prius Hybrid Electric Drive System" (Staunton et al., 2006), published by U.S. Department of Energy, was used to validate the developed electric motor/generator model. The report includes tests performed by the Oak Ridge National Laboratory and data provided by manufacturer.

Torque speed characteristics, plotted based on published data from Toyota and the simulation of the developed models, are shown in Figures 36 and 37, respectively.

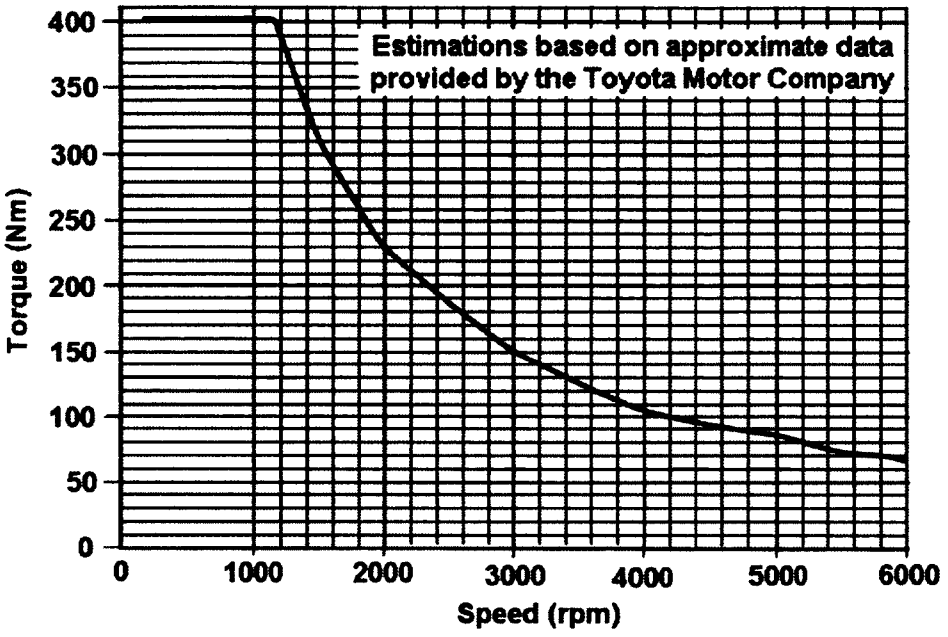

Figure 36. Torque-speed performance specifications for the 2004 Prius (Staunton et al., 2006).

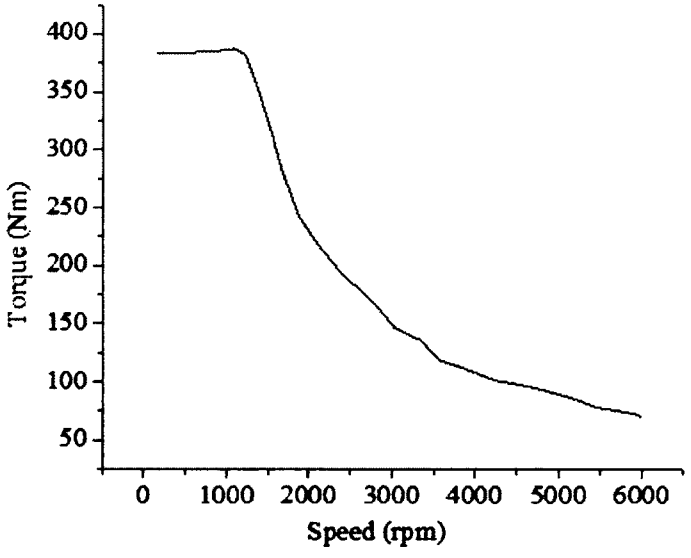

Figure 37. Torque-speed characteristics of electric motor/generator model.

As shown in Table 4, the difference between manufacturer data and simulation data is less than 5%, which is an acceptable range for the vehicle simulation, according to the Argonne National Laboratory (Pasquier & Rousseau., 2001).

Table 4

Comparison of Manufacturer Data and Model Torque Values in Different Speeds

Motor Speed (rpm)	Torque (Manufacturer Data) (Nm)	Torque (Simulation Data) (Nm)	% Difference
1000	400	387	3.25
2000	225	215	4.44
3000	149	142	4.70
4000	105	101	3.81
5000	86	83	3.49
6000	68	65	4.41

Torque-current relationship is another important aspect of PMDC that requires validation. As shown in equation 10, torque can be expressed as a constant multiple (torque constant, K_a) of armature current. Test results from Oak Ridge National Laboratory show that K_a is equal to 1.315 V.s/rad in the 2004 Prius. According to simulation results developed in this study, the PMDC model is 1.326. The difference between the test and the simulation results is only 0.8%, which is confidently within acceptable limits.

Internal Combustion Engine (ICE) Subsystem

The internal combustion engine (ICE) engine subsystem consists of an engine, mechanical rotational inertia, mechanical rotational viscous damper, ideal torque sensor, mechanical rotational motion sensor, and a mechanical rotational reference, as shown in Figure 38.

The generic engine block from the Simulink SimDriveline library is used as an internal combustion engine (ICE) for the dual-engine hybrid vehicle. It models the torque-speed or, equivalently, power-speed characteristics of an internal combustion engine, which the user can specify as either a spark-ignition or a diesel, type (The MathWorks, 2012). The signal that passes the position of the throttle directly controls the generated torque by the engine and indirectly controls the speed of the engine. If the engine speed exceeds the maximum that the user specifies, the engine does not generate torque. The engine model in Figure 36 limits maximum engine speed to prevent negative power and torque. The power turns to zero if the speed reaches its maximum value.

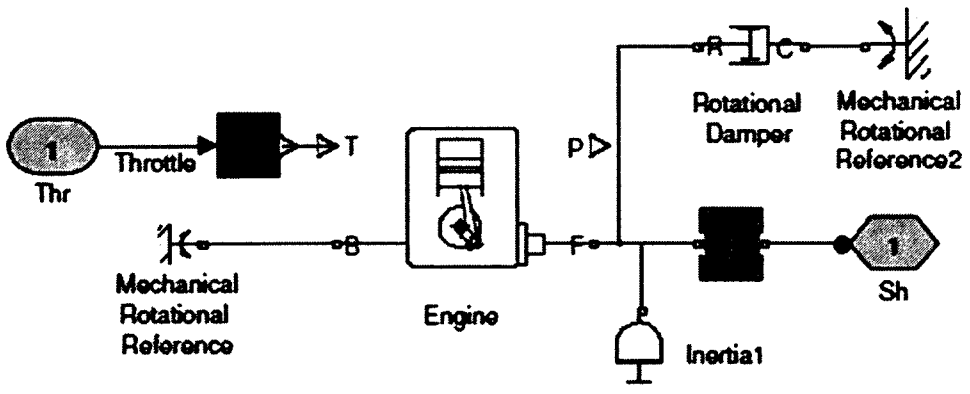

Figure 38. ICE engine subsystem.

Engine Model Used in the Engine Subsystem

The engine model used in the engine subsystem has one input, one output, and two conserving ports. The physical input signal at pin T (Figure 36) specifies engine torque as a fraction of the maximum torque possible, in a steady state, at a fixed engine speed, with values between 0 and 1. The block computes the generated engine power as a physical output signal at port P. Pin F and Pin B represent rotational conserving ports (respectively), the engine crankshaft, and the engine block.

The engine model is specified by an engine power demand function, $g(\Omega)$, which provides the maximum power available for a given engine speed, Ω. The block parameters (maximum power, speed at maximum power, and maximum speed) normalize this function to the physical maximum torque and speed values. The normalized throttle input signal, T, specifies the actual engine power delivered as a fraction of the maximum power possible in a steady state at a fixed engine speed, as shown in Figure 39. It modulates the actual power delivered to P from the engine: $P(\Omega,T) = T \cdot g(\Omega)$. The engine torque is $\tau = P/\Omega$ (The MathWorks, 2005). Table 5 shows the parameter values for the engine model used in this study.

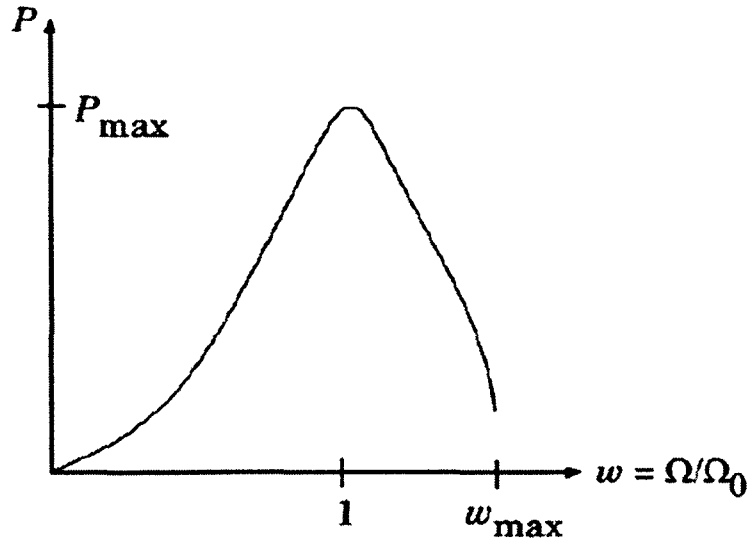

Figure 39. Engine power demand function.

Table 5

ICE Engine Parameters

Parameter	Values	Units
Maximum power	11400	W
Speed at maximum power	5000	rpm
Maximum speed	6000	rpm
Stall speed	500	rpm
Speed threshold	100	rpm
Shaft Inertia	0.25	kg*m^2
ICE Friction	0.2079	N*m/(rad/s)

Figure 40 shows rotational speed and torque measurement blocks for engine speed, torque, and power. Since the engine speed output from the ideal rotational motion

sensor is in rad/s, the output is multiplied by 60/(2*pi) to convert it to rpm. Block passes torque value from ideal torque sensor unchanged. Engine power is calculated as:

$$P_{engine} = \tau_{engine} * \omega_{engine}$$

where P_{engine} is the engine power (W);

τ_{engine} is the engine torque (Nm); and

ω_{engine} is the engine velocity (rpm).

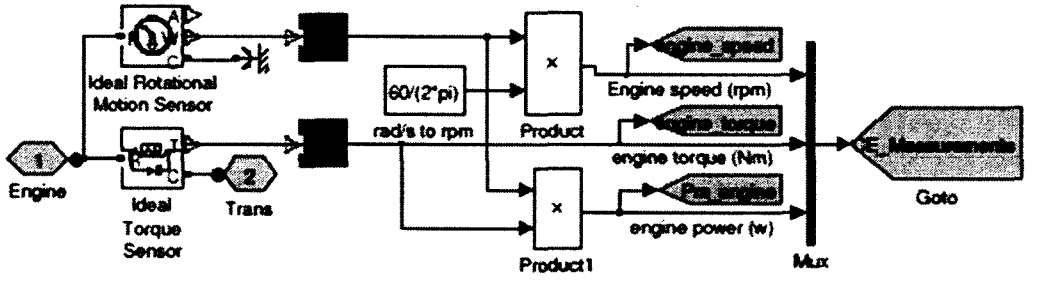

Figure 40. ICE engine subsystem rotational speed and torque measurement block.

DC-DC Controller

Figure 41 illustrates a simple DC-DC converter model developed for the DE-HEV. It consists of a transformer, two resistors, a voltage sensor, and a current sensor. The transformer is the ideal power-conserving transformer. It satisfies $V_1 = N*V_2$ and $I_2 = N*I_1$, where N is the Winding ratio, V_1 and V_2 are the primary and secondary voltages, I_1 is the current flowing into the primary + terminal, and I_2 is the current flowing out of

the secondary + terminal. The winding ratio, N, is 2.5. It steps up input voltage from the generator to a 500 V nominal battery, or steps down the battery voltage as an output to the EMs. The DC-DC converter model includes fixed losses, which are independent of the load current, and load dependent losses, which are due to resistive heating. Parallel and series resistors represent fixed losses and load dependent losses, respectively. Current and voltage sensors measure input current and voltage.

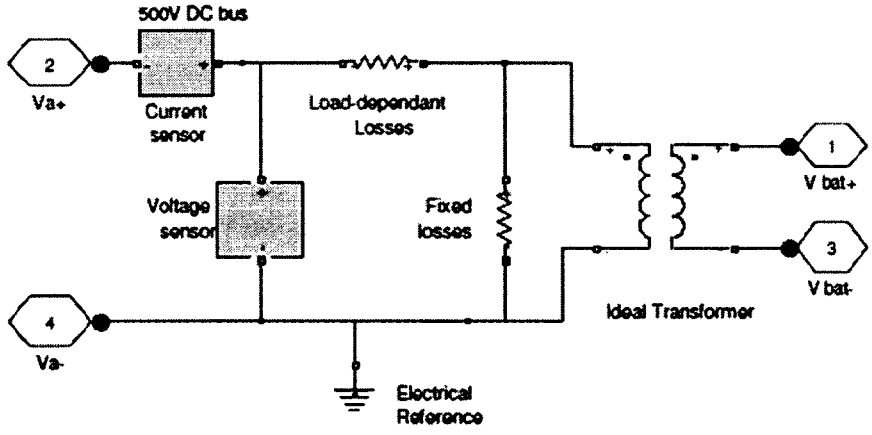

Figure 41. DC-DC converter model.

DC-DC Converter Model Validation

Figure 42 shows the DC-DC converter test module to validate the DC-DC converter module. It consists of a battery model, sensors, the DC-DC converter model, electrical load, and sensors. The model is simulated in constant input voltage and different electrical loads. Output current and voltage values are determined and input and

output power values are calculated. To validate the DE-HEV model, the simulation results were compared with the actual test results, as reported on the Oak Ridge National Laboratory's study. Input and output power values were calculated. Oak Ridge National Laboratory`s (Burress et al., 2008) report on the 2004 hybrid Camry was used as a source for validation of the model. As shown in Figure 43, the developed model succeeded in corresponding test results, with less than 3% error.

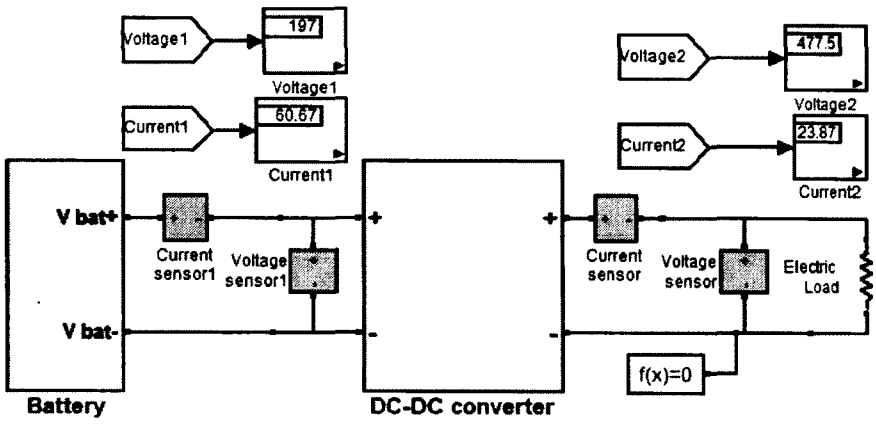

Figure 42. DC-DC Converter test and verification module.

Battery Pack Model

A generic battery block from the Simulink library was used to model the DE-HEV battery, as shown in Figure 44. According to the MathWorks` Simulink Getting Started Guide (2012), experimental validation of the model shows a maximum error of 5%, which is an acceptable limit for the vehicle simulation.

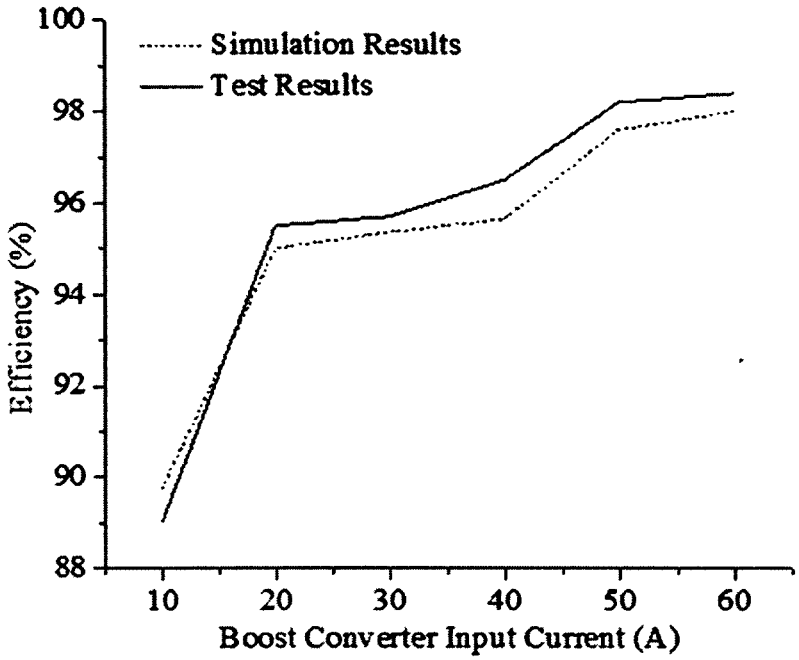

Figure 43. Comparison of actual DC-DC converter and developed model.

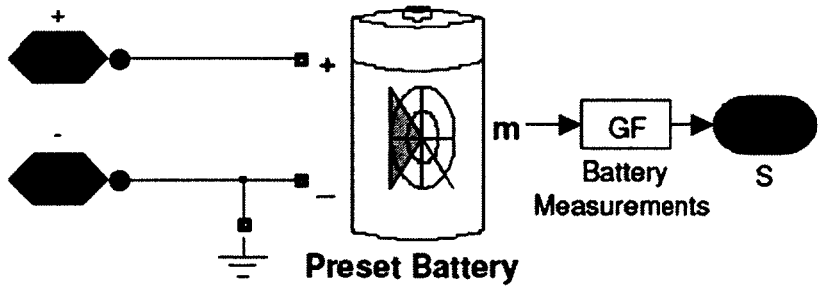

Figure 44. Battery model.

Based on the study, "Evaluation of the 2007 Toyota Camry Hybrid Synergy Drive System" (2008), completed by the U.S. Department of Energy, battery model parameter values are shown in Table 6.

Table 6

Battery Model Parameters

Battery Model	
Paramaters	Values
Nominal Voltage (V)	500
Rated Capacity (Ah)	8.1
Maximum Capacity (Ah)	8.7
Nominal Discharge Current (A)	1.62
Internal Resistance (Ohms)	0.24691
Capacity (Ah) at Nominal Voltage	7.7285
Battery response Time (s)	30

Controller Design

The goal of the controllers is to create a module that mimics the response of real-life conditions. In real road conditions, both torque and speed demand dynamic change based on the driver's demand for speed and road conditions. Controllers monitor the difference between desired and actual values of the component parameters and feed the error value into a proportional controller. The proportional–integral controller (PI controller) is used to develop the controller for the electric motor, the generator, and the ICE. The PI controller was used in this study rather than proportional–integral–derivative

controller (PID), because the PI controller provides satisfactory response in terms of improving rise time and eliminating steady-state errors. Besides, the derivative component generally does not add much responsiveness, but adds complexity, and can be difficult to tune. The transfer function of the PI controller is defined as:

$$PI(s) = K_p + \frac{K_I}{S} \tag{18}$$

where,

K_p is the Proportional gain; and

K_i is the Integrated gain.

The PI controller in a closed-loop system schematic is shown in Figure 45. The variable (e) represents the tracking error—the difference between the desired input value (R) and the actual output (Y). The error signal (e) is sent to the PI controller, and the controller computes the integral of the error signal. The signal (u), optioned by error signal (e), passes through the controller and is equal to the proportional gain (K_p) times the magnitude of the error, plus the integral gain (K_i), times the integral of the error, as shown in equation 19.

$$u(t) = K_p e + K_i \int e dt \tag{19}$$

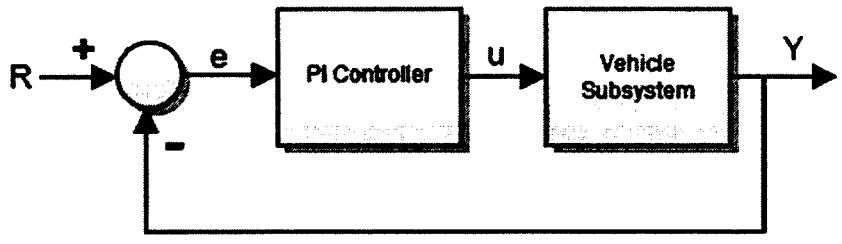

Figure 45. Closed-loop PI controller system block diagram.

The signal (u) passed through the plant, and the new output (Y) was obtained. Derived output (Y) was sent back to the sensor to find the new error signal (e). The controller took the new error signal and computed the integral once again. This process repeats continuously, as long as the subsystem is on.

The Simulink Discrete PID Controller block and the PID tuner tool were used to develop a PI controller for the motor, generator, and the ICE controller. Figure 46 shows Simulink PID controller design model, developed by Arkadiy Turevskiy (2011), and published on the Matlab File Exchange website. All PI controllers in this study were developed using this model.

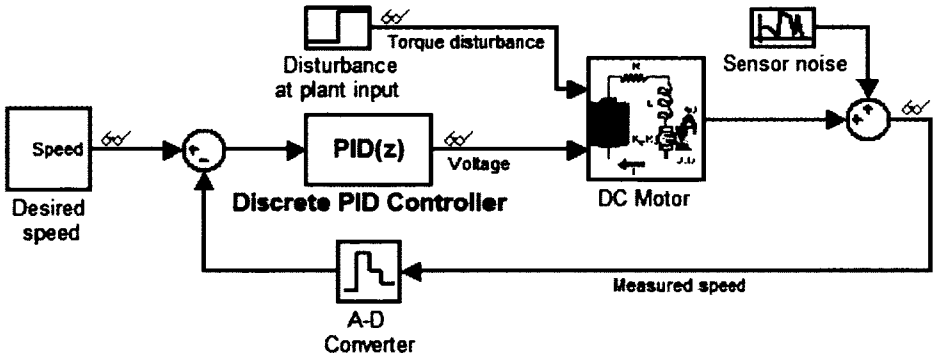

Figure 46. PID controller design model template.

Motor Controller

This closed-loop PI controls the motor speed. First, the PI controller parameters, K_p and K_i, were determined and tuned using the template model in Figure 46. They were substituted with the motor model developed for this study, shown in Figure 47. The template model is simply a digital control system model that controls the rotational speed of the motor shaft. The control system will took the error signal between desired speeds, measured speed, and used it to calculate voltage necessary to run the DC motor.

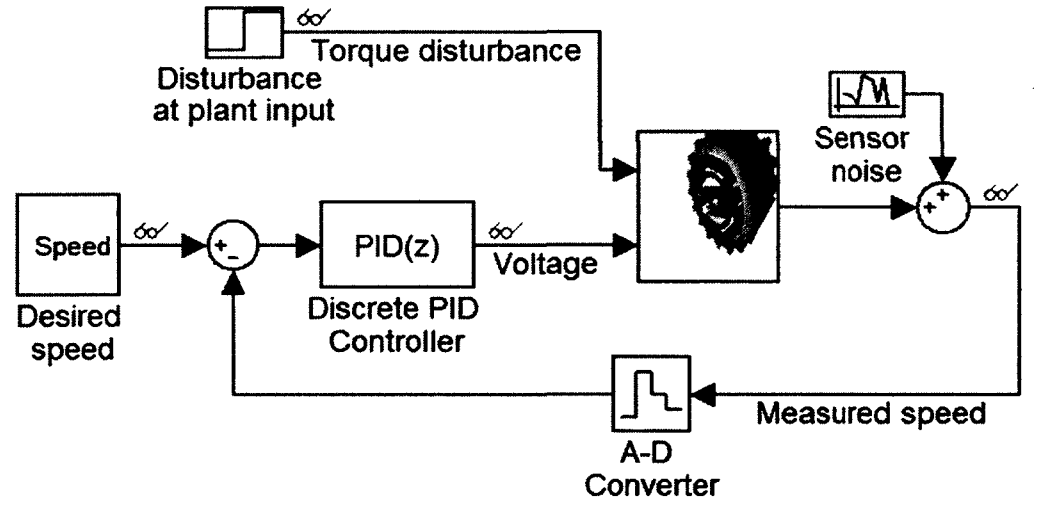

Figure 47. PID controller design model template for PMDC Motor.

PI controller parameters, K_p and K_i, were tuned as 500 and 300, respectively, to find the optimum point between the fastest response time and the noisiest voltage request signal. The PI controller was implemented in the motor controller subsystem, as shown in

Figure 48. First order, low-pass filter was used after the generator RPM signal to remove high frequency noise.

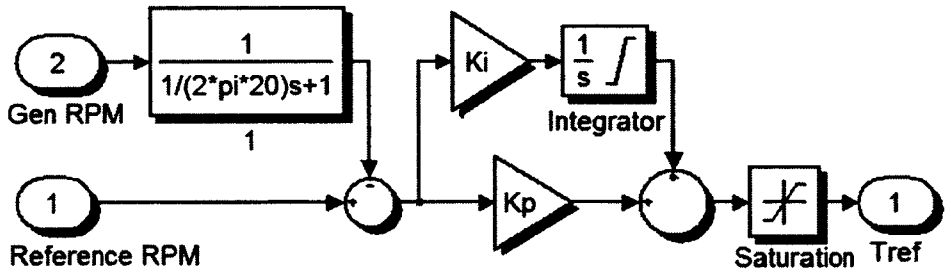

Figure 48. PMDC motor controller subsystem.

The controller takes the error signal between the generator and reference speeds to calculate the voltage needed to run the DC motor. The error signal passed through the PI controller. The saturation block placed before the output port limited the input signal to the upper and lower saturation values, and kept the signal within the range of [-5, 5], as in the input port. The maximum value for the reference voltage was 5 volts, which is equivalent to a speed demand of 6,500 rpm.

Generator Controller

As shown in Figure 49, the generator controller subsystem is almost identical with the generator controller block subsystem. It includes a 20 Hz low pass filter block, integrator block, saturation block, and a closed-loop PI controller in motor controller subsystem. The PI controller parameters, K_p and K_i, were determined as ten and three,

respectively, using the Simulink PI tuner tool. The value of maximum reference voltage for generator control subsystem was five volts, which is equivalent to a speed demand of 10,000 rpm.

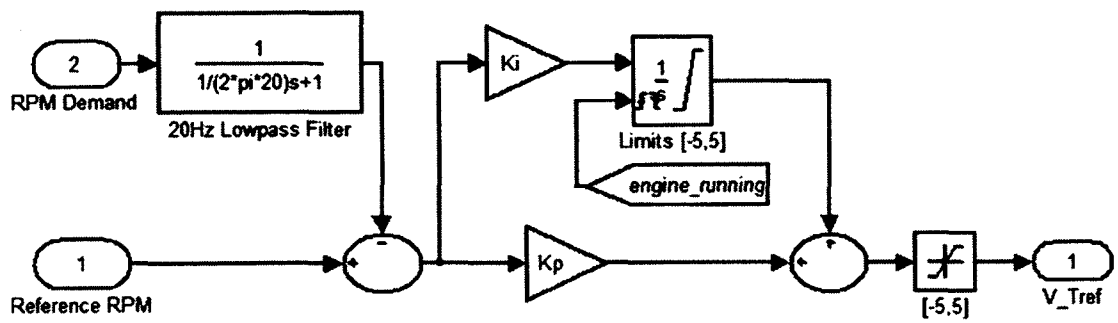

Figure 49. PMDC generator controller subsystem.

Engine Controller

As shown in Figure 50, the generator controller subsystem is very similar to the motor controller subsystem. PI controller parameters, K_p and K_i, were determined as 0.02 and 0.01, respectively. It has a switch block to enable the main controller to turn on and off the generator as required. If the speed demand is less than the idle speed of 800 rpm, the speed demand is set to zero. The controller takes the error signal between engine the RPM signal, and switches the output signal. Then, the error signal passes through the PI controller. The saturation block is placed before the throttle output port to keep the signal within the range of [-5, 5] as in input port.

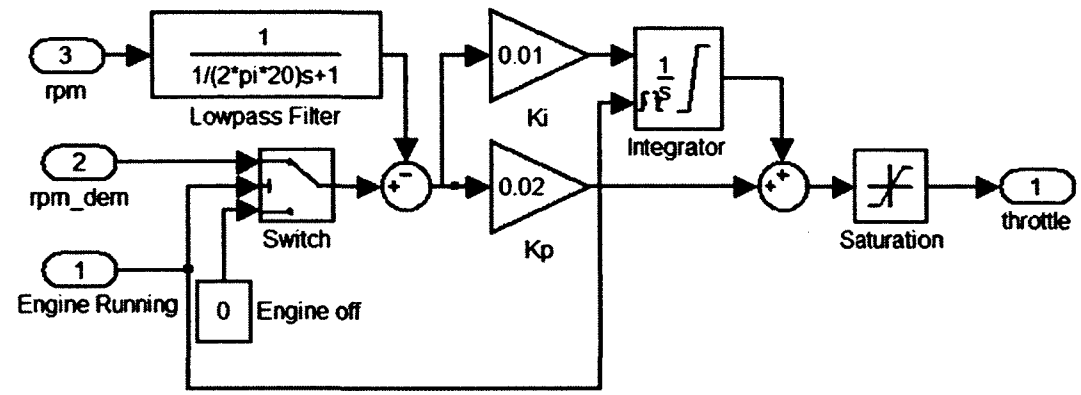

Figure 50. ICE controller subsystem.

Vehicle Dynamics

The mechanical power required to drive a vehicle is determined by several factors. These factors include, but are not limited to, the vehicle weight, engine efficiency, driveline efficiency, aerodynamic drag, rolling resistance, road grade, and accessory loads. Research indicates that "A vehicle traveling at a particular speed in air encounters a force resisting its motion. This force is referred to as aerodynamic drag. It mainly results from two components: shape drag and skin friction" (Ehsani et al., 2005, p. 23). The aerodynamic drag on a vehicle is based on the density of the air it travels in, its velocity, its drag coefficient, and its frontal area. It is the force required to push the vehicle through the air (Smith, 2001).

Aerodynamic drag is expressed as:

$$F_d = \frac{\rho V^2 C_d A}{2} \tag{20}$$

where F_d is the drag force;

ρ is the mass density of the fluid (air);

V is the speed of the object relative to the fluid;

C_d is the drag coefficient; and

A is the reference area.

Figure 51 illustrates the Simulink model of aerodynamic drag. The model converts speed input from kilometers per hour (kph) to miles per second (mps). Then, the function block gets the square of the speed input. Finally, it multiplies the speed value with other constant values in the equation.

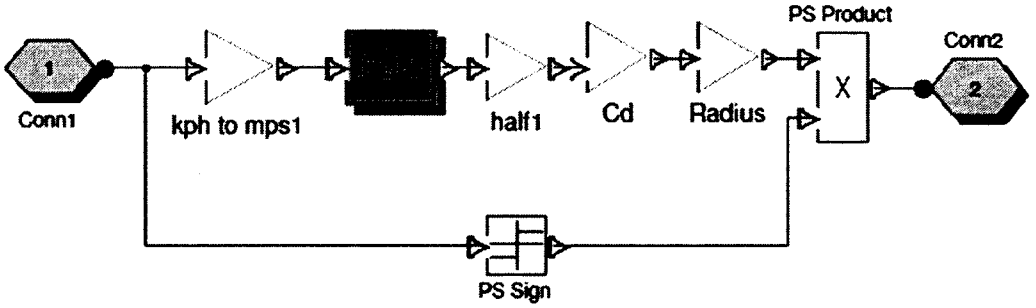

Figure 51. Vehicle aerodynamic drag model block.

According to Smith (2001), "Rolling resistance comes from a combination of the weight of the vehicle deforming the shape of the tire, the friction between the tire and the roadway, and air friction across the tire surface" (p. 21). The rolling resistance

coefficient, μ, is a function of the tire material, structure, temperature, and inflation pressure; it is also a function of tread geometry, road roughness, road material, and the presence or absence of liquids on the road (Ehsani et al., 2005). The typical values of rolling resistance coefficients on various roads are given in Table 7.

Table 7

Rolling Resistance Coefficients.

Conditions	**Rolling resistance coefficient**
Car tires on concrete or asphalt	0.013
Car tires on rolled gravel	0.02
Tar macadam	0.025
Unpaved road	0.05
Field	0.1-0.35
Truck tires on concrete or asphalt	0.006-0.01
Wheels on rail	0.001-0.002

Rolling resistance force is expressed as:

$$F = \mu mg \tag{21}$$

where,

μ is the friction coefficient;

m is the weight of the vehicle; and

g is the acceleration of gravity.

Accordingly, "The force on a vehicle due to road grade is due to a portion of the vehicle's weight vector being directed against the direction of travel when θ is positive and with

the direction of travel when θ is negative" (Nennelli, 2001, p. 26). The force on a vehicle due to road grade is expressed as follows:

$$F_\theta = mgSin\theta \tag{22}$$

where,

F_θ is the force on a vehicle due to road grade; and

θ is the angle of inclination.

Using basic statics, any vehicle has an accompanying inertial force:

$$F_i = m\frac{dV}{dt} \tag{23}$$

Combining forces on the vehicle yields,

$$\Sigma F = m\frac{dV}{dt} = -\left(1/2\,\rho V^2 C_d A + \mu mg + mgSin\theta\right) + F_w \tag{24}$$

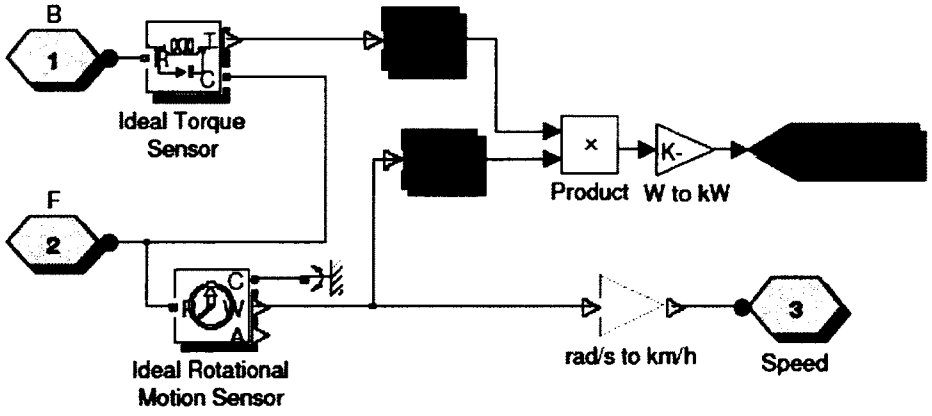

Figure 52. Vehicle torque and speed measurement and calculation.

Required power to keep the vehicle at a certain speed can be calculated, as:

$$Power = Force * Velocity$$

$$\text{or, } P_w = mV\frac{dV}{dt} - \left(\frac{1}{2}\rho V^2 C_d A + \mu mg + mgSin\theta\right) \quad (25)$$

Overall, a vehicle dynamics subsystem model that contains aerodynamic drag, rolling resistance, and force due to road grade, is shown in Figure 53. It has one input and one output. The subsystem gets rotational speed and torque input through the drive shaft input. It is connected to a rotational damper block and vehicle speed and power measurement blocks. A rotational damper block is a mechanism that transmits continuous torque and protects connected machines by dampening alternating torque vibrations. Vehicle speed and the power measurement block measures rotational speed and torque. it then calculates power based on these two variables, as shown in Figure 52. It passes vehicle speed to the aerodynamic drag block. The aerodynamic drag block then generates an output signal to ideal torque sources based on the speed input. The ideal torque source block generates a torque proportional to the input signal.

Supervisory Power Management and Control Strategy

The most important target of the HEV design is to maximize energy conversion on the powertrain through appropriate controls. Overall effectiveness was checked against standard drive cycles in the EU, USA, or Japan to make fair comparisons. Therefore, controller design is a key point of the HEV design process. HEV control strategies aim to satisfy a number of goals. There are four key roles (Chan & Wong, 2004):

- Maximum fuel economy;
- Minimum emissions;

- Minimum system cost; and
- Good driving performance

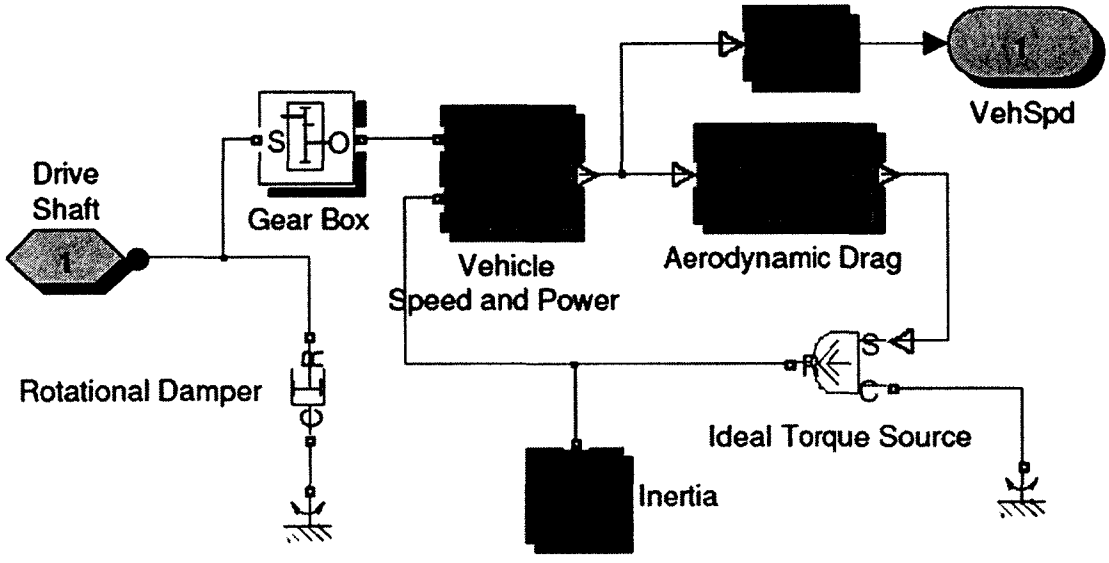

Figure 53. Vehicle dynamics subsystem model.

Hardware configurations and powertrain considerations need to be designed together to find an optimum solution (Katsargri, 2009). To some extent, the hardware configuration dictates what control strategy can be used in the HEV controller design. In the literature, while a lot of work can be found related to energy management in single engine hybrid vehicles, very little can be found regarding DE-HEV architectures. In this part of the study, the proposed energy management strategy for the DE-HEV vehicles is presented.

Although there are some similarities, the DE-HEV hardware configuration proposed in this study has some significant differences compared with conventional parallel and series HEV powertrain configurations. It has a pair of engines, generators, and motors. Since there is no direct mechanical connection between the internal combustion engine (ICE) and the wheels, it is similar to a series HEV configuration. In fact, it might be considered as two series HEVs in parallel. A DC-DC converter and battery are used as common electric energy conversion and storage mediums, respectively.

As shown in Figure 54, not having a mechanical connection between ICEs and the wheels make the control structure relatively simpler as in series HEV. All the propulsion power comes from the electric motors (EMs), while the ICEs are only used to charge the battery. The biggest advantage of the proposed DE-HEV configuration is the simplicity of its powertrain, which is due to the decoupling between the ICEs and the wheels, which permits the ICEs to operate at their most efficient. ICE can maintain an optimal running state with an optimized fuel-economy despite variation of load. This allows an ICE to maximize fuel efficiency for generating power needed by the EMs.

Peak energy demand from the vehicle is one of the most important factors to take into consideration during the sizing of a vehicle's engine. The design of a vehicle's engine to meet energy needs in a fully loaded condition is not an optimal solution in terms of fuel efficiency; larger engines mean more fuel consumption. Hence, with the help of advances in electronic converter systems, the evolution of HEV technologies are as shown in Figure 55.

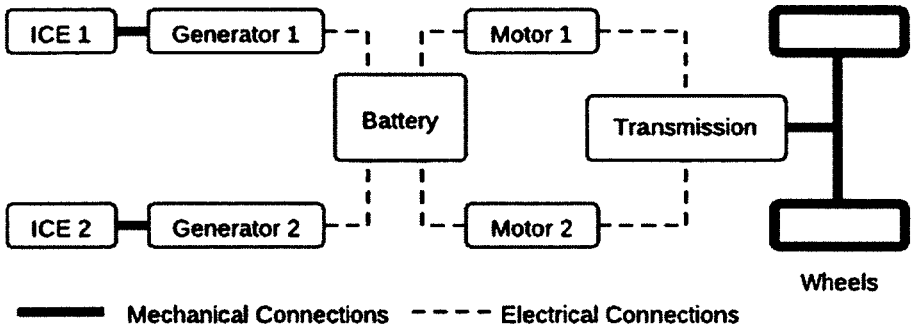

Figure 54. Mechanical and electrical connections.

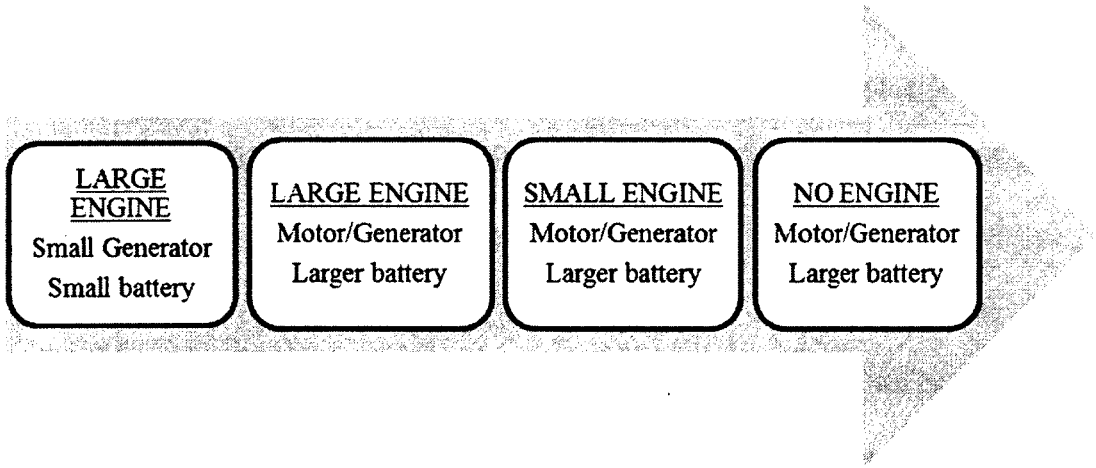

Figure 55. The evolution steps of HEV technologies.

The proposed DE-HEV design eliminates the aforementioned problem by offering two small engines instead of one single engine. In this design, ICEs are coupled with electric generators. During low power demand, a single engine provides mechanical

power to the electric generator, and the generator charges the battery to provide electric power to the EM for vehicle propulsion. When power demand is high, both ICEs charge the battery, and both EM1 and EM2 run to meet high power demand.

Although each subsystem has a controller in the DE-HEV design, a high-level power management and control system is necessary from the fact that increased complexity, when compared to a conventional ICE, requires coordination among the vehicle's drivetrain subsystems.

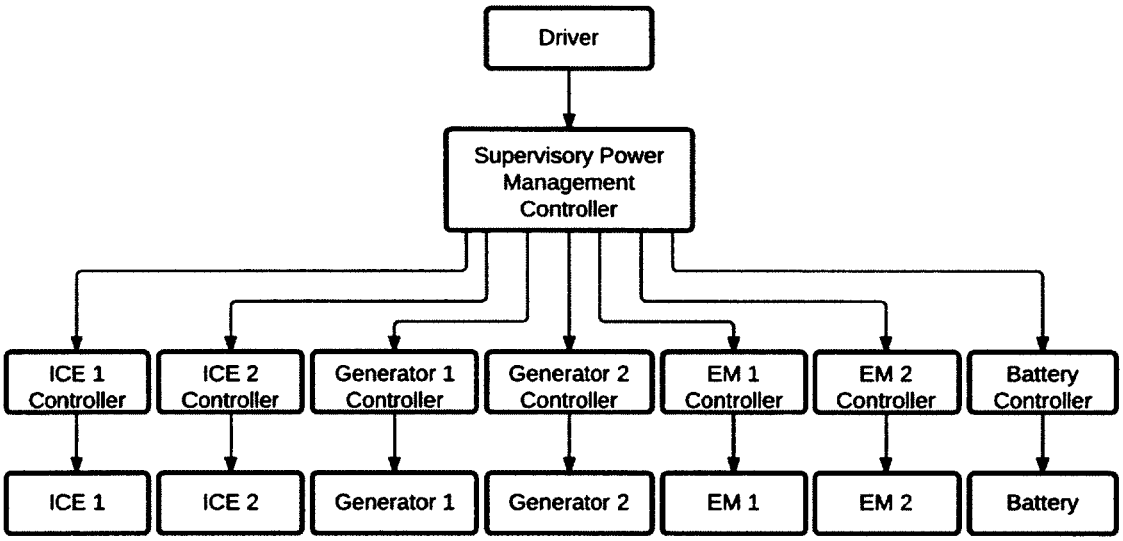

Figure 56. Relationship between DE-HEV components and controllers.

As shown in Figure 56, each subsystem has its own controller. There is also a high-level supervisory power management controller to control each vehicle's subsystem

by interacting with their controllers. Overall, the DE-HEV design contains five subsystems, five low-level controllers, and one high-level controller. Figure 57 shows a flowchart for the DE-HEV supervisory energy management controller. There are two parameters that decide which engine or EM should be on or off. These are P_{EM1_max} (maximum power that EM1 can provide) and state of charge (SOC) of the vehicle's battery.

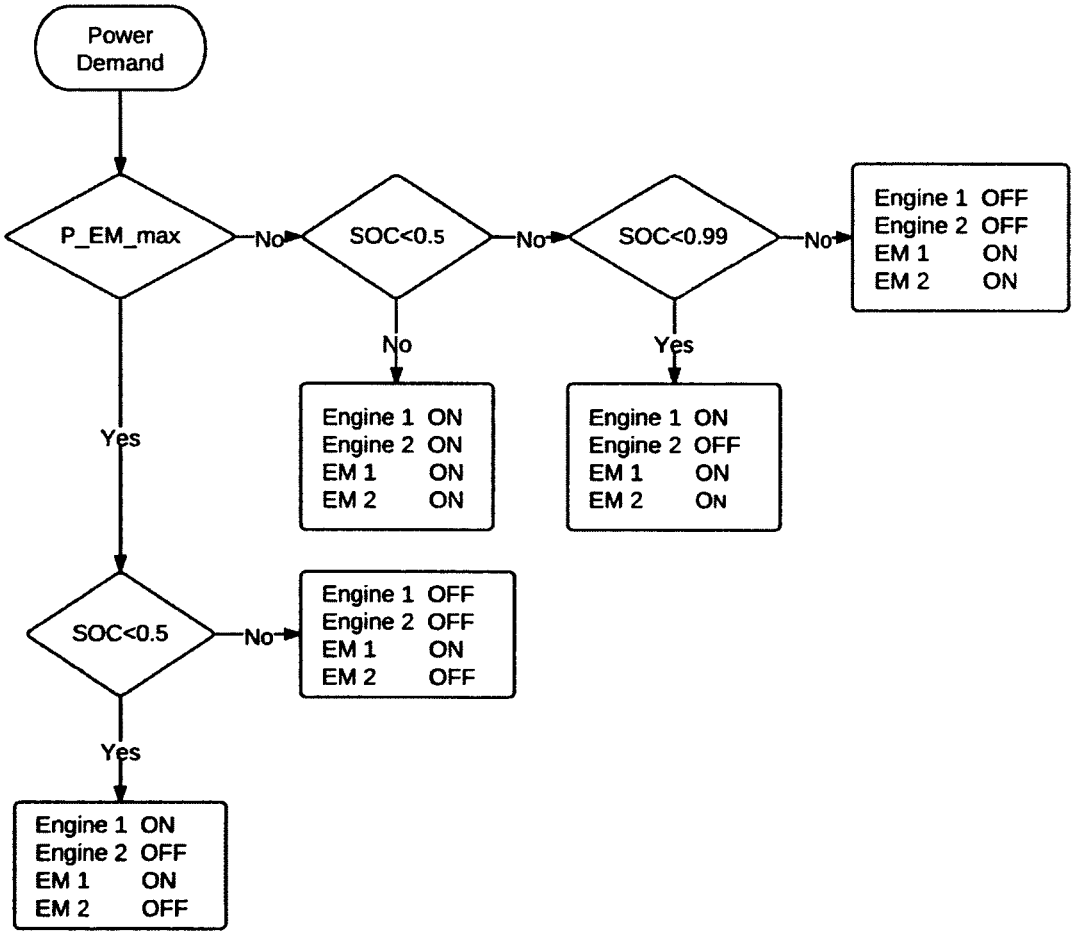

Figure 57. Flowchart for DE-HEV supervisory energy management controller.

The supervisory power management controller first compares power demand with P_{EM1_max}. It decides whether to run a single or double motor based on this comparison. If the power demand is smaller than the P_{EM1_max}, only one EM provides propulsion to the vehicle. Then, the control system checks for the SOC parameter. If the SOC is greater than 0.5, both engines stay off, as shown in Figure 58. If the SOC is smaller than 0.5, engine 1 will turn on, and engine 2 will stay off, as shown in Figure 59. Since power demand is not high enough, both engines are able to provide enough energy to keep battery charged above its current state.

If the power demand is greater than P_{EM1_max}, both EMs are required to run. Then, the control system checks the SOC parameter. As shown in Table 8, there are three conditions for SOC. If the SOC is smaller than 0.5, both engines turn on to maintain the current SOC, or even to increase it depending on the power demand from the battery, as shown in Figure 60. If it is greater than or equal to 0.5, but smaller than 0.99, only one engine will run, as shown in Figure 61. If the SOC is greater than or equal to 0.99, both engines will turn off to avoid overcharging the battery, as shown in Figure 62. As shown in Table 8 and Figures 57 and 59, both engines run only at high power demand with the SOC<0.5 mode.

Table 8

Truth Table for DE-HEV Supervisory Energy Management Controller

Control Parameters		Engine 1	Engine 2	EM 1	EM 2
Pdemand< PEM_Max	SOC<0.5	On	Off	On	Off
Pdemand< PEM_Max	SOC>=0.5	Off	Off	On	Off
Pdemand>=PEM_Max	SOC<0.5	On	On	On	On
Pdemand>=PEM_Max	0.5=<SOC<0.99	On	Off	On	On
Pdemand>=PEM_Max	SOC>=0.99	Off	Off	On	On

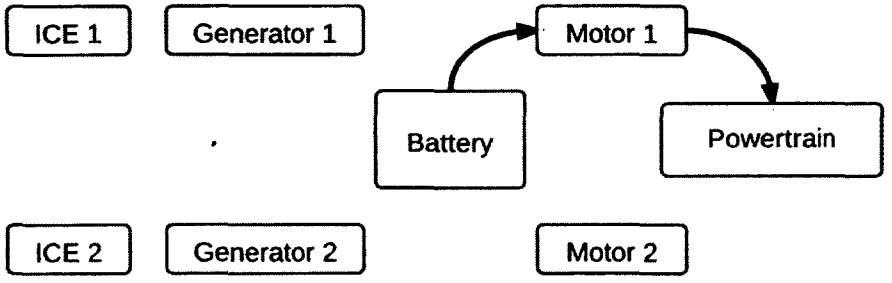

Figure 58. Low power demand with SOC>=0.5.

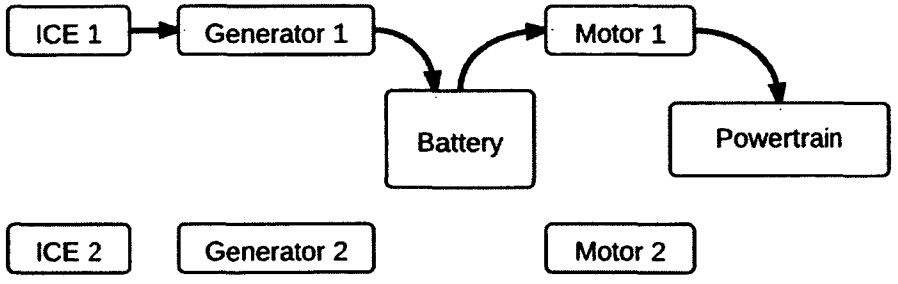

Figure 59. Low power demand mode with SOC<0.5.

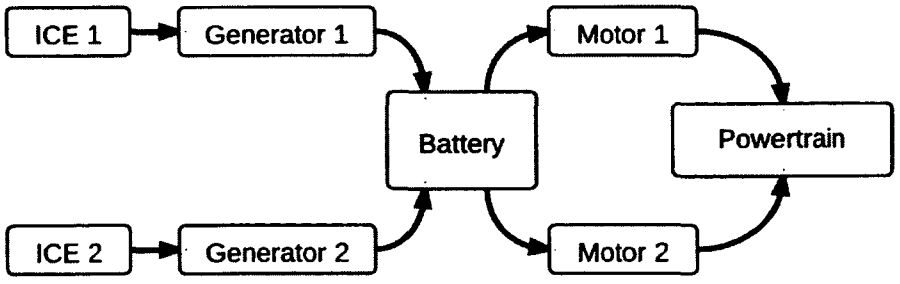

Figure 60. High power demand mode with SOC<0.5.

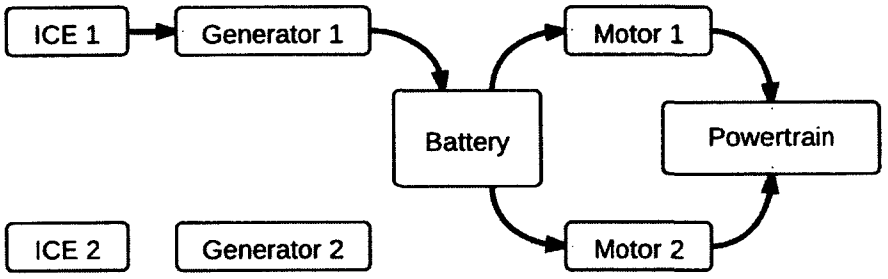

Figure 61. High power demand mode with 0.5<=SOC<0.99.

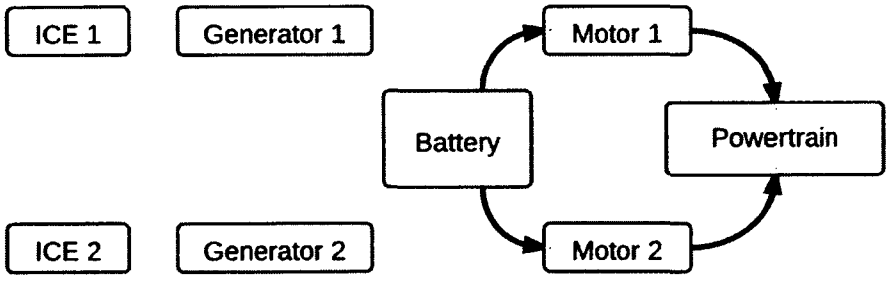

Figure 62. High power demand mode with SOC>=0.99.

Simulink® Stateflow® software is used to implement supervisory power management logic in the Matlab Simulink® environment. The Matlab Product Documentation identifies, "Stateflow® extends Simulink® with a design environment for developing state charts and flow diagrams. Stateflow software provides the language elements required to describe complex logic in a natural, readable, and understandable form" (The MathWorks, Inc., 2012, p. 1). The resulting model is shown in Figure 63. As seen there, the Stateflow® control module applies the exact same logic described in the flowchart in Figure 51 and Truth table in Table 5. The vehicle start mode, which has similar low power demand as the SOC>0.5 mode, is included on the top of the flow chart logic. As shown in Figure 63, the vehicle starts with a single EM. Both engines are off when the vehicle starts. Since EM has better efficiency in starting than ICE, it improves fuel efficiency, especially in urban driving, which contains frequent stops and starts. The Stateflow® model also includes a brake mode that enables the vehicle to recover some energy that is otherwise wasted, as in conventional ICE engine vehicles.

In conclusion, DE-HEV supervisory control model was developed using Simulink® Stateflow® software. The primary goal of the control model is to satisfy the driver's power demand by managing power flows from the various vehicle components to minimize fuel consumption and simultaneously satisfying other constraints, such as SOC and emissions. A rule-based control technique was used to develop the controller. The objective of the DE-HEV supervisory control was to discover the sequence of optimal power splits at each instant of time that minimizes fuel consumption over a given driving

cycle. Five different states are modeled among possible driving situations, according to event-triggered rules that depend on the SOC of the battery and the request of power.

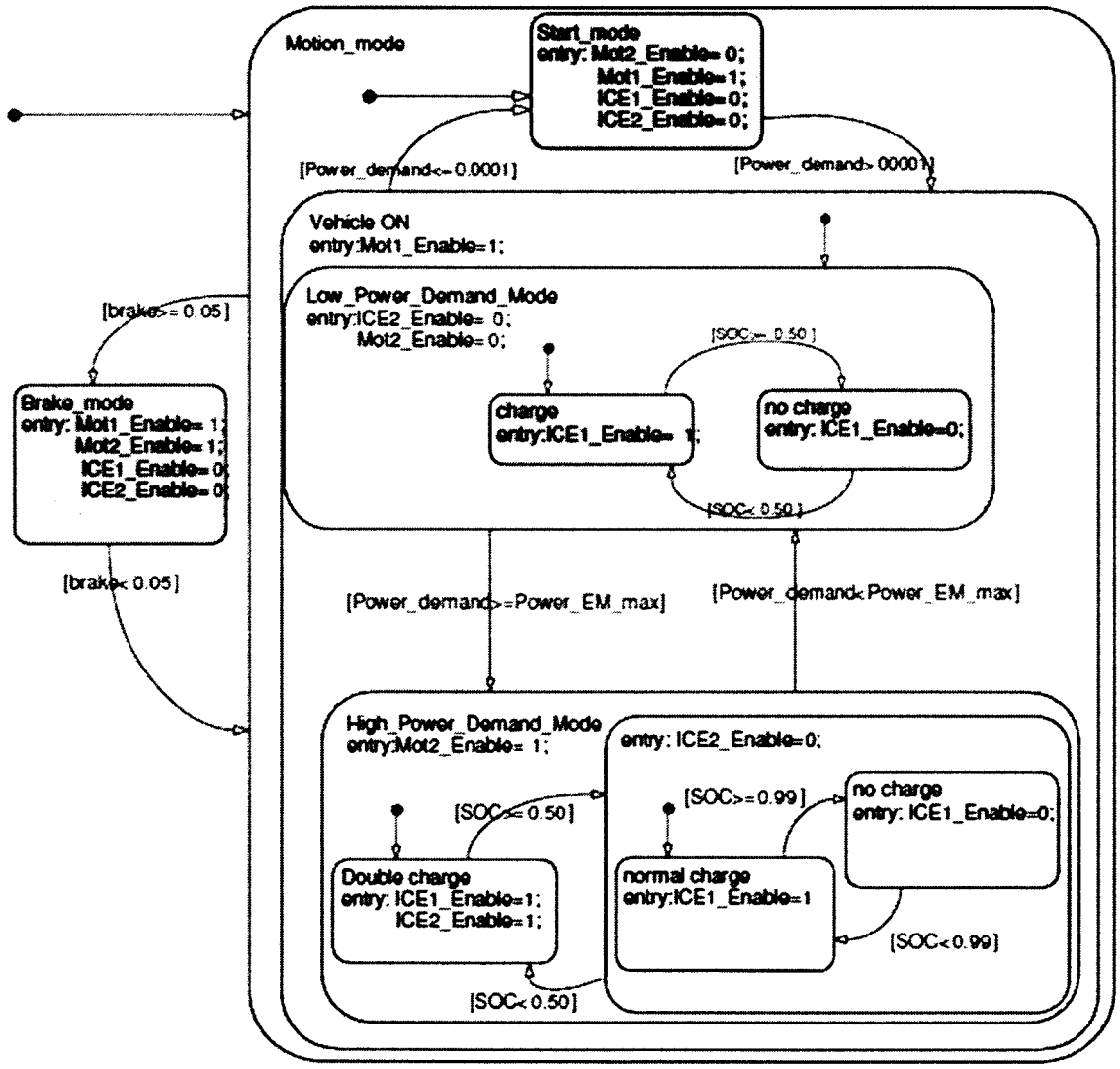

Figure 63. Energy management subsystem block developed in Simulink® Stateflow.®

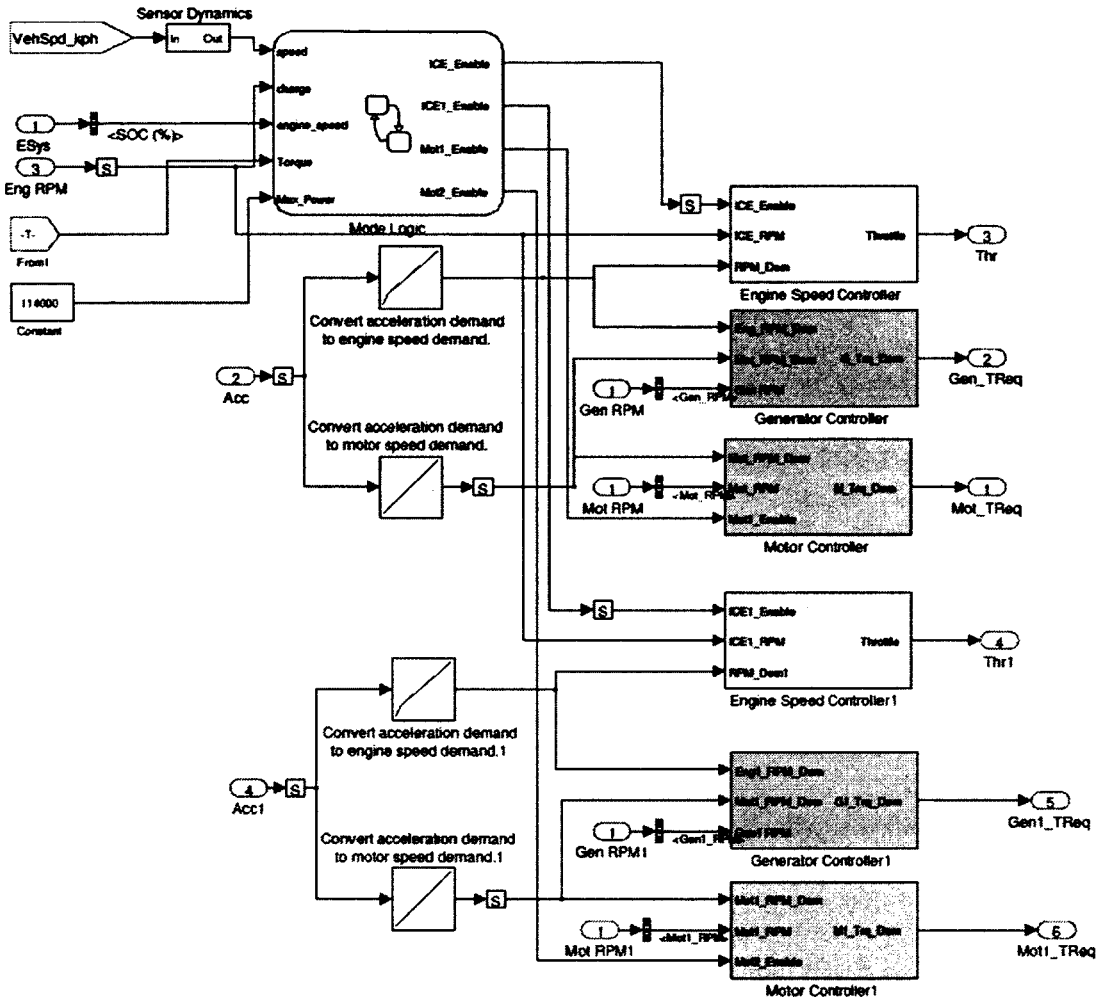

Figure 64. Overall Simulink control module for DE HEV.

The overall control system consists of a supervisory controller, two ICE controllers, two EM controllers, and two generator controllers, as illustrated in Figure 64. The interaction between the control system and vehicle components is shown in Figure 65.

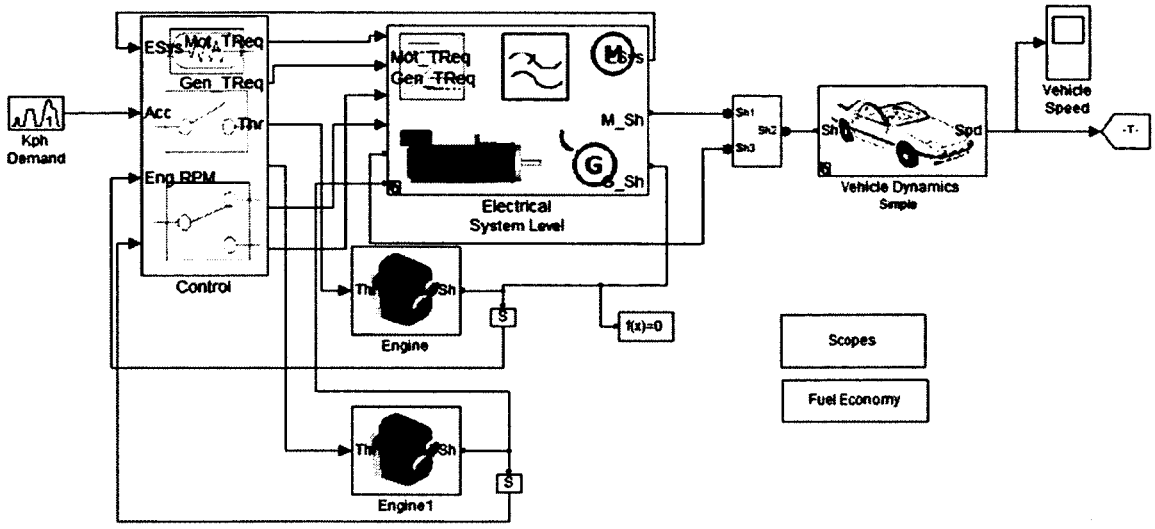

Figure 65. Overall Simulink DE HEV model.

Driving Cycle

A driving cycle is a series of data points representing the speed of a vehicle versus time. Usually, speed is in kph or mph and time in seconds. Driving cycles are formed by different organizations and countries to evaluate vehicles in various ways, in terms of performance, fuel consumption, and polluting emissions (Brundell-Freij & Ericsson, 2005; Ericsson, 2001).

Another use for driving cycles is in vehicle simulation. More specifically, they are used in drivetrain system simulation to predict performance of ICEs, electric drive systems, batteries, etc. One of the first vehicle simulators that used driving cycle was the ADVISOR, produced by AVL Engineering (Fan, 2007).

There are two types of driving cycles: transient driving cycles and modal driving cycles. Yu, Wang, and Shi (2010) stated that "Transient driving cycles involve many

changes such as frequent speed changes during typical on-road driving. Modal driving cycles involve protracted periods at constant speeds. This means that there are parts in these cycles where the speed is constant" (p. 12). The most common driving cycles are the European NEDC, the Japanese10-15, and the American FTP-75 (Cho, 2008).

Description of Driving Cycles Used in the Study

Driving cycles used worldwide can be categorized into three groups:

- European driving cycles;
- US driving cycles; and
- Japanese driving cycles.

Five driving cycles were used in this study; three of them European, one U.S. driving cycle, and one Japanese driving cycle. Data sets for all these driving cycles were taken from the U.S. Environmental Protection Agency (EPA) modeling, testing, and research website.

European Driving Cycles

These driving cycles are modal cycles. This means there are parts in these cycles where speed is constant. Figure 66 represents an urban driving cycle; more specifically, a UN/ECE elementary urban cycle characterized by low vehicle speed (max.50 km/h), low engine load, and low exhaust gas temperature.

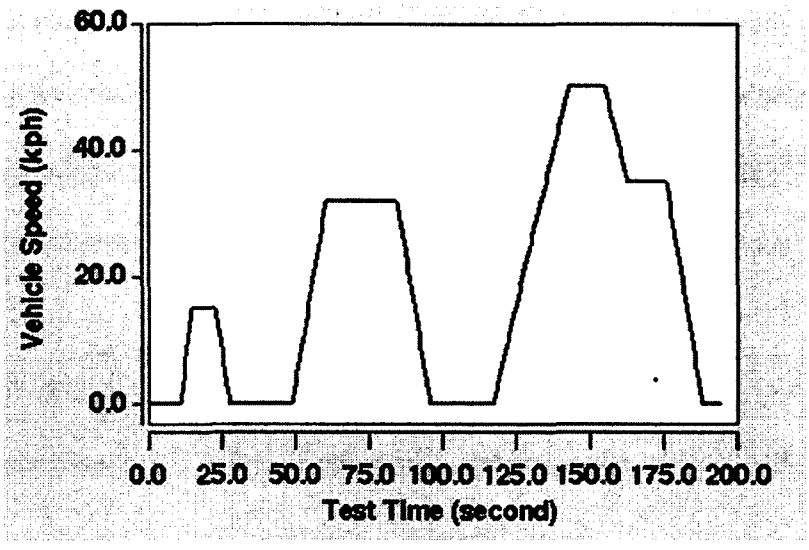

Figure 66. UN/ECE elementary urban cycle.

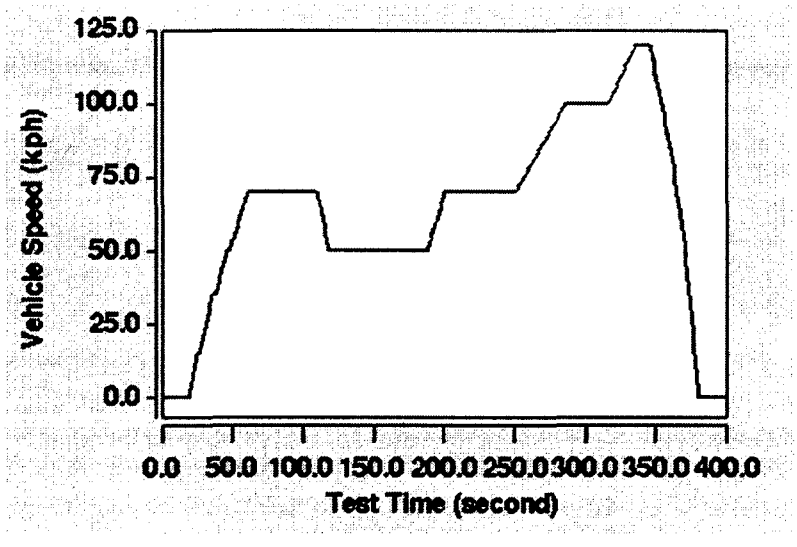

Figure 67. The UN/ECE extra-urban driving cycle.

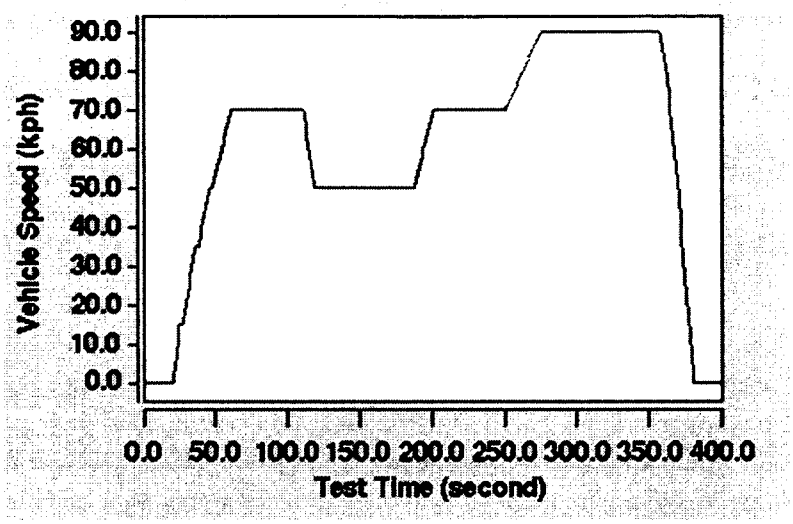

Figure 68. The UN/ECE extra-urban driving cycle (Low powered vehicles).

US Driving Cycles

These driving cycles are transient cycles. They give a better representation of real driving patterns than the model cycles shown in Figure 69. The U.S. drive cycle named FTP 72 (Federal Test Procedure) was used in this study. It has been developed to describe an urban route: "The U.S. FTP-72 cycle is also called Urban Dynamometer Driving Schedule (UDDS) or LA-4 cycle" (Dieselnet, 2000).

Japanese Driving Cycles

Japanese driving cycles belong to modal cycles. In this study, the Japanese 10-15 mode driving cycle was used. There are three cycles for the urban mode. These are "10 mode" for urban routes, "15 mode" for extra-urban routes, and "10-15 mode," which is a combination of the first two driving cycles. This cycle is currently used in Japan to meet

emission certification and fuel economy for light duty vehicles. It is derived from the 10-mode cycle by adding another 15-mode segment of a maximum speed of 70 km/h.

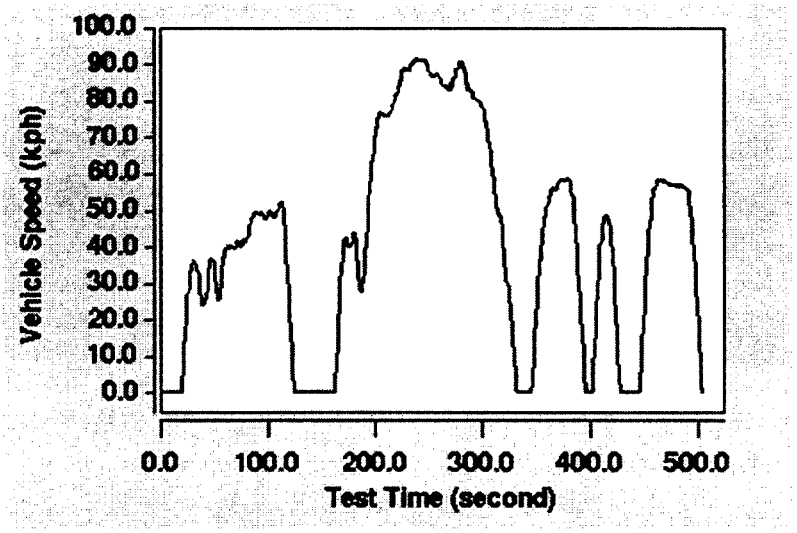

Figure 69. FTP 72 driving cycle.

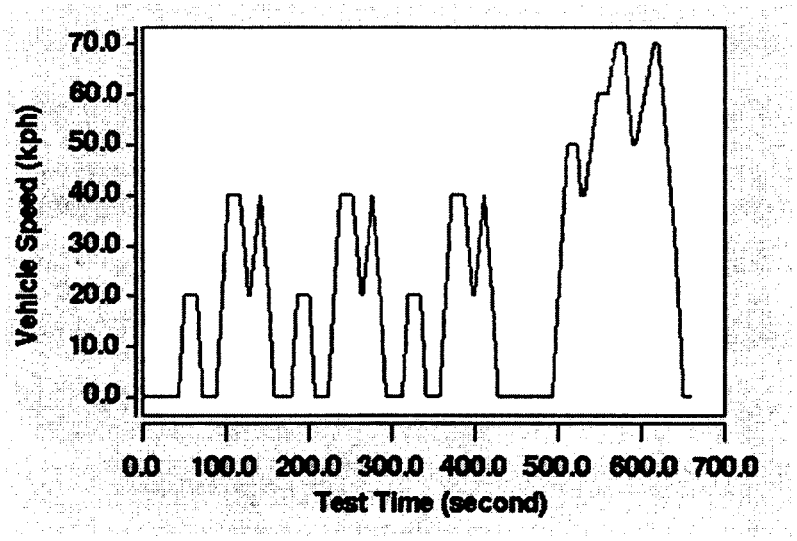

Figure 70. The Japanese 10.15-Mode driving cycle.

Summary of Driving Cycles

As mentioned earlier, five driving cycles were applied to the developed vehicle drivetrain. The driving cycle subsystem gives a time/speed vector as an input to the vehicle control subsystem. Driving cycle 1 is a UN/ECE elementary urban cycle. Its length is 0.944 km in 195 seconds, with an average speed of 18.25 km/h and a maximum speed of 50 km/h. Drive cycle 2 is the UN/ECE extra-urban driving cycle, which runs 6.955 km/h in 400 seconds, with average speed of 62.60 km/h and top speed of 120 km/h, as shown in Figure 67.

Drive cycle 3 is the UN/ECE extra-urban cycle (ECE-EULP), which is an alternative for low-powered vehicles. As illustrated in Figure 68, the duration of this cycle is the same as the UN/ECE driving cycle. Its length is a little bit higher than a UN/ECE, with 6.609 km, and its average speed is significantly lower than the UN/ECE drive cycle, with 90 km/h, as illustrated in Table 9.

Table 9

Driving Cycles Characteristics

Driving Cycle	Duration (Second)	Distance (km)	Average Speed (km/h)	Max Speed (km/h)
UN/ECE Elementary	195	0.994	18.35	50
UN/ECE Extra-Urban	400	6.955	62.59	120
UN/ECE Extra-Urban Low	400	6.609	59.48	90
FTP 72	505	5.78	41.2	91.2
Japanese 10.15 Mode	660	4.16	22.7	70

Drive cycle 4 is the FTP-72 urban drive cycle (Figure 69). This cycle simulates an urban route of 5.78 km with frequent stops. The maximum speed is 91.2 km/h, and the average speed is 41.2 km/h, as shown in Table 9 (Dieselnet, 2000). Driving cycle 5 is a Japanese 10-15-mode driving cycle. The distance of the cycle is 4.16 km, with an average speed 22.7 km/h, and duration 660 seconds, as shown in Figure 70. The duration, distance, average speed, and maximum speed characteristics of all driving cycles were used in this study are summarized in Table 9.

Driving Cycle Subsystem

The vehicle control system block gets its speed demand signal as an input from the vehicle speed demand block. As shown in Figure 71, the vehicle speed demand block allows users to run vehicle simulations individually or with all of them, one after the other. For any driving cycle, it uses speed as a reference speed input, compares it with vehicle speed, and creates the correct acceleration signal output for the vehicle control block.

Component Cost Modeling

Cost Calculation Method

HEV manufacturers use new and developing technologies to produce more efficient and high-performing cars to compete with conventional vehicles. Thus, cost assessments are difficult to determine. However, two significant studies have been done by the Electric Power Research Institute (EPRI) using industry examples to determine vehicle component costs (Golbuff, 2007).

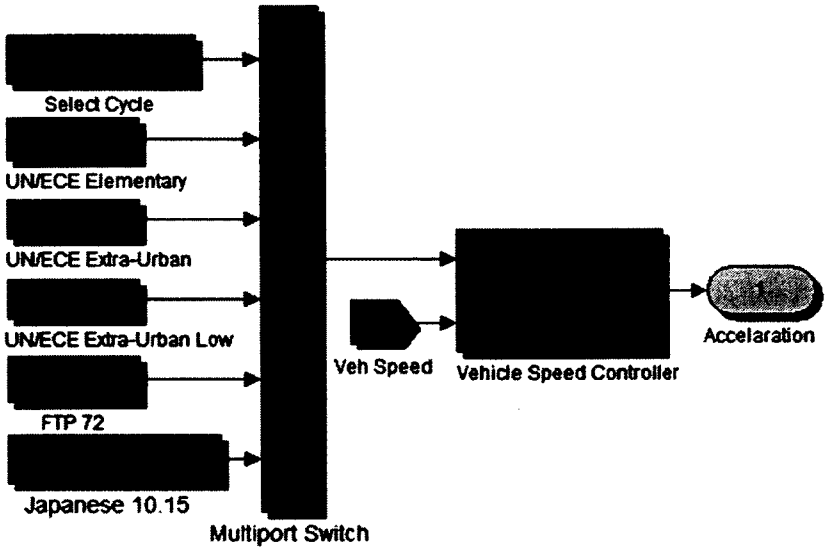

Figure 71. Vehicle speed demand block.

These studies were completed in collaboration with a team that contained representatives from all the major HEV manufacturers. Cost estimates included manufacturing materials and manufacturing volume considerations, and assumed a production of 100,000 units per year (Simpson, 2006).

Component Costs

ICE cost. The EPRI study (2006) was used to estimate engine size cost. Only 4-cylinder ICE was considered consistent with model developed in this study (Pesaran, Simpson, & Markel, 2006). The cost of the ICE, $C_{ICE}(\$)$, was calculated with following equation:

$$C_{ICE}(\$) = \$12.00 * P_E + \$424 \quad (26)$$

where P_E is the peak power of the engine in kW. This equation is valid as long as P_E is lower than 90kW, because an ICE above 90kW P_E becomes a 6-cyclinder ICE with a different cost function.

Electric Motor/ Generator Cost. The cost calculation method for the electric motor also comes from an EPRI study. EPRI estimated the cost of the electric motor, $C_m(\$)$, as:

$$C_M(\$) = \$13.70 * P_M + \$190 \quad (27)$$

where P_m is the peak power of the electric motor in kW. Since it is the most common type of motor used in HEV, a brushless permanent magnet motor was used to derive this equation. Same equation can be used to calculate the cost of an electric generator in HEV.

Besides the electric motor/generator, HEVs also need power electronics to control the electric motor/generator. The EPRI estimated the average cost of typical power electronics systems, $C_{PE}(\$)$, as:

$$C_{PE}(\$) = \$8.075 * P_M + \$235 \quad (28)$$

Battery Pack Cost. Battery pack cost consisted of the cost of the battery manufacturing, thermal management, hardware, and mounting (Golbuff, 2007). Since they are the most advanced type of battery, and will take the place of other types of batteries in the future, according the EPRI (Markel & Simpson, 2006), battery manufacturing cost calculation is based on Lithium-Ion (Li-Ion) batteries. Since Li-Iion batteries are not yet common in the automotive industry, it is difficult to obtain an accurate cost model. Golbuff (2007) stated:

> As a compromise, an industry estimate based on small scale consumer use is used, which is $650 per kWh for Li-Ion batteries. This might be a relatively high

> estimate and as production volumes increase and technology develops, this estimate could be reduced substantially. (p. 43)

The following equation was used to calculate the cost of Li-Ion batteries:

$$C_{Batt,Li-Ion}(\$) = \$650 * Capacity\ [kWh] \quad (29)$$

where $C_{batt,\ Li\text{-}Ion}(\$)$ is the cost of the Li-Ion batteries.

The following equation was used to calculate the cost of battery accessories (hardware, the tray, and thermal management):

$$C_{BattAcc}(\$) = \$1.2 * Capacity\ [kWh] + \$680 \quad (30)$$

where $C_{BattAcc}(\$)$ is the cost of all battery pack accessories (Markel & Simpson, 2006).

Mathematical equations developed for the cost analysis of battery accessories, motor, engine, and power electronics are summarized in Table 10.

Table 10

HEV Powertrain Cost Analysis

	Near-Term Scenario	Long-Term Scenario
Battery Pack cost	Cost($) = ($/kWh + 13) x kWh + 680	Same
Battery Accessories Cost	Cost($) = 1.2*Capacity [kWh]+ $680	N/A
Motor Cost	Cost($) = $21.7 x kW + $425	Cost($) = $16 x kW + 385
Engine Cost	Cost($) = $14.5 x kW + $531	Same
Power Electronics for EM/GM	Cost($) = $8.075 x PM + $532	N/A

Total Powertrain Cost.

Using the aforementioned cost equations for each individual component, the total powertrain cost, $C_{Total}(\$)$ can be calculated as follows:

$$C_{Total}(\$) = C_{ICE}(\$) + C_{M}(\$) + C_{PE}(\$) + C_{Batt,Li-Ion}(\$) + C_{BattAcc}(\$) \quad (31)$$

CHAPTER IV

RESULTS

Fuel Efficiency of the DE-HEV

The DE-HEV model was simulated over standard city and highway drive cycles to demonstrate the fuel efficiency of DE-HEVs over comparable HEVs. The EPA`s fuel economy measurement method was used to calculate the fuel consumption of the DE-HEV. Since fuel consumption is different in city and highway driving, two separate tests were used. An average of city and highway fuel economy values, 55% and 45%, respective, were used to determine combined fuel consumption.

An urban dynamometer driving schedule (UDDS) was used to simulate city driving. It simulates an urban route of 7.5 miles (12.07 km) with frequent stops. As shown in Figure 72, its maximum speed is 56.7 mph (91.2 km/h), and the average speed is 19.6 mph (31.5 km/h; U.S. Environmental Protection Agency, 2010).

In this study, a highway fuel economy driving schedule (HWFET) was used to simulate highway driving. As illustrated in Figure 73, it represents highway driving conditions under the speed of 60 mph. The cycle lasts 765 seconds, covering 10.26 miles (16.45 km), with an average speed of 48.3 mph (77.7 km/h; U.S. Environmental Protection Agency, 2010).

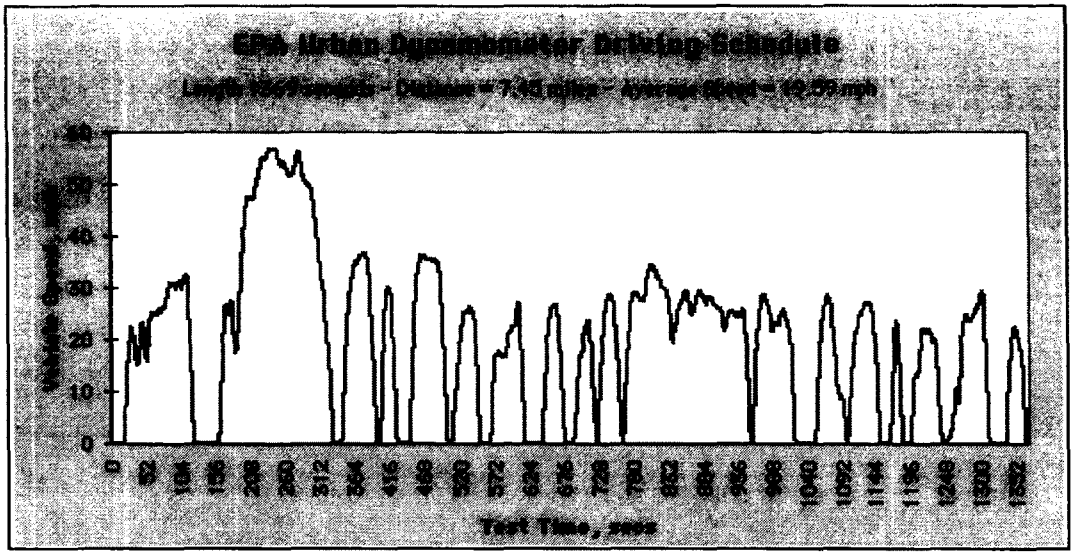

Figure 72. Urban Dynamometer Driving Schedule (UDDS; U.S. Environmental Protection Agency, 2009).

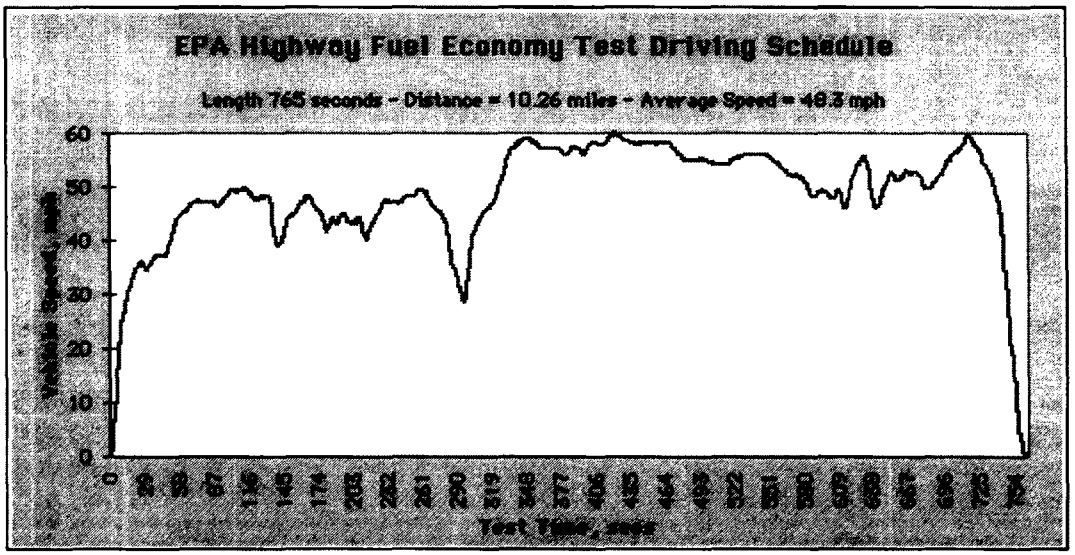

Figure 73. Highway Fuel Economy Driving Schedule (HWFET; U.S. Environmental Protection Agency, 2009).

Figure 74 illustrates the simulation results for the UDDS test. The results show that the proposed DE-HEV model has a fuel consumption rating of 41 mpg. Based on the EPA`s ratings, UDDS testing indicates three mpg higher rating than the 2007 Hybrid Toyota Camry.

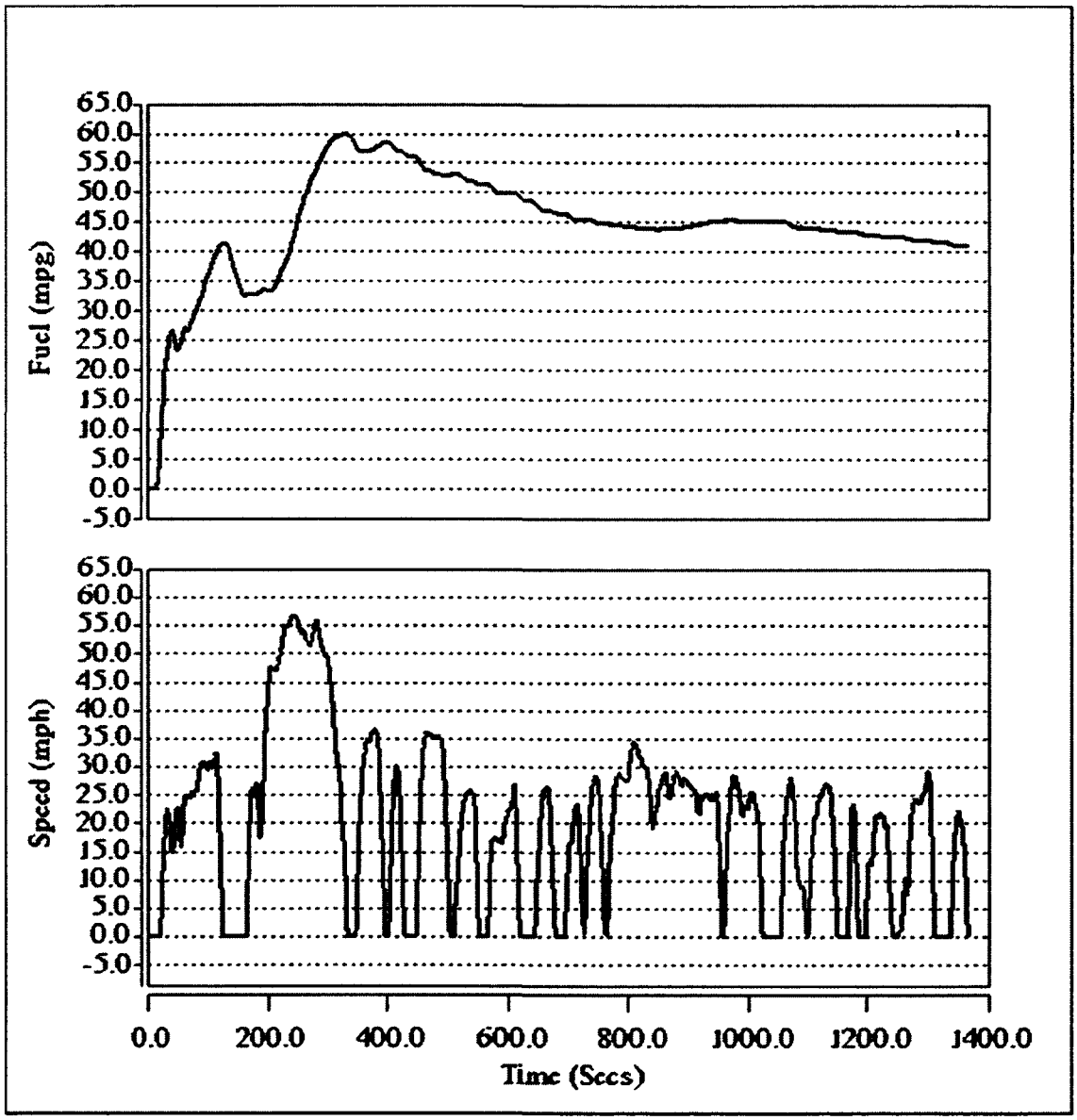

Figure 74. Fuel consumption results for the UDDS drive cycle test.

Figure 75 shows the simulation results for the HWFET test. The proposed DE-HEV model has a 42.3 mpg fuel consumption rating, which is 2.3 mpg higher than the 2007 Hybrid Toyota Camry.

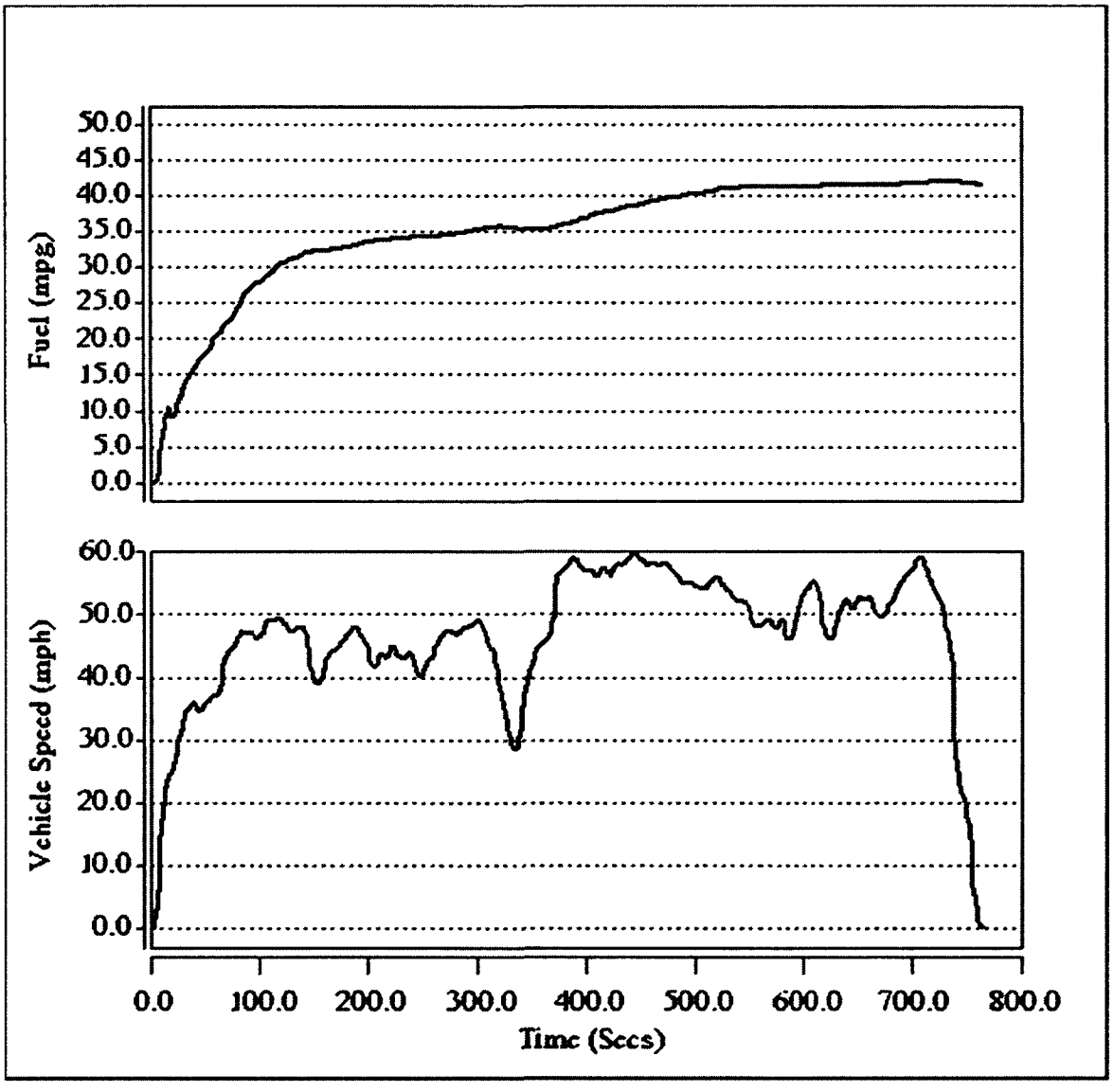

Figure 75. Fuel Consumption results for the HWFET drive cycle test.

Combined fuel consumption rating was calculated as follows:

$$EPA_{overall} = \frac{1}{\left(\frac{0.55}{EPA_{City}} + \frac{0.45}{EPA_{Highway}}\right)} = \frac{1}{\left(\frac{0.55}{41} + \frac{0.45}{42.3}\right)} = 41.6\ mpg$$

The DE-HEV fuel consumption simulation results are summarized and compared with the 2007 Hybrid Toyota Camry, as shown in Table 11. It shows that the simulation of the DE-HEV was successfully performed over the UDDS and the HWFET. It was found that the DE-HEV model demonstrated 2.5% and 10.15% fuel economy improvement over the 2007 Hybrid Toyota Camry for the UDDS and HWFET drive cycles, respectively. The reason for less fuel efficiency improvement in the city driving cycle than in the highway driving cycle is a lack of regenerative breaking logic in the simulated DE-HEV design.

Table 11

Fuel Consumption Comparison of 2007 Hybrid Toyota Camry and the DE-HEV

Fuel Consumption			
	City Driving (mpg)	Highway Driving (mpg)	Combined Driving (mpg)
2007 Hybrid Toyota Camry	40	38	39
Simulated DE-HEV	41	42.3	41.6
% Difference	2.5	10.15	6.25

Vehicle Performance

After the DE-HEV model was completed, it was tested with standardized driving cycles to explore and compare the performance of the developed model. In this section, road performance of the DE-HEV vehicle model was presented based on five drive cycles. The simulation results on these drive cycles were first compared with speed requested (drive cycle) to assess the HE-HEV's performance.

Figure 76, 77, and 78 show the simulation results of vehicle speed following the UN/ECE elementary driving urban cycle, the UN/ECE extra-urban driving cycle, and the UN/ECE extra-urban driving cycle for low-powered vehicles.

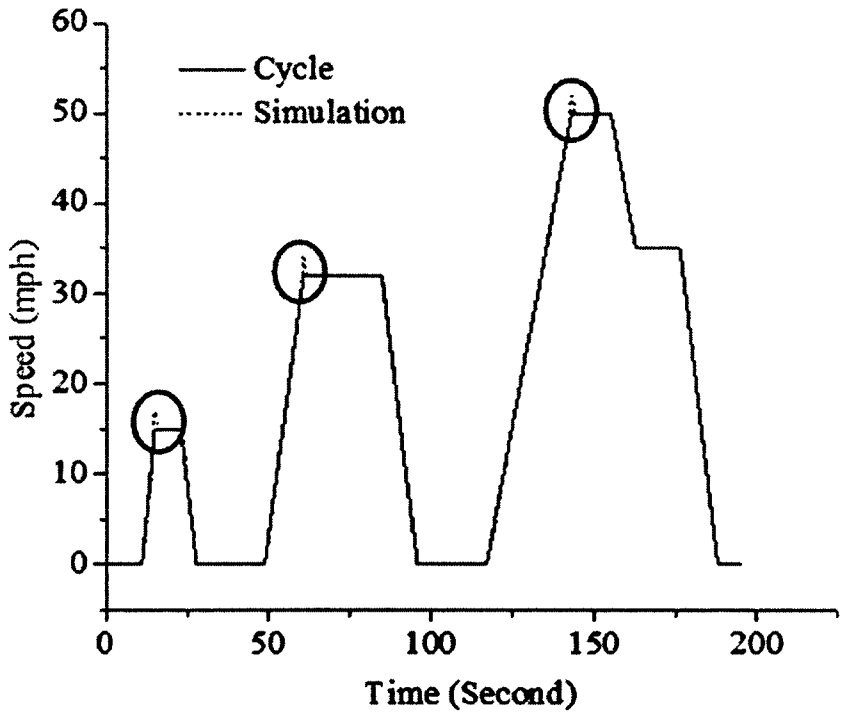

Figure 76. DE-HEV speed on the UN/ECE elementary urban drive cycle.

The UN/ECE elementary urban drive cycle consisted of a gradual acceleration, cruise, and then a deceleration back to stop. These steps were repeated three times, with different peak speed values. The UN/ECE extra-urban drive cycle and the UN/ECE extra-urban drive cycle for low-powered vehicles consisted of a gradual acceleration, cruise, and a deceleration. The solid lines below are driving cycle speed values requested, while the dashed lines are the vehicle speed achieved. Since two lines overlap, is it difficult to see the dashed line in most part of the graphs, as seen in Figure 77. Speed differences between the two are circled in the figures. There were barely noticeable differences between the two, which are circled in the figures.

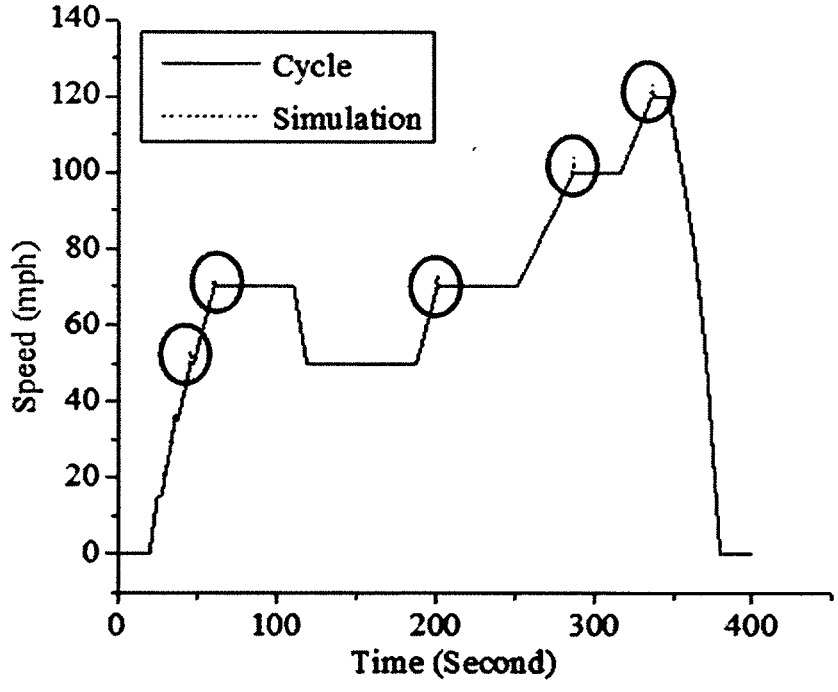

Figure 77. Vehicle speed on the UN/ECE extra-urban driving cycle.

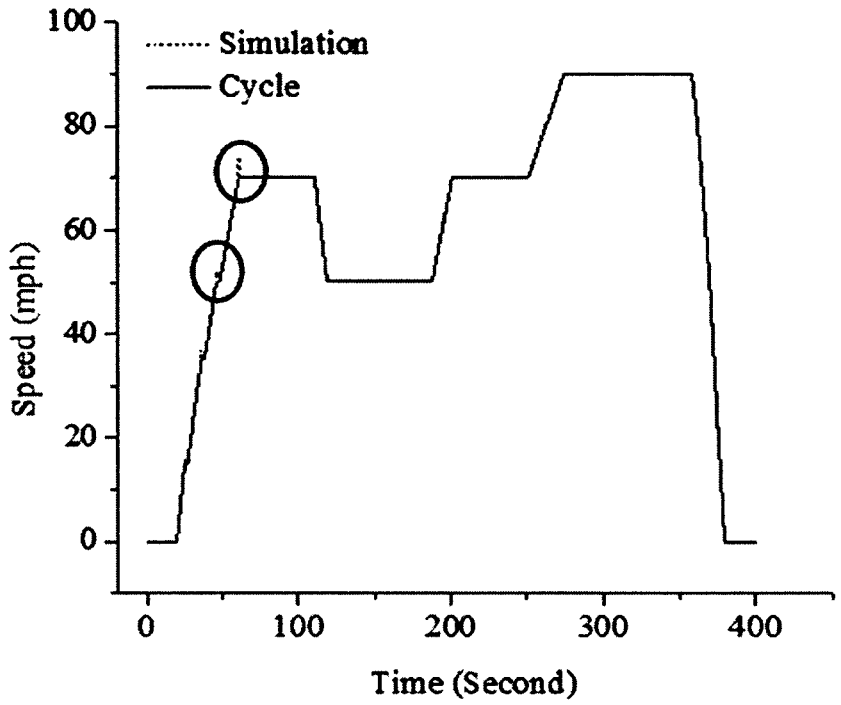

Figure 78. Vehicle Speed on the UN/ECE Extra-Urban Driving Cycle (Low-Powered Vehicles)

Figure 79 shows the simulation results of the vehicle speed on the FTP 72 driving cycle. The solid line is drive cycle speed, while the dashed line is vehicle speed in the simulated vehicle. The speed differences between the two are circled in the figure. The simulated DE-HEV showed as slightly underpowered during rapid acceleration. It was also not able to follow requested speed values when the speed request change was fast. The DE-HEV behaved significantly different than the requested speed, as seen in Figure 79; however, the difference was within the acceptable range. Overall, the vehicle showed adequate power supply.

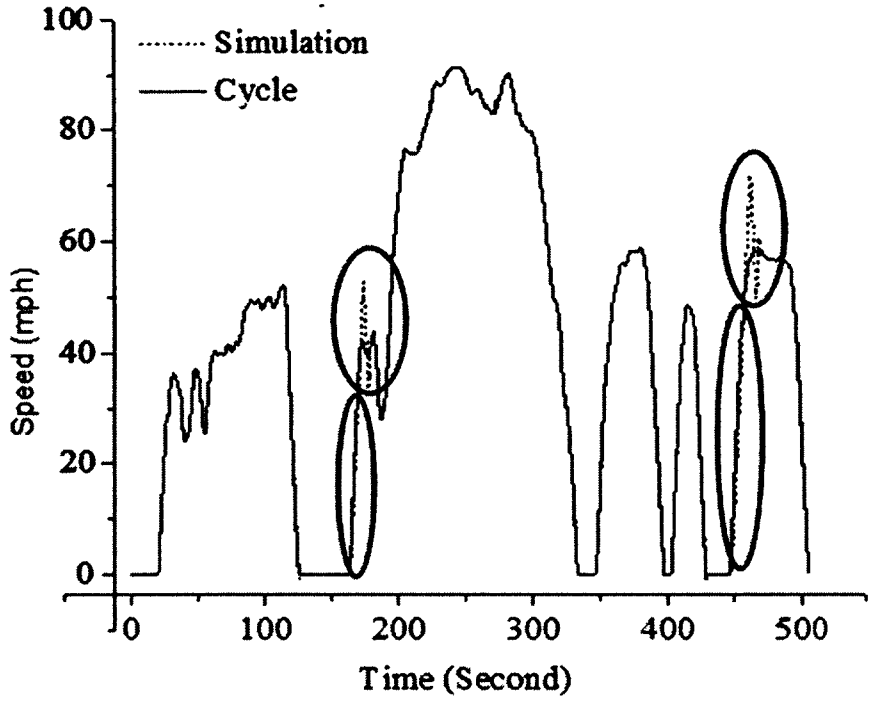

Figure 79. Vehicle speed on FTP 72 driving cycle.

Figure 80 shows the simulation results of vehicle speed on the Japanese 10.15 driving cycle. This cycle contains examples of aggressive acceleration and deceleration in low and high speed values. The solid line is a drive cycle speed, while the dashed line is vehicle speed in the simulated vehicle. The speed differences between the two are circled in the figure. The simulated DE-HEV performed slightly under power during rapid acceleration; however, the difference was within the acceptable range (Pasquier & Rousseau., 2001).

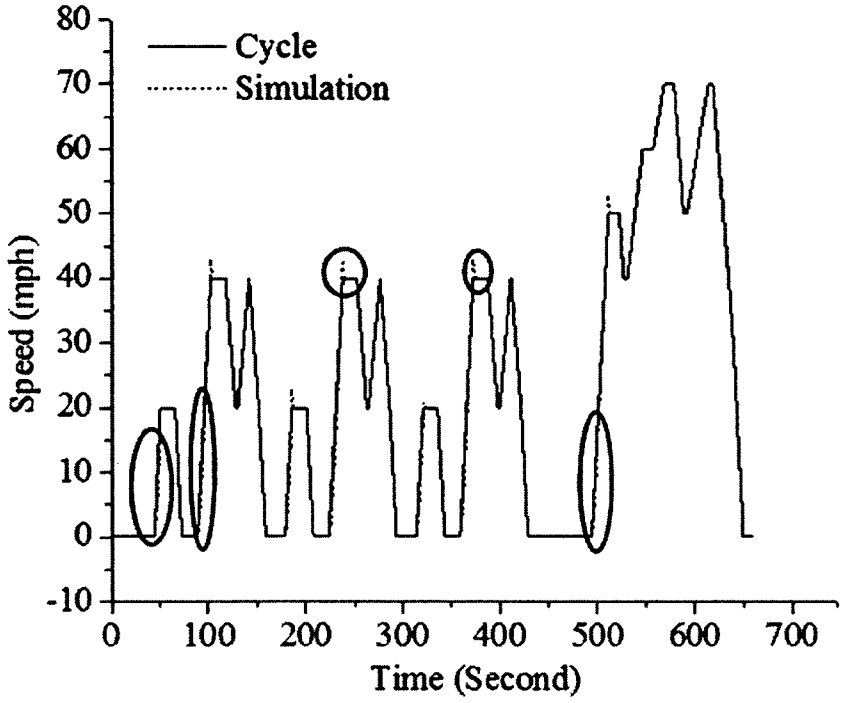

Figure 80. Vehicle speed on the Japanese 10.15 mode driving cycle.

Overall, the simulated DE-HEV succeeded in completing five driving cycles with no significant cycle miss-match. This indicated that the DE-HEV powertrain provided adequate power for the vehicle propulsion in all driving cycles.

Cost of the DE-HEV Powertrain

As in all new technologies, the success of DE-HEV depends on its manufacturing cost. It needs to be significantly more fuel efficient than current HEVs, and also cost competitively to be a viable option and have a future chance of commercialization. The cost of powertrain components (ICE, electric motor, electric generator, power electronics, and battery) has been studied for both the 2007 Toyota Hybrid Camry and the proposed

DE-HEV. A cost analysis model of each component was done based on two studies from the EPRI. This cost model was simplified by ignoring the time variable due to the complexity of the model (Burress et al., 2008). Cost model equations reflect the most updated information and parameters from 2010.

Figure 81 illustrates variations of the HEV EM/generator and the cost of power electronics components at peak power, based on the EPRI's study.

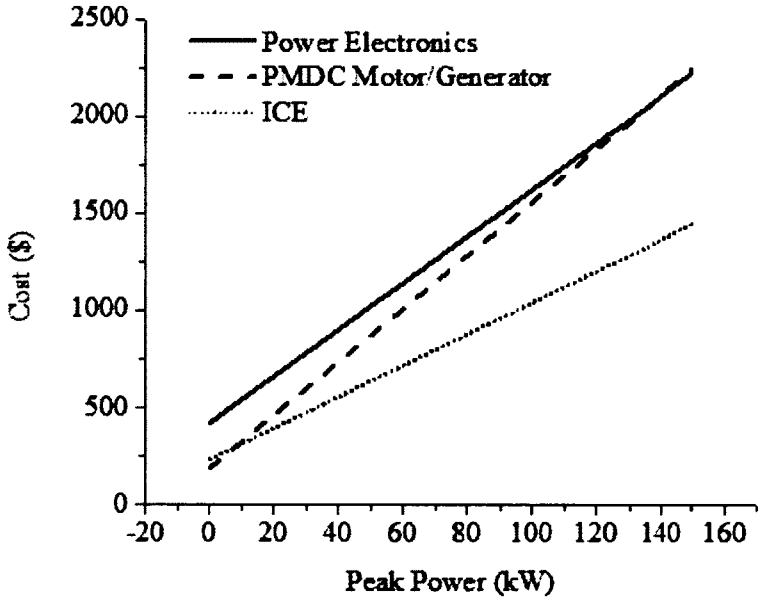

Figure 81. Variation of HEV component cost by peak power.

ICE Cost

The cost of the ICE, C_{ICE}($), was calculated with following equation:

$$C_{ICE}(\$) = \$12.00 * P_E + \$424 \quad (26)$$

where P_E is the peak power of the engine in kW.

Using above equation, the cost of an ICE for a Hybrid Camry and the DE-HEV was calculated as follows:

$$C_{ICE\_Hybrid\_Camry}(\$) = \$12.00 * 147 + \$424 = \$2188$$

$$C_{ICE\_DE\_Hybrid\_Camry}(\$) = 2 * (\$12.00 * 73 + \$424) = \$2600$$

Electric Motor/ Generator Cost

EPRI estimates the cost of the electric motor, $C_m(\$)$, as:

$$C_M(\$) = \$13.70 * P_M + \$190 \quad (27)$$

where P_m is the peak power of the electric motor in kW.

Using the equation, the cost of the EM and generator for the Hybrid Camry and the DE-HEV was calculated as follows:

$$C_{M\_Hybrid\_Camry}(\$) = \$13.70 * 105 + \$190 = \$1628$$

$$C_{M\_DE\_Hybrid\_Camry}(\$) = 2 * (\$13.70 * 50 + \$190) = \$1750$$

Power Electronics Cost

EPRI estimates the average cost of typical power electronics, $C_{PE}(\$)$, as:

$$C_{PE}(\$) = \$8.075 * P_M + \$235 \quad (28)$$

Using above equation, the cost of power electronics for the Hybrid Camry and the DE-HEV was calculated as follows:

$$C_{PE\_Hybrid\_Camry}(\$) = \$8.075 * 105 + \$235 = \$1082$$

$$C_{PE\_DE\_Hybrid\_Camry}(\$) = 2 * (\$8.075 * 50 + \$235) = \$1277$$

Battery Pack Cost

Battery is the most important component in defining the cost of the HEV. Since the DE-HEV is a series type of HEV, its reliance on a battery is higher in peak power demand. Hence, a slightly bigger battery capacity was chosen for the DE-HEV to avoid performance failure during high power demand.

Figure 82 presents the battery and battery accessories cost function in the capacity range from 0.8 kWh to 2 kWh. As mentioned in Chapter 3, a Li-Ion battery was used in DE-HEV, as in the 2007 Hybrid Camry. The following equation was used to calculate cost of Li-Ion batteries:

$$C_{Batt,Li-Ion}(\$) = \$650 * Capacity\ [kWh] \quad (29)$$

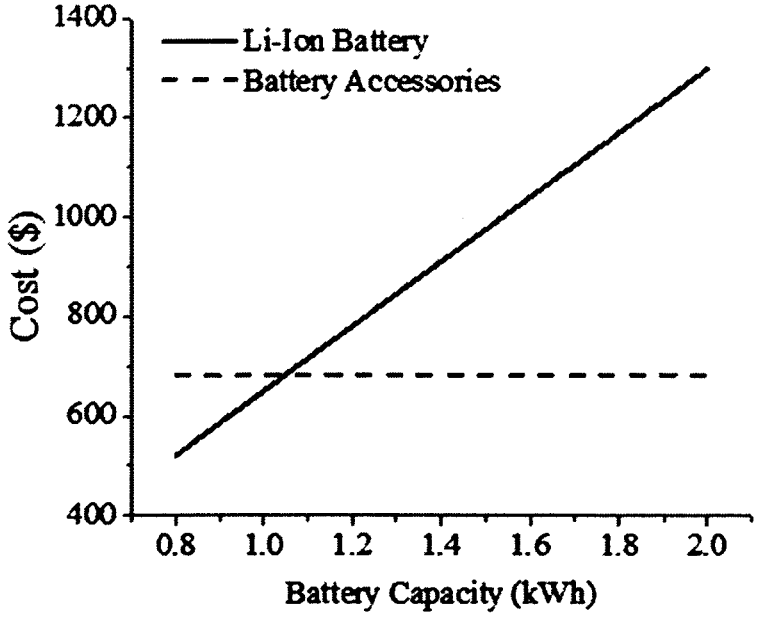

Figure 82. Variation of battery and cost of accessories by battery capacity

Using the equation, the cost of the battery for the Hybrid Camry and the DE-HEV was calculated as follows:

$$C_{Batt\_Hybrid\_Camry}(\$) = \$650 * 1.591 = \$1034$$

$$C_{Batt\_DE\_Hybrid\_Camry}(\$) = \$650 * 1.872 = \$1216$$

where $C_{batt,\ Li\text{-}Ion}(\$)$ is the cost of the Li-Ion batteries.

The following equation was used to calculate the cost of battery accessories (hardware, the tray, and the thermal management):

$$C_{BattAcc}(\$) = \$1.2 * Capacity\ [kWh] + \$680 \quad (30)$$

where $C_{BattAcc}(\$)$ is the cost of all battery pack accessories.

Using the equation, the cost of battery accessories for the Hybrid Camry and the DE-HEV was calculated as follows:

$$C_{BattAcc\_Hybrid\_Camry}(\$) = \$1.2 * 1.6\ [kWh] + \$680 = \$681.9$$

$$C_{BattAcc\_DE\_Hybrid\_Camry}(\$) = \$1.2 * 1.875\ [kWh] + \$680 = \$682.25$$

Total Powertrain Cost

Total powertrain cost was calculated as follows:

$$C_{Total}(\$) = C_{ICE}(\$) + 2 * C_M(\$) + C_{PE}(\$) + C_{Batt,Li-Ion}(\$) + C_{BattAcc}(\$) \quad (31)$$

Using the aforementioned cost equations for each individual component, the total powertrain cost, $C_{Total}(\$)$ can be calculated as follows:

$$C_{Total\_Hybrid\_Camry}(\$) = \$2188 + 2 * \$1628 + \$1082 + \$1034 + \$682$$

$$C_{Total\_Hybrid\_Camry}(\$) = \$8242$$

$$C_{Total\_DE\_Hybrid\_Camry}(\$) = \$2600 + 2 * \$1750 + \$1277 + \$1216 + \$682$$

$$C_{Total\_DE\_Hybrid\_Camry}(\$) = \$9275$$

Table 12

Cost of Powertrain Components

Cost of Powertrain Components ($)		
Component	2007 Toyota Hybrid Camry	DE-HEV
ICE	2188	2600
Electric Motor	1628	1750
Electric Generator	1628	1750
Power Electronics	1082	1277
Battery	1034	1216
Battery accessories	682	682
TOTAL	8242	9275

The calculated cost of each powertrain component, and the overall cost of the DE-HEV are summarized in Table 12.

The percentage difference of the DE-HEV and the Hybrid Camry was calculated as follows:

$$\%\, Diff = \frac{C_{Total\_DE\_Hybrid\_Camry}(\$) - C_{Total\_Hybrid\_Camry}(\$)}{C_{Total\_DE\_Hybrid\_Camry}(\$)}$$

$$\%\, Diff = \frac{\$9275 - \$8242}{\$9275} = \%11.1$$

As seen in the above equation, the DE-HEV cost %11.1 more than conventional hybrids for the configuration in this study.

According to the report, "Hybrid-Electric Vehicle Design Retail and Lifecycle Cost Analysis," published by Lipman and Delucchi (2003), it was estimated that HEV retail prices ranged from approximately $2,500 to $6,700 more than the estimated retail

price of baseline ICE vehicles. This means that HEVs cost 12% to 33.5% more than ICE vehicles, depending on the hybridization ratio, and adding around 11.1% on top of the current manufacturing cost of HEVs makes the DE-HEV cost 23% to 45% more than ICE vehicles. Considering the high initial cost, a weak global economy, and sluggish HEV sales, the DE-HEV option may not have a good chance unless it offers significant fuel-efficiency increases compare with HEVs and ICE vehicles.

CHAPTER V

CONCLUSIONS, SUMMARY, AND RECOMMENDATIONS

In the previous chapter, the DE-HEV model simulation results were presented and discussed. The simulation results showed that the DE-HEV has better fuel efficiency and it performs as good as other comparable vehicles; but it costs significantly more than HEVs and traditional vehicles.

In this chapter, results of the DE-HEV model simulation will be discussed, guided by the research hypothesis. Then the summary of the study and recommendations for future are presented.

Research Questions of the Study

A set of four questions were used as the basis of this study. The objective of this study was to develop and validate the dual-engine hybrid vehicle power train simulation model.

The research hypotheses were:

1. Modeling of the dual-engine hybrid vehicle components can be developed in MATLAB®/Simulink® simulation software, meeting the industry requirements.
2. There will be measurable efficiency increase in the dual-engine hybrid vehicle model compared to conventional combustion engine models.
3. The simulation model developed for the dual-engine hybrid vehicle will perform similarly to actual vehicle operation.

4. The overall cost of the simulation model will not be higher than the conventional, combustion engine model.

Component validation results show that component models can be developed with less than +-5% margin of error. Based on validation results of power train component models, it can be said that dual-engine hybrid vehicle components can be developed using MATLAB®/Simulink® simulation software, meeting industry requirements.

The fuel consumption of the DE-HEV model, and its HEV equivalent, were compared over the same standard drive cycles. It is shown that the DE-HEV model successfully performed over the EPA Urban Dynamometer Driving Schedule (UDDS) and the Highway Fuel Economy Cycle (HWFET). The hybrid vehicle model demonstrated a 2.5% and a 10.15% improvement in fuel economy over the conventional hybrid vehicle for the UDDS and HWFET drive cycles, respectively. Due to lack of regenerative logic in the overall control system, the vehicle is not able to take advantage of regenerative braking comparable to a HEV; hence, the increase in fuel economy in UDDS was less than in HWFET.

Unlike what has been hypothesized, the overall cost of the simulation model was significantly higher than the conventional combustion engine vehicle and the HEV model. Simulation results show that the developed DE-HEV model costs 11.1% higher than its HEV equivalent. Previous studies show that HEVs cost 12% to 33.5% more than ICE vehicles, depending on the ratio of hybridization. Adding around 11.1% on top of the current manufacturing cost of HEVs makes the DE-HEV model cost 23% to 45% more than the ICE vehicle equivalent.

The DE-HEV model performance was simulated over European ECE, U.S. FTP-72 and Japanese 10.15 drive cycles. Simulation results showed that the DE-HEV performed with high accuracy in following drive cycles, except that it showed minor underpowered issues in the FTP-72 driving cycle.

In conclusion, simulation results showed that DE-HEV has a 2% to 10% higher efficiency than comparable HEVs. Cost analysis results showed that the manufacturing cost of DE-HEV is 11% higher. Performance of the vehicle was tested with standard drive cycles, and the results are satisfactory. Although there was a significant increase in fuel-efficiency, because of its higher initial manufacturing cost and complexity, DE-HEVs may have challenges in the short term. With expected decreases in the manufacturing cost of battery storage and power electronics technology, the DE-HEVs is a feasible option in the near future.

Summary of the Study

With increasing oil prices, and growing environmental concerns, cleaner and sustainable energy solutions are in demand. At present, different types of HEVs offer less oil dependent, cleaner, and more efficient solutions; but the demand for hybrid vehicles is still not on a desired level. More research is needed to develop more efficient and better-performing vehicles. The objective of this study was to develop a DE-HEV that provides a significant increase in fuel economy while maintaining the performance of HEVs and traditional vehicles.

MATLAB®/Simulink® software was used to simulate the DE-HEV. Component models, such as engines, generators, motors, and DC-DC converters were modeled.

Models were validated by means of lab tests completed in the literature and on manufacturer's datasheets for actual components. Controller modules were developed for engine, electric motor, and generator subsystems. A supervisory power management was established to control each subsystem by interacting with their controllers. A complete DE-HEV model was simulated using developed component models and an energy management system. Necessary changes in component models and energy management strategies were made based on the simulation results to find an optimum configuration and energy management strategy in terms of performance and fuel economy. Simulation results were compared with the HEV equivalent on the market to see if the dual engine, power train model is viable option for heavy-duty vehicles.

Recommendations for Future Study

The MATLAB®/Simulink® DE-HEV model offers a simulation platform that is modular, flexible, and can be easily modified for different sized components. In addition, simulation results demonstrated the fuel economy advantage of the DE-HEV over the comparable HEVs; however, additional work is recommended to further optimize the efficiency of the supervisory power management controller and other controllers, including the ICE controller and the motor controller. Since the current power management controller covers a limited number of possible conditions in the vehicle, and does not contain regenerative braking logic, it is recommended that a more sophisticated power management controller to be implemented to optimize the overall efficiencies of the engine and the motor/generator.

Although already developed component models were validated with the test data, and a 5% margin of error was achieved, the accuracy of the DE-HEV can be greatly improved by utilizing a more detailed component model. A more detailed component model should be developed to increase accuracy reliability.

Simplified cost analysis has been done for this study. A more detailed cost-benefit analysis should be implemented to better assess the viability of the DE-HEV design. In this study, equal sized engines and motors/generators were used. The results indicate that power train component sizing optimization may increase fuel efficiency of the DE-HEV.

REFERENCES

Adeli, S., & Sarvi, M. (2010). A neural network method for estimation of battery available capacity. 45th International Universities' Power Engineering Conference, UPEC 2010. *Proceedings of the Universities Power Engineering Conference*.

Anderson, J. D. (1997). *A history of aerodynamics and its impact on flying machines*. Cambridge: Cambridge University Press.

Argonne National Laboratory. (2010, 9). *Transportation Technology R&D Center*. Retrieved February 23, 2011, from http://www.transportation.anl.gov/modeling_simulation/PSAT/index.html

Banjac, T., Trenc, F., & Katrasnik, T. (2009, January 01). Energy conversion efficieny of hybrid electric heavy-duty vehicles operating according to diverse drive cycle. *Energy Conversion and Management, 50*(12), 2865-2878.

Bayindir, K. C., Gözüküçük, M. A., & Teke, A. (2010, February 01). A comprehensive overview of hybrid electric vehicle: Powertrain configurations, powertrain control techniques and electronic control units. *Energy Conversion and Management, 52*(2), 1305–1313.

Brown, D., Alexander, M., Brunner, D., Advani, S. G., & Prasad, A. K. (2008). Drive-Train simulator for a fuel cell hybrid vehicle. *Journal of Power Sources*, 275-281.

Brundell-Freij, K., & Ericsson, E. (2005, May). Influence of street characteristics, driver category and car performance on urban driving patterns. *Transportation Research Part D Transport and Environment, 10D*(3), 213-229.

Burress, T. A., Coomer, C. L., Campbell, S. L., Seiber, L. E., Marlino, M. D. (2008). *Evaluation of the 2007 Toyota Camry Hybrid Synergy Drive System.* Oak Ridge, TN: Oak Ridge National Laboratory.

Chan, C. C., & Wong, Y. S. (November 01, 2004). Electric vehicles charge forward. *IEEE Power and Energy Magazine, 2,* 6, 24-33.

Chau, K. T., & Chan, C. C. (2001). *Modern electric vehicle technology*. New York, NY: Oxford University Press.

Cho, B. (2008).*Control of a hybrid electric vehicle with predictive journey estimation.* (Doctoral Dissertation). Retrieved from https://dspace.lib.cranfield.ac.uk/handle/1826/2589

Dieselnet. (2000, April). Retrieved September 16, 2011, from http://www.dieselnet.com/standards/cycles/ftp72.php

Duty Cycle. (2011). Retrieved September 10, 2011, from http://www.radartutorial.eu/18.explanations/ex28.en.html

Ecolife Dictionary. (2006). Retrieved September 14, 2011, from http://www.ecolife.com/define/greenhouse-gas.html

ECU. (2000). *websters-online-dictionary.org*. Retrieved August 30, 2005, from http://www.websters-online-dictionary.org/definitions/Electronic+control+unit?

Ehsani, M., & Gao, Y. (2006, May). Parametric Design of the Traction Motor and Energy Storage for Series Hybrid Off-Road and Military Vehicles. *IEEE Transactions on Power Electronics, 21*(3), pp. 749-755.

Ehsani, M., Gao, Y., Gay, S. E., & Emadi, A. (2005). *Modern electric, hybrid electric, and fuel cell vehicles: fundamentals, theory, and design.* Boca Raton, FL: CRC press.

Ehsani, M., Gao, Y., Gay, S. E., & Emadi, A. (2010). *Modern electric, hybrid electric, and fuel cell vehicles: fundamentals, theory, and design* (2nd ed.). Boca Raton, FL: CRC Press.

Electric motors and generators. (2007). Retrieved September 14, 2008, from http://www.physclips.unsw.edu.au/jw/electricmotors.html#DCmotors.

Electric Power Research Institute (EPRI). (2001). *Comparing the Benefits and Impacts of Hybrid Electric Vehicle Options.* Palo Alto, CA: EPRI.

Emadi, A., Mi, C., & Gao, D. W. (2007). Modeling and Simulation of Modeling and Simulation of. *Proceedings of the IEEE*, (pp. 729-745).

Ericsson, E. (2001). Independent driving pattern factors and their influence on fuel-use and exhaust emission factors. *Transportation Research Part D Transport and Environment, 6*(5), 325-345.

F1 technical glossary. (2008). Retrieved August 21, 2011, from http://www.f1technical.net/glossary/g

Fan, B. S.-M. (2007). *Modeling and simulation of a hybrid electric vehicle using MATLAB/Simulink and ADAMS.* Waterloo, Ontario: University of Waterloo.

Fang, L., & Qin, S. (2006). Optimal Control of Parallel Hybrid Electric Vehicles Based on Theory of Switched Systems. *Asian Journal of Control*, 274-280.

Fuhs, A. (2009). *Hybrid Vehicles and the Future of Personal Transportation.* Boca Raton, FL: CRC Press.

Gao, W., & Musunuri, S. (2006). Hybrid Electric Vehicle Modeling and Analysis in Generic Modeling Environment. *Vehicle Power and Propulsion Conference* (pp. 1-6). Windsor, United Kingdom: IEEE.

Global Smart Energy. (2011). *Smart Grid Focus Cruising the Electric Vehicle Fast Lane.* Seattle, WA.

Golbuff, S. (2007). *Design optimization of a plug-in hybrid electric vehicle* (Doctoral Dissertation). Retrieved from http://search.proquest.com/docview/28969735?accountid=10906

History of Hybrid Vehicles. (2006, April 27). Retrieved September 8, 2010, from Hybridcars: http://www.hybridcars.com/history/history-of-hybrid-vehicles.html

Hou, J., & Guo, X. (2008). Modeling and Simulation of Hybrid Electric Modeling and Simulation of Hybrid Electric Vehicles Using HEVSIM and ADVISOR. *IEEE Vehicle Power and Propulsion Conference (VPPC)* (pp. 1 - 5). Harbin, China: Institute of Electrical and Electronics Engineers (IEEE).

How Motors Work. (2008). Retrieved May 30, 2008, from http://www.stefanv.com/rcstuff/qf200212.html

Huff, M. R. (1999). *A LabVIEW based wind tunnel data acquisition system.* (Master Thesis). Retrieved from http://search.proquest.com/docview/23953011?accountid=10906

Husain, I. (2005). *Electric and hybrid Vehicles Design Fundamentals.* Boca Raton, FL: CRC Press.

HybridCARS. (2006, April 03). Retrieved September 6, 2010, from Regenerative Braking: http://www.hybridcars.com/components/regenerative-braking.html

Internal Combustion Engine. (2008). Retrieved September 14, 2011, from http://www.sccs.swarthmore.edu/users/08/ajb/tmve/wiki100k/docs/Internal_combustion_engine.html

Jackson, T. (2010, July 19). *Emissions regulations: Challenges and solutions.* Retrieved October 5, 2010, from SAE International: http://www.sae.org/mags/sohe/8554

Jensen, M. (2006). *Improving System Reliability Using the Saber® Simulator in a Robust Design Flow.* Mountain View, CA: Synopsys, Inc..

Katrasnik, T. (2009, January 01). Analytical framework for analyzing the energy conversion efficency of different hybrid vehicle topologies. *Energy Conversion and Management, 50*(8), 1924-1938.

Katsargyri, G. E. (2008). *Optimally controlling hybrid electric vehicles using path forecasting.* (Master Thesis). Retrieved from http://dspace.mit.edu/handle/1721.1/44455

Kellermeyer III, W. F. (1998, May). *Development and Validation of a Modular Hybrid Electric Vehicle.* Retrieved November 15, 2010, from ProQuest Dissertations and Theses: http://www.proquest.com/en-US/

Levine, W. S., & Hristu-Varsakelis, D. (2005). *Handbook of networked and embedded control systems.* Boston: Birkha□user.

The Library of Congress. (2007, July 27). *Today in History.* Retrieved September 11, 2010, from http://lcweb2.loc.gov/ammem/today/jul30.html

Lipman, T. E., & Delucchi, M. A. (2003, March 01). Hybrid-Electric Vehicle Design Retail and Lifecycle Cost Analysis. *Transportation Research Part D, 11*(2), 115-132.

Lorenzo, S. (2009). *A comparative analysis of energy management strategies for hybrid electric vehicles.* (Doctoral Dissertation). Retrieved from http://search.proquest.com.proxy.lib.iastate.edu:2048/docview/304986201/13753B1FBEA765F4765/1?accountid=10906

Markel, T., Brooker, A., Hendricks, T., Johnson, V., Kelly, K., Kramer, B., . . . Wiple, K. (2002). ADVISOR: a systems analysis tool for advanced vehicle modeling. *Journal of Power Sources*, 255–266.

Markel, T., & Simpson, A. (2006). Cost-Benefit Analysis of Plug-In Hybrid-Electric Vehicle Technology (Presentation). *The 22nd International Electric Vehicle Symposium*, (pp. 1-13). Yokohama, Japan.

The MathWorks. (2005, December). *Learning MATLAB 7.* Retrieved February 27, 2011, from MathWorks: http://www.mathworks.com/academia/student_version/learnmatlab_sp3.pdf

The MathWorks. (2012, March). Simulink Getting Started Guide. Natick, MA. Retrieved May 16, 2012, from http://www.mathworks.com/help/pdf_doc/simulink/sl_gs.pdf

The MathWorks, Inc. (2012). Stateflow. Retrieved September 12, 2011, from: http://www.mathworks.com/academia/student_version/r2012a_products/stateflow.pdf

McBroom, S. T. (1997). Toolkit for Tomorrow's Car. *Technology Today, 18*(1), pp. 10-13.

Mi, C. (2004). *University of Michigan.* Retrieved August 13, 2011, from http://groups.engin.umd.umich.edu/vi/w4_workshops/Mi%20_W04.pdf

Moore, T. C. (1996). Tools and Strategies for Hybrid-Electric Drivesystem Optimization. *Future Transportation Technology Conference & Exposition* (p. 66). Vancouver: Society of Automotive Engineers (SAE).

National Instruments. (2011). *NI LabVIEW Data Visualization and User Interface Design.* Retrieved December 12, 2011, from http://www.ni.com/labview/whatis/user-interface/

Nennelli, A. D. (2001). *Simulation of Heavy-Duty Hybrid Electric Vehicles.* (Doctoral Dissertation). Retrieved from ProQuest Dissertations & Theses database. (UMI No. 1408993)

NREL. (2002, June 11). Retrieved January 12, 2011, from National Renewable Energy Laboratory: http://www.nrel.gov/news/press/2002/2102_advisor_tool.html

On-Road Heavy-Duty Vehicle Program. (2011, January 26). Retrieved February 5, 2011, from The California Air Resources Board (ARB): http://www.arb.ca.gov/msprog/onroadhd/onroadhd.htm

Pasquier, M., & Rousseau, A. (2001). *Validation of a Hybrid Modeling Software (PSAT) Using Its Extension for Prototyping (PSAT-PRO).* Detroit, MI: Argonne National Laboratory.

Pesaran, A. A., Simpson, A., & Markel, A. J. (2006). *Cost-benefit analysis of plug-in hybrid electric vehicle technology.* Golden, CO: National Renewable Energy Laboratory.

Petinrin, M. O. (2010, July 01). Development of graphical user interface for finite element analysis of static loading of a column using MATLAB. *Leonardo Electronic Journal of Practices and Technologies, 9*(17), 131-142. Retrieved October 12, 2011

Pogula, S. S. (2005). *Developing neural network applications using LabVIEW.* (Master Thesis). Retrieved from http://search.proquest.com/docview/305456807?accountid=10906

Reemer, B. R. (2007, March 30). *DC to DC Conversion:Boost Converter Design.* Retrieved from http://www.egr.msu.edu/classes/ece480/capstone/spring/group05/docs/AppNote-reemmerb.pdf

Sanna, L. (2005). *Driving the Solution: The Plug-in hybrid Vehicle Lucy Sanna.* Retrieved July 12, 2011, from Electric Power Research Institute: http://mydocs.epri.com/docs/CorporateDocuments/EPRI_Journal/2005-Fall/1012885_PHEV.pdf

Serway, R. A., & Jewett, Jr. J. W. (2003). *Physics for Scientists and Engineers.* 6th Ed. Pacific Grove, CA: Brooks Cole. ISBN 0-53440-842-7.

Simpson, A. (2006). *Cost-Benefit Analysis of Plug-In Hybrid Electric Vehicle Technology.* Washington, DC: Dept. of Energy.

Smith, J. B. (2001). Optimum Hybrid Vehicle Configurations for Heavy Duty Applications. Morgantown, WV: West Virginia University Libraries.

Staunton, R. H., Ayers, C. W., Marlino, M. D., Chiasson, J. N., & Burress, T. A. (2006). *Evaluation of 2004 Toyota Prius Hybrid Electric Drive System.* Oak Ridge, TN: Oak Ridge National Laboratory.

Synopsys, Inc. (2006, March 01). *Mechatronics System Design, Analysis, and Verification.* Mountain View, CA: Synopsys, Inc.

Synopsys, Inc. (2011). Retrieved January 16, 2011, from Saber for Automotive Systems: http://www.synopsys.com/Systems/Saber/Pages/Automotive.aspx

Tóth-Nagy, C. (2000). *Investigation and simulation of the planetary combination hybrid electric vehicle* (Doctoral Dissertation). Retrieved from ProQuest Dissertations & Theses database. (UMI No. 1404683)

Toyota Gibraltar Stockholdings Ltd. (n.d.). *TGS glossary of 4x4 terms.* Retrieved September 12, 2011, from http://ecom.toyota-gib.com/English/Vehicles/4x4%20Guide/glossary.htm

Travis, J., & Kring, J. (2007). *LabVIEW for everyone: Graphical programming made easy and fun.* Upper Saddle River, NJ: Prentice Hall.

Turevskiy, A. (2011, April 26). *Matlab Central.* Retrieved from http://www.mathworks.com/matlabcentral/fileexchange/authors/32123

Uses for Gears. (2008). Retrieved August 12, 2011, from http://www.howstuffworks.com/gear-ratio4.htm

U.S. Environmental Protection Agency. (2009, September 17). Retrieved September 12, 2011, from Emission Standards Reference Guide: http://www.epa.gov/oms/standards/light-duty/udds.htm

Vehicle Technologies Program. (2004). *Energy Efficiency & Renewable Energy.* Retrieved August 16, 2004, from http://www1.eere.energy.gov/vehiclesandfuels/pdfs/success/psat.pdf

Vlach, M. (1990). Modeling And Simulation with Saber. *ASIC*

Wakefield, E. H. (2008). *History of the Electric Automobile: Hybrid Electric Vehicles.* Society of Automotive Engineers (SAE). Warrendale, PA

What is Global Warming? (2011). Retrieved June 10, 2012, from http://gcmd.nasa.gov/Resources/FAQs/glob_warmfaq.html

What is NI LabVIEW? (2011). Retrieved September 10, 2011, from http://singapore.ni.com/labviewlearningcenter

Wipke, K., Cuddy, M., & Burch, S. (1999). ADVISOR 2.1: a user-friendly advanced powertrain simulation using a combined backward/forward approach. *IEEE Transactions on Vehicular Technology*, 1751-1761.

Wishart, J. D. (2008). *Modelling, simulation, testing, and optimization of advanced hybrid vehicle powertrains.* (Doctoral Dissertation). Retrieved from http://search.proquest.com/docview/304445804?accountid=10906

Wouk , V. (1995, July). Hybrids: then and now. *IEEE Spectrum Magazine*, pp. 16-21.

Yu, L., Wang, Z., & Shi, Q. (2010). *PEMS-based Approach to Developing and Evaluating Driving Cycles for Air Quality Assessment.* Houston, Tex. : Center for Transportation Training and Research, Texas Southern University.

Yue, Bonnie. (2011). *A Hardware-in-the-Loop Test Platform for Planetary Rovers.* (Master Thesis). Retrieved from http://uwspace.uwaterloo.ca/bitstream/10012/6055/1/Yue_Bonnie.pdf